Tissue Electrical Impedance Determination via Microneedles

by

Laura L. Proctor
B.S., Mechanical and Aerospace Engineering
B.S., Mathematics
University of Missouri – Columbia, 1999

Submitted to the Department of Mechanical Engineering
in Partial Fulfillment of the Requirements for the Degree
of

Master of Science in Mechanical Engineering

at the

Massachusetts Institute of Technology

June 2002

Signature of Author: .....
Department of Mechanical Engineering
8 May 2002

Certified by: .....
Ian W. Hunter
Hatsopoulos Professor of Mechanical Engineering and Professor of BioEngineering
Thesis Supervisor

Accepted by: .....
Ain A. Sonin
Chairman, Department Committee on Graduate Students

Tissue Electrical Impedance Determination via Microneedles

by

Laura L. Proctor

Submitted to the Department of Mechanical Engineering on May 24, 2002 in Partial Fulfillment of the Requirements for the Degree of Master of Science in Mechanical Engineering

Abstract

A new system of drug delivery requires knowledge of depth of needle penetration into skin. Electrical impedance is proposed as a method to measure the insertion depth of microneedles by applying a small current through the skin and measuring the voltage output. The theory is that impedance values will vary with changes in the make-up of the skin. The impedance will decrease with increased depth into the skin. As the needles penetrate the stratum corneum and move into the viable epidermis, there will be a decrease in the impedance values. The impedance drops sharply again when the needles move into the dermis and finally into the subcutaneous layer. These different impedance values are measured and programmed in the microcontroller used in the drug-delivery device. This will make the drug-delivery system an autonomous system. Once the impedance goes down to a pre-determined level, it will trigger the microcontroller to actuate the pumping of the drug into the skin. Not only will this prevent the drug being wasted by pumping when the needles haven't penetrated the skin, but it will also ensure repeatable results where the amount of drug is controlled and the delivery region is specific.

Thesis Supervisor: Ian W. Hunter

Title: Hatsopoulos Professor of Mechanical Engineering

Biographical Note

As an undergraduate, I attended the University of Missouri in Columbia, Missouri; the same city in which I was born. I earned the Bright Flight scholarship given to all Missouri residents who scored well on the ACT to keep these students in the state. After analyzing both the English and Math departments at the university, I decided to major in Mathematics.

My second year at the University, I received a letter from the Learning Center inviting me to become a math tutor. I took the offer and began as a Calculus tutor. I met several other tutors in the program who were not only great friends, but also helped me make decisions that would influence my future.

About a year later, I made a decision to start taking more Physics classes and eventually took enough classes to have a minor in Physics. At that time, I also started tutoring Differential Equations and a few elementary Physics classes.

At the end of my fourth year, I understood that my draw to math was primarily in applied math rather than theoretical math, and thus took a few engineering courses. Before the year was over, I went to a few schools to look at graduate school in mechanical engineering. I soon realized that I wanted to get a better base knowledge of the subject, and with one year left on my scholarship, I stayed an undergrad at Mizzou and took engineering classes.

After I finished my fifth year, I had only one year left to get a degree in engineering, and with the momentum that I had built up I didn't want to stop there. I also had more opportunities to do internships in engineering, so I decided to apply for a few. I ended up deciding on Anheuser-Busch, and worked there from June 1998 to January 1999.

After finishing my internship there, I went back to school for my last year with more focus and determination than before. I applied to graduate school in the fall of 1999, and graduated cum laude in the winter.

I had one semester to wait to receive word on graduate school, so I decided to start a research project at the University of Missouri until I heard from my schools. I worked on a satellite trajectory program written in Fortran for NASA-Glen in Lewiston, Ohio for Doctor Craig Kleuver. I would also teach his class in System Dynamics in his absence. In the time that I had been involved at the University of Missouri, I had received two awards for Excellence in Teaching for my work as a tutor (the only tutor to receive the award twice at that point).

In April of 2000, I heard from MIT, and I made the decision to come. In the fall of 2000, I joined Professor Ian Hunter's BioInstrumentation Lab and started on the drug delivery project shortly thereafter.

In the fall of 2001, I started working as a Graduate Resident Tutor (GRT) in the Burton 3rd undergraduate dorm. The GRT position is for mentoring undergraduates at MIT and being a liaison between the students and the system.

Thus far I have had a blessed life and I can only look forward to what the future holds.

Acknowledgements

First I want to thank Professor Ian Hunter for being the very best advisor. I couldn't have made it through without his guidance and understanding. He has created the ultimate environment in which to foster and stimulate the mind. I am eternally thankful for his patience and desire to let his students work in areas that spark their interest. The BioInstrumentation lab is an incredible environment that I have been given the opportunity in which to work.

Thanks also to Professor Peter Hunter of the University of Auckland in New Zealand for his help in deriving an equation for fluid flow through a tapered tube. He pointed out an assumption that I had clearly overlooked that proved to simplify the Navier-Stokes equation incredibly.

I would like to thank Dr. John Madden, who spent many hours of his week not only helping me struggle through my research problems, but also several other students in the lab. Dr. John Madden has an incredible gift for patience. Without his help and support, this work could have never been done.

I also want to thank Paul Horowitz and Tom Hayes, who truly taught me the "Art of Electronics." After taking the course at Harvard, I felt like I could conquer the world of electronics. It not only gave me the know how to work with circuits, but the confidence to do so.

A special thanks to Bryan Crane, a fellow Missouri Tiger. I wouldn't have been introduced to the lab without him. Thanks to Peter Madden for helping me struggle through even the simplest of electronics problems. Peter has a talent and knack to teach in a way that is never boring and always stimulating. Thanks to Peter for helping me trudge through the first draft of my thesis. Thanks to Dr. Sylvain Martel for letting me in on the cutting-edge technology in electronics. Dr. Sylvain Martel has always been there to answer my questions, even with his schedule full. I truly appreciate the time that he took out of his busy schedule to teach me. Big thanks to his crew for helping me find parts for my circuit, especially Johann Burgert and Jan Malasek. I would also like to thank Johann and Jan for helping me troubleshoot my circuit...a tedious task for anyone. Thanks to Robert David for being in the lab at those hours where you would never expect anyone to be in lab! He has been a great deal of help to me in proofing my thesis. Thanks to Patrick Anquetil for being the computer guru that he is. He took many hours helping myself and others troubleshoot our computer problems. I would also like to thank him for his time spent in proof-reading my thesis. I also want to thank James Tangorra for all his time and help and laughter (and 4:00 coffee breaks – I would have never been addicted to caffeine without him).

Thanks to my mom and dad for lending me an ear during the hard times; also, for their support and great advice. I also would like to thank my wonderful grandparents. Thanks to my brother, Mike, and his wife, Johanna, for giving me an outlet in Portland, Oregon. Also, thanks to my brother, John, and his wife, Jayma who have been so kind to me. Thanks to their son and my nephew, Kellen, who brightens my day every time I think of him! Also, thanks to my dear friends who have listened to my frustrations and my joys, and love me just the same: Robin Prica, Chi Collins, and Cavanaugh Noce. I would also like to thank my boyfriend, Kevin Flaherty and his parents Larry and Edna, who have been fabulous supporters of me. They have been genuinely wonderful and understanding and treat me like part of the family. Now, when I go visit them in Maine I feel as if I'm heading to my second home.

This is dedicated to the memory of Fred Morris Aussieker, the best granddaddy a kid could ever want.

TABLE OF CONTENTS

Chapter 1: INTRODUCTION

The area of drug delivery is an ever-expanding field. Almost everyone in the world has taken one drug or another. On a daily basis, it is not uncommon for one to ingest a pill, like a vitamin or an aspirin. Aside from ingestion, there are primarily three other methods by which a person may receive drugs: inhalation, injection, and transdermal delivery. Asthmatics may take their medicine using an inhaler. This allows the medicine to act immediately, especially useful during an asthma attack. Type I Diabetics are not able to take insulin orally because the body's digestive juices destroy it. Therefore, insulin must be administered via injection into fat in the body. This is also done on a daily basis. Transdermal drug delivery, like the nicotine patch, only works for drugs that are suitable to pass through the stratum corneum. There are several ways to administer drugs in modern society, yet we still predominantly rely on invasive, painful, and to some people, scary needles. Needles may be used wither to get the drug into the circulatory system quickly, or to avoid a chemical breakdown that would occur through any other processes. The goal of this project is to find an alternative method for injection of drugs that is less invasive; especially drugs that need to be delivered via needles.

The goal of the limpet microneedle drug delivery system is to deliver drugs into the lower epidermal layer of the skin or even the upper dermal layer of the skin. This would be shallow enough to not hit nerves, and deep enough to penetrate the stratum corneum, the primary skin barrier.

During the design process of the drug delivery device, knowledge of the pressure needed to push the drug through the needles is important in order to determine the size of the needles and the parameters for the pumping mechanism. A detailed analysis of the pressures needed for needles of different profiles was done to determine the ideal conditions.

The drug delivery device should require very little human interaction; the more independent the device is, the better. Thus, the use of electrical impedance to determine when the device is on the skin, or how far the device has gone into the skin is an important factor. This is so that the drug is safely and effectively delivered to the correct

area and in the prescribed dosage. The electronic circuit discussed herein (a.k.a. the impedance circuit) has been designed to determine the impedance value of the skin using the microneedles in the limpet design.

1.1 The Human Skin

Skin is the largest organ on the human body with a surface area of approximately two square meters and a mass of about 4.5 to 5 kilograms.[43] It is important to have a good understanding of the different layers of skin and their roles in the body. Specifically to this project the different layers will put restraints upon the optimum depth of penetration for the needles.

Understanding the different layers of skin, and specifically the thickness of the layers will provide insight as to how the impedances may change with depth of penetration of the microneedles. "Different tissues are characterized by wave impedances and also by equivalent impedances at various tissue interfaces representing discontinuities."[41]

Skin is made up of two principal layers: the epidermis and the dermis. Skin serves to protect the underlying tissues from ultra-violet light, extreme temperature, bacterial invasion, physical abrasion, dehydration, and more.

The epidermis may be divided into two parts: the stratum corneum and the viable epidermis. The stratum corneum is the outermost layer of the skin, the primary protective layer. The viable epidermis is the rest of the epidermis that is made up of living cells as opposed to the stratum corneum, which is composed of striated layers of dead cells.

The stratum corneum is the outer 10 to 15 micrometers of skin, consisting of 20 to 30 rows of flat, dead, keratinized cells. The epidermis goes through a desquamation cycle that takes two to four weeks. The cells at the base of the stratum corneum are constantly being replaced with newly keratinized cells as the topmost layer of cells is sloughed off. Keratin is a protein which forms waterproof layers, so it protects the skin not only from liquids leeching into the inner organs, but it also prevents fluids from leaking out of the body. The stratum corneum is the most protective layer of the skin, and thus is considered the primary barrier for transdermal drug delivery.

The viable epidermis is composed of three to four layers depending on the location on the body. These layers are: stratum lucidum, stratum granulosum, stratum spinosum, and stratum basale. The cells that make up the epidermis are: keratinocytes, melanocytes, Langerhans cells, and Merkel cells. Keratinocytes produce the protein keratin and form about 90% of epidermal cells. Desmosomes bind the keratinocytes in the epidermis together. Melanocytes are responsible for producing the pigment melanin which is responsible for skin color. Langerhans cells come from bone marrow and have a role in immune responses. Merkel cells are located only in hairless skin in the stratum basale; they detect touch.

Skin on the palms and soles (hairless skin) contains the stratum lucidum layer just below the stratum corneum. For the purposes of drug delivery, since it is unlikely the drug will be injected in these areas, the stratum lucidum will not be discussed.

Stratum granulosum is then the layer just below the stratum corneum. It consists of three to five layers of flattened cells. Some of the cells in this layer do contain nuclei as they are in various stages of decomposition. The cells contain granules of keratohyalin, a precursor of keratin, which is found in the stratum corneum.

The stratum spinosum is the next layer down, and contains 8 to 10 rows of cells. The spiny desmosomes that connect the keratinocytes to one another give the layer its name.

The stratum basale, which is the lower layer of the stratum germinativum (the upper layer being the stratum spinosum), is the lowest layer of the epidermis, which is connected to the dermis. It is a single layer of cells and it contains stem cells. The stem cells multiply and make keratinocytes. The keratinocytes migrate toward the surface and in the process enucleate and loose all organelles. These cells will eventually become part of the stratum corneum and shed off. Stem cells may also move into the dermis and become sebaceous glands, sweat glands or hair follicles. The stratum basale also contains Merkel discs that are sensitive to touch, but it does not contain free nerve endings.

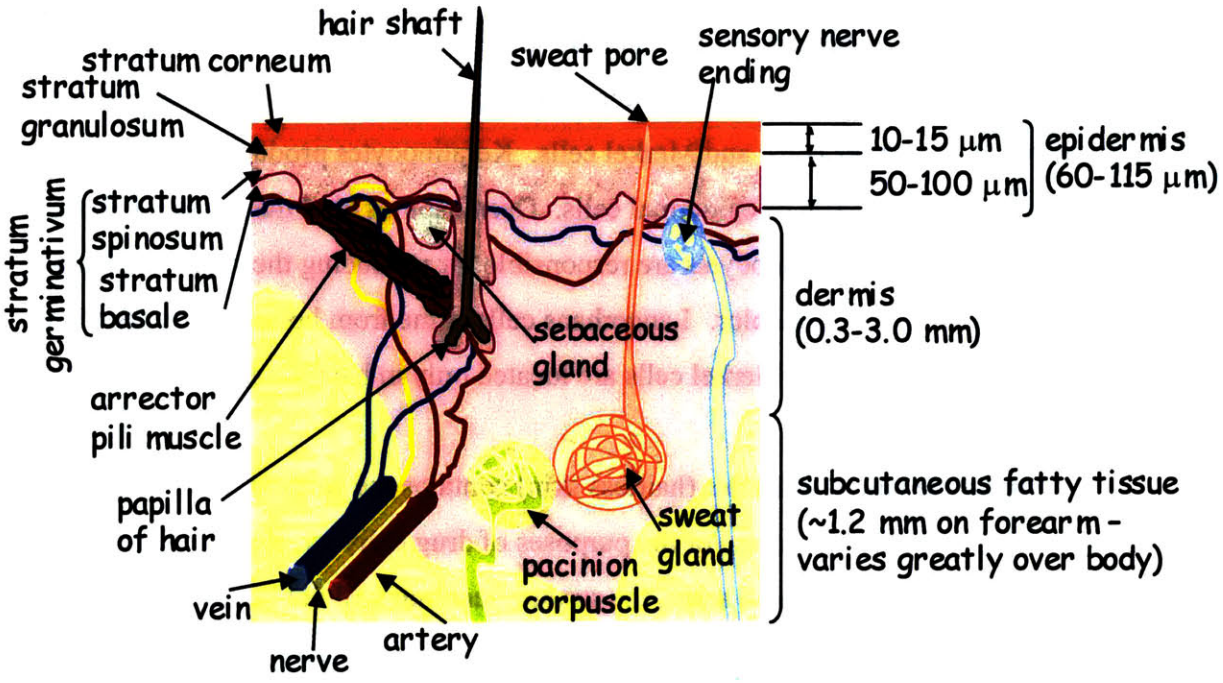

Figure 1-1: Illustration of the different layers of skin.[36, 43]

The dermis is mainly composed of collagen and elastin fibers. The layers of the dermis are the papillary and reticular region. Below the dermis is the subcutaneous layer.

The papillary region is just below the stratum basale. The dermal papillae help connect the epidermis and dermis together. This region contains fine capillaries, which bring nutrients to the skin and carry away waste. There are also branched nerve endings in the dermal papillae, which can detect pressure, pain, and temperature. Since this region can detect pain, it is important to not penetrate into this region. The drug should absorb down from the stratum spinosum through the stratum basale and into the capillaries in the papillary region.

The reticular region in the dermis contains interwoven connective tissue. In between the interlaced collagen and elastin fibers there are nerves, sweat glands, hair follicles, and oil glands. This region composes the bulk of the skin and gives skin most of its mechanical properties.

In order to have a drug delivery system that is less invasive and less painful, it is important to know where the nerves are in the skin. An overview of the layers of skin and their different thickness values are given in Figure 1-1.

1.2 Porcine Skin: A Model for Human Skin

How does porcine skin relate to human skin? The histology of porcine skin is nearly identical to that of human skin. Thus, it is a good representation for human skin. The porcine model used in testing later in Chapter 5: Testing and Results, is skin taken from the shoulder of the pig. Initial testing was done on skin from the leg of the pig, but the skin from the shoulder is softer and more like skin that would be found on the site for drug delivery into human skin. See Figure 1-2 shows the shoulder skin that is used in testing.

Figure 1-2: Porcine Model – skin from the shoulder of the pig.

1.3 Impedance and Drug Delivery

Why would impedance be a useful measurement to make for drug delivery applications? The idea of delivering the drug through the stratum corneum and into the viable epidermis or dermis is a novel idea, and in doing so it would be useful to determine what depth is optimal for the delivery of the particular drug. Most other injection systems using needles deliver the drug into the connective tissue underneath the dermis and transdermal patches apply the drug directly to the stratum corneum. As of yet, there are no drug delivery systems that effectively by-pass the stratum corneum.

Using impedance would assure repeatability in the delivery of the drug to the specified depth.

The overall goal of this project, the limpet drug-delivery system (see Figure 1-3), is to create a pain-free or less painful method of drug delivery by injection into the superficial layers of tissue rather than going directly into the subcutaneous tissue where there are more free nerve endings and a greater likelihood of painful delivery. Not only will smaller needles be less painful, but a shallower delivery site will hit fewer pain receptors.

Another aspect of this drug-delivery project is to have a device that is small and portable. It should have minimal interference with the patient, and so a small design is necessary. The patient should be able to carry on with daily life while the limpet is injecting drug into their tissue.

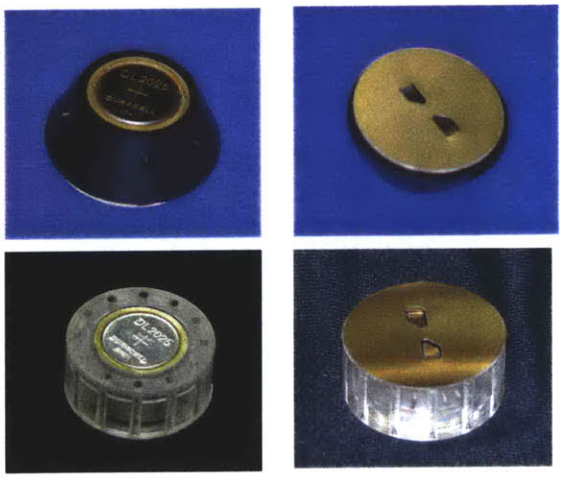

Figure 1-3: Limpet design for drug delivery via microneedles.[3]

Using the principle of impedance, a small AC current is run through the microneedles where the voltage output will be monitored by the microcontroller. When the voltage drops down to a pre-programmed value, to be determined by extensive testing of the circuitry, this will trigger the limpet to stop moving into the skin. Then, the drug will be delivered to the precise layer of skin. This method of impedance measurement will prevent the drug from being delivered into air if it is accidentally activated without contact to skin. It will also prevent drug delivery to layers of skin that

might be too shallow to effectively distribute the correct amount of drug into the circulatory system.

Given that the different layers of skin are made-up of different compositions of materials, the impedance value should change at different depths of penetration into the skin. So, when the needles are touching the skin and penetrated into the skin to a depth of approximately 10 μm, the depth of the stratum corneum, the impedance value may see a small decrease as the skin is all keratinized cells. The next few microns may see a sharper decline in impedance values as the cells are in varying stages of decay. At the top of the stratum germinativum there should be a more drastic downward change as the needles penetrate into a layer of live keratinocytes and connective desmosomes. Impedance values tend to decrease as the amount of fluid in the skin increases. The theory is that the dry stratum corneum will have a much larger impedance value than the wetter dermis. The whole epidermis of a human forearm is on the order of 150 μm in depth. It would be useful to observe the changes through the epidermis and into the dermis; changes in impedance value measured to a depth of one millimeter are useful measurements.

The purpose of this project is to make a small-scale electronic circuit that can measure impedance through the limpet's microneedles. The device must be portable, so size is a major concern. The device must also be accurate enough to differentiate between small changes in depth of penetration of the needles. Since the epidermis itself is only 150 μm thick, a change in 10 μm is substantial and must be readable by the impedance circuitry.

1.4 Fluid Flow and Drug Delivery

The fluid flow through microneedles in this method of drug delivery is important for many reasons. The needle size will affect how the drug flows through the needles. A model of the fluid flow shows the pressure needed to push drug through different shaped needles and will give an idea of what type of actuator will be needed for the drug delivery pump. A general derivation of fluid flow through the needles, considering the needles to have a fairly smooth profile and minimal resistance, will give a general idea of the pressure needed to push the drug through the needles. Initially, the shape of the

needles was undetermined, so it was important to determine the flow through several geometries of needles as seen in Appendix A: Fluid Flow Through Microneedles (see Figure 1-4). A typical drug dose, say, of insulin, can be approximately 1.5 mL. A minimum drug delivery speed of 1 μL/s would mean that the device should be in contact with the skin for 25 minutes. This would be the upper limit of the design. Having the drug delivery limpet applied to the forearm for much longer than 25 minutes would be uncomfortable for the user. Achieving a delivery rate of 1 μL/s or faster is desirable. See Appendix A: Fluid Flow Through Microneedles for a derivation and discussion of fluid flow.

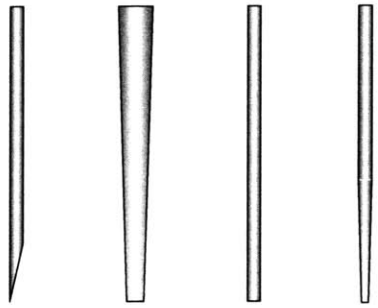

Figure 1-4: Different needle geometries considered for microneedle drug delivery.

Chapter 2: ELECTRICAL IMPEDANCE APPLIED TO DRUG DELIVERY

Electrical impedance is the "measure of the total opposition to current flow in an alternating current circuit, made up of two components, ohmic resistance and reactance, and usually represented in complex notation as $Z = R + iX$, where R is the ohmic resistance and X is the reactance."[13] For a more in-depth overview of impedance and its meaning, refer to Appendix B: .

Impedance is the proposed method to determine needle depth in the skin for drug delivery actuation purposes. The theory is that by applying a current through the skin and measuring the output voltage, the depth of the needles in the skin may be determined. This chapter lays the foundation for this theory by showing some background testing which relates impedance values to various levels of stratum corneum stripping and also using the microneedles to penetrate porcine skin and measuring impedance.

2.1 Biological Impedance

Impedance has been used to measure several biological properties. The measured properties vary from fat percentage to power deposition over the body to Electrical Impedance Tomography (EIT) imaging.

One daily use of impedance measurements in conjunction with biology is body impedance measurements which are currently used to measure one's body fat percentage. However, the credibility of such measurements and their relation to exact body fat is in question since it is likely that the measurements are simply finding a value for water content in the body which is not an exact correlation to the amount of body fat. Impedance measurements may also be done on segments of the body rather than over the whole body.[42]

The impedance method was developed to make numerical computations in the presence of electrical fields and currents of the human body. Essentially, a "3-D resistance network represents the computational cells within a volume, that completely encloses the model analyzed."[44] Power deposition throughout the body in the presence of time-varying electromagnetic field sources were measured "to examine the coupling

of radio frequency magnetic fields with the human body vis-à-vis that of a vertically polarized electric field."[30]

EIT imaging is a small, inexpensive method for imaging that may be used as an alternative to x-ray tomography and positron emission tomography. Its drawbacks are its low spatial resolution and large variability of images between subjects. "Recordings are typically made by applying current to the body or system under test using a set of electrodes, and measuring the voltage developed between other electrodes. To obtain reasonable images, at least one hundred, and preferably several thousand, such measurements must be made."[10]

Stuchly and Stuchly did extensive work on electrical properties of tissues in the early 80's. The graph seen in Figure 2-1 is typical of all high-water content tissue.[39] They designed a probe which was then used to measure the electrical properties of different tissues in vitro and in vivo to compare the values against theoretical values, especially in the area of cancer research.[39]

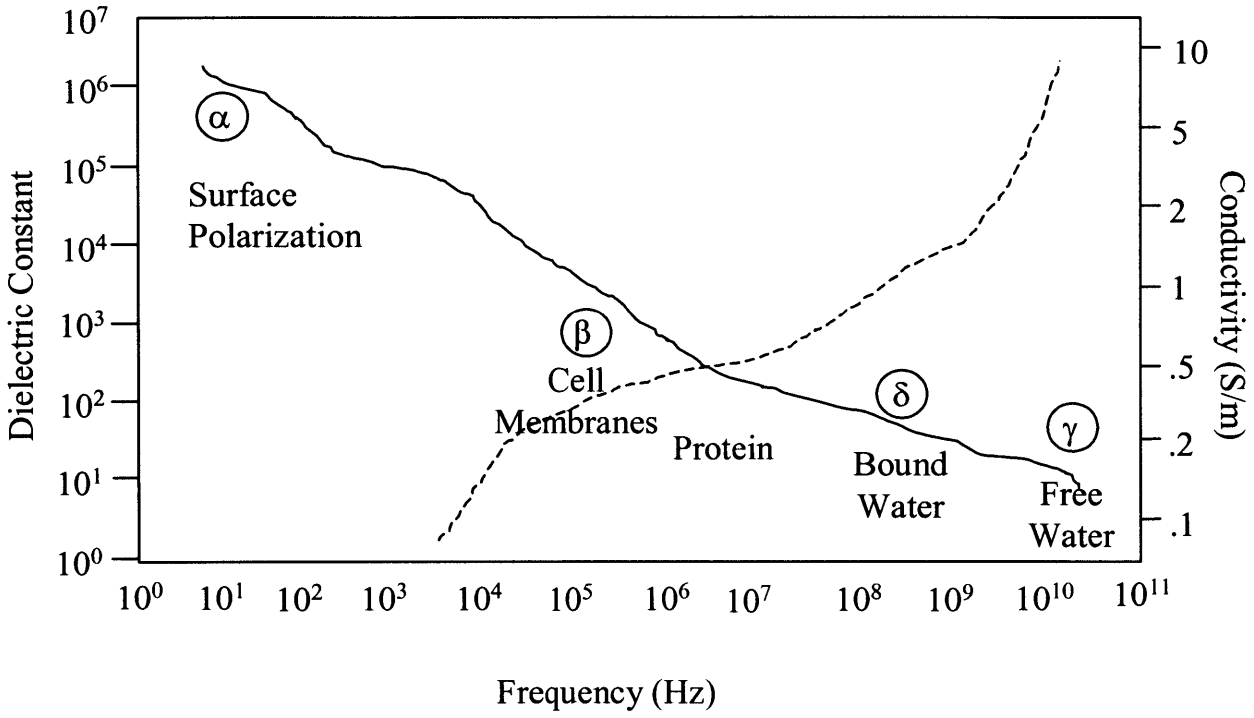

Figure 2-1: Permittivity of muscle tissue as a function of frequency.[39]

As far as we know, no measurements have been done that relate the depth of penetration into skin to impedance values. Although, several measurements have been made where a "3-D impedance network is formulated to represent the biological body using the anatomical data and the anisotropic, spatially varying complex resistivity"[16] to estimate the mass-normalized rate of energy deposition (specific absorption rates or SAR's). But, these tests make assumptions that are not relevant when measuring the impedance of skin; they tend to be more generalized.

2.2 Impedance Measurements

The Hewlett Packard Impedance Analyzer, HP 4194A, has been used to make several preliminary measurements of skin impedance. The HP 4194A measures impedance over the range of 100 Hz to 40 MHz. The results achieved using the HP 4194A will give values near where the skin impedance values should be. Two major areas of testing have been done on skin impedance measurements in the BioInstrumentation Lab: testing on human subjects and testing on in vitro pigskin. The testing that was done on human subject was done with copper electrodes placed on the skin surface. The tests that were performed upon in vitro pigskin were done using needles from the proposed drug delivery device, placed both on the surface of the skin and in the skin. These results provide a starting point for estimating results with the impedance circuit that will be discussed in Chapter 4: .

2.2.1 Impedance Measurements on Human Skin In Vivo

James Tangorra, a doctoratal candidate in the BioInstrumentation Lab, performed tests upon human subjects using the HP 4194A Impedance Analyzer. The copper electrodes, seen in Figure 2-2, were used to do the testing. The polycarbonate block is used to house the electrodes and is non-conductive so that it won't interfere with the tests. Several tests were done with varying degrees of preparation of the forearm.

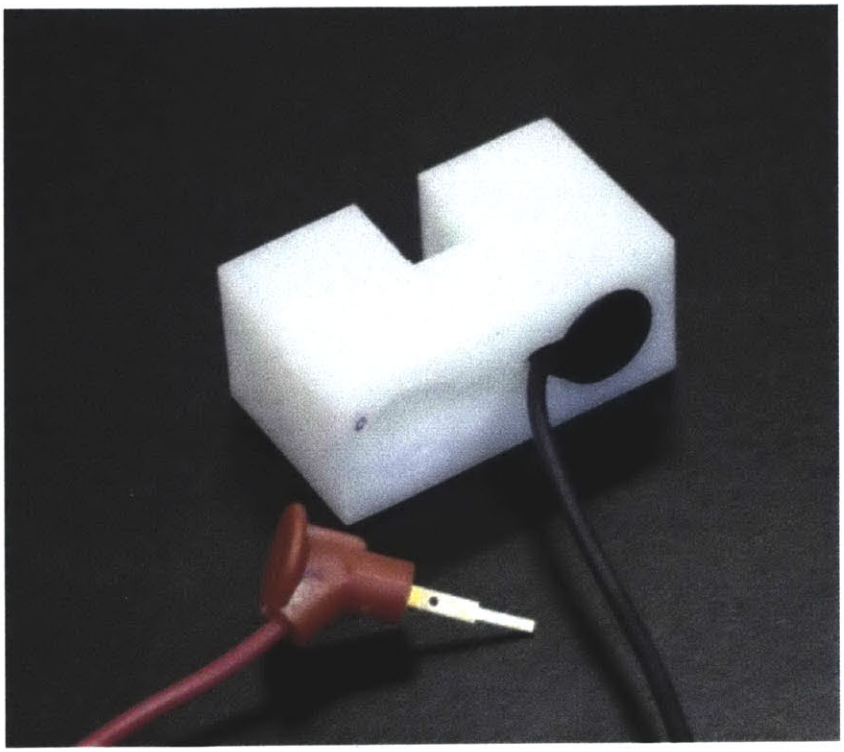

Figure 2-2: Copper electrodes in machined in polycarbonate (Delrin) used to do impedance testing on humans in vivo.

As seen in Figure 2-3, the impedance levels dropped with what seems to be an increase in the stripping of cells from the stratum corneum. With no skin prep, there are dead cells on the arm which are presumably ready to be sloughed off. Once the arm is shaved, the dead cells that would have fallen off or been washed off in the near future are likely shaved off with the dry shave process. This is only a cellular penetration into the stratum corneum. The Nuprep gel is a gel that is used in application of electrodes onto people for medical purposes and is helpful in creating a better electrical connection to the surface of the skin by lowering the skin's impedance; it is lightly abrasive. The sandpaper was rubbed onto the skin of the forearm and produced visible changes in the skin's appearance. The skin was red in color from the irritation of the sandpaper, and looked slightly watery. This means that the stratum corneum is removed, and most likely the rest of the epidermal layer is also removed. These results were very promising for the future tests. At 1 kHz, the change in impedance between the stratum corneum and the dermis is at least three orders of magnitude from approximately 20 MΩ to 10 kΩ. The goal of the project is to penetrate the stratum corneum, thus the impedance values under 1 MΩ are of the most interest.

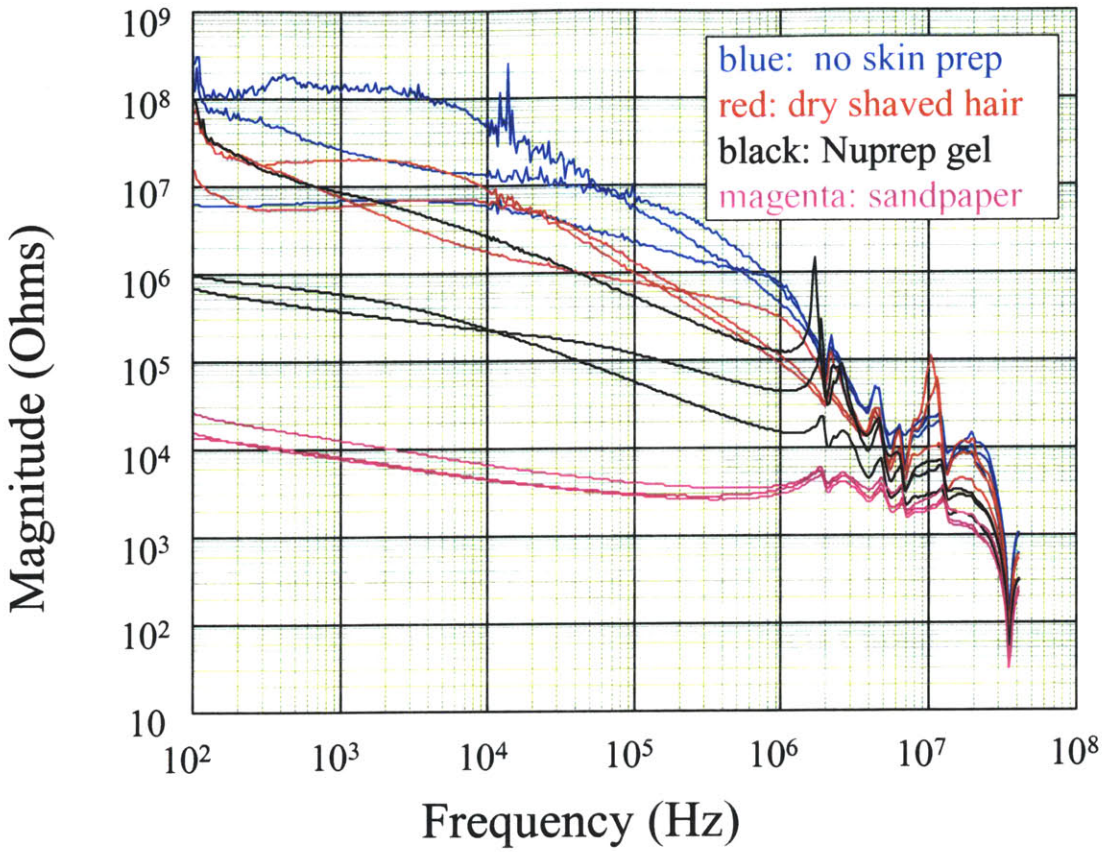

Figure 2-3: Forearm impedance measurements done on the HP4194A Impedance Analyzer with the electrodes seen in Figure 2-2 limited to 500 mV.

2.2.2 Impedance Measurements on Pigskin In Vitro

Tests using 100 μm outer diameter stainless steel needles as electrodes were performed upon excised porcine skin taken from pigs' legs. This again shows that the impedance value is expected to decrease as depth into the skin increases. The impedance change with respect to change in depth into the pigskin cannot yet be determined from these graphs since there are only two measurements shown. The needles were initially rested on the skin (Figure 2-4). The needles were then plunged into the skin (blue lines, Figure 2-4); the depth of penetration was deep enough to be into the dermis and probably into the subcutaneous tissue. The configuration of the needles can be seen in Figure 2-5.

The change in impedance between these two layers of skin is three orders of magnitude different at 1 kHz. The outer layer is 2 MΩ while the inner layer of skin has an impedance value of 2 kΩ.

For the needles resting on skin, the impedance levels are within one order of magnitude between the testing seen in Figure 2-3 with the electrodes on skin without preparation and those seen in Figure 2-4 where the needles are resting on the skin.

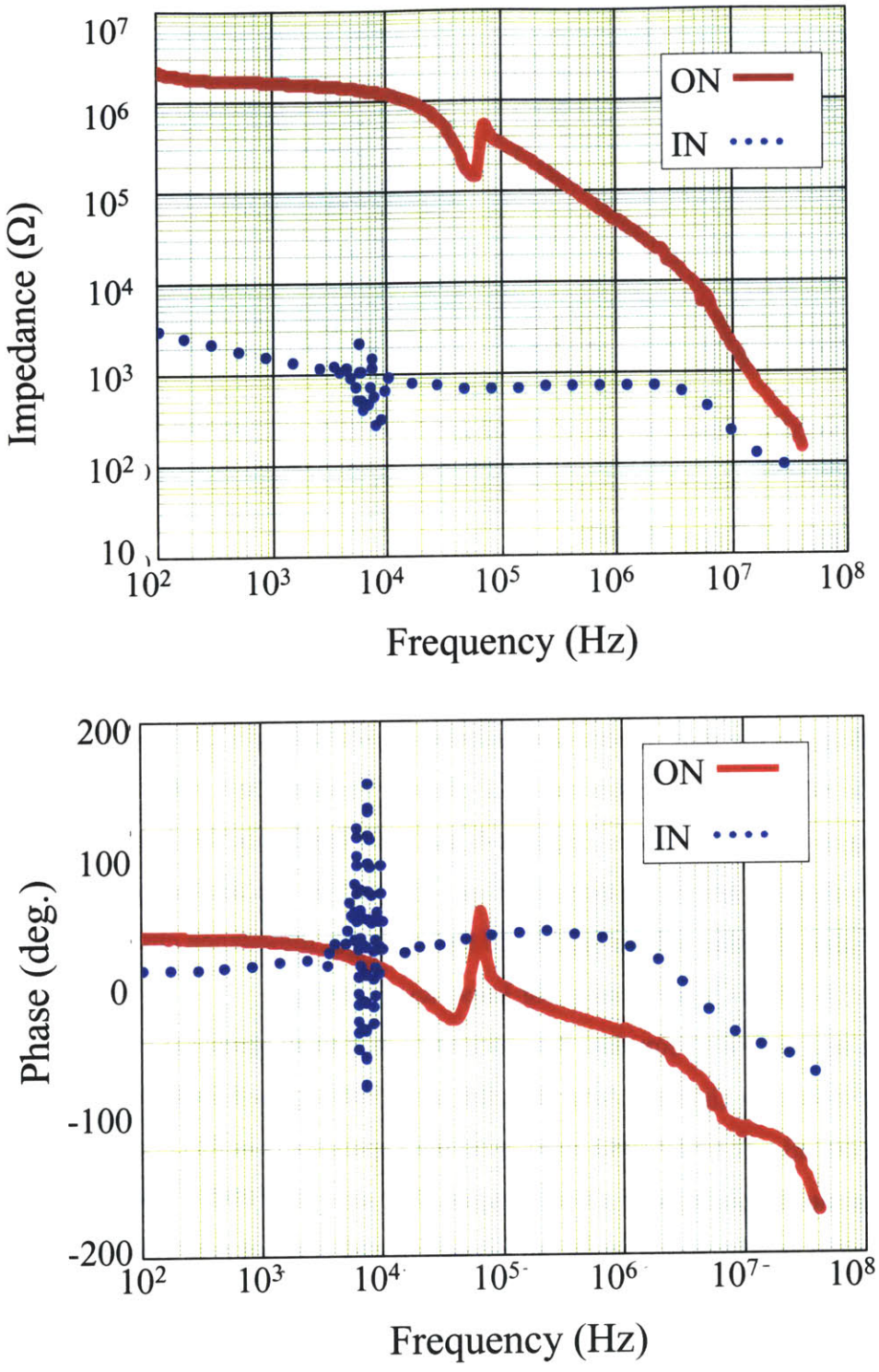

Figure 2-4: Impedance values measured with the HP4194A tested on and in porcine feet.

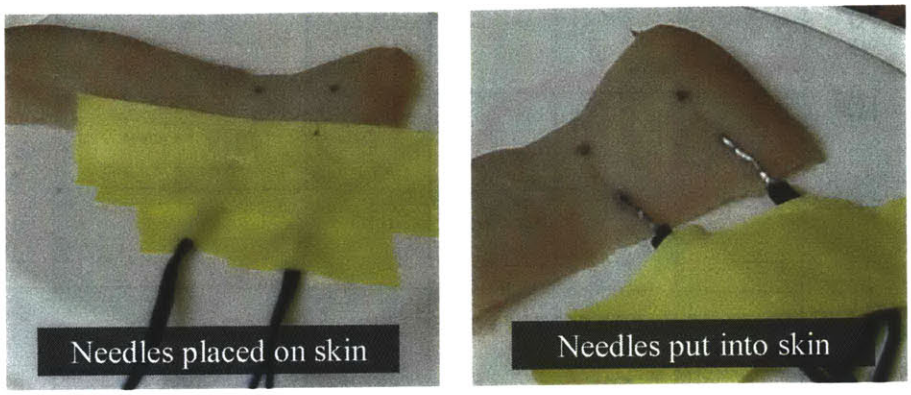

Figure 2-5: Needle placement in excised porcine skin tests using the impedance analyzer.

2.2.3 Analysis of Experiments

The purpose of doing these preliminary tests is to see what kind of impedance values there are at different depths in the skin. From the in vivo experimental results in Figure 2-3, at 1 kHz there is a sharp difference between the sandpapered skin and the other tests done on the skin. There also seems to be some degree of impedance drop from the skin without any preparation to the shaved skin and then to the Nuprep gel. From the pigskin experiments, in Figure 2-5, at 1 kHz the distinction between the impedance values on and in the skin are clear. Because of this distinction, the frequency value of 1kHz will be used to do testing in the impedance circuit discussed in Chapter 4: Electrical Circuit Design for Impedance Testing.

The next step is to simulate the reaction of skin to an electrical stimulus. This is done in the following chapter. After that, the next challenge will be to make a portable impedance circuit. The HP4194A used to do the experiments in this chapter gives incredibly accurate results over a wide range of frequencies (100 Hz – 40 MHz), but is too large and expensive to use in the limpet design and thus not practical.

Chapter 3: SKIN MODELS

Because of the laborious nature of using human skin, or even pigskin, to test the circuit, a model of skin was made using capacitors and resistors. Several electrical models of human skin have been proposed. Often, values for specific resistances or capacitances are not given because of the variation between individuals. It is important that the circuit determines impedance values of human skin.

3.1 Background

Skin has been modeled using several different electrical circuits (Figure 3-1). But, none of them are the same nor do any of them have even approximate values for the components that make up the circuit. Therefore, it was necessary to make electrical models for skin using the results obtained in Section 2.2.2

Impedance Measurements on Pigskin In Vitro (see Figure 2-4).

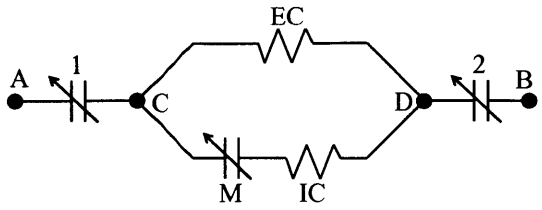

a. Thomasset's model of the skin[42]

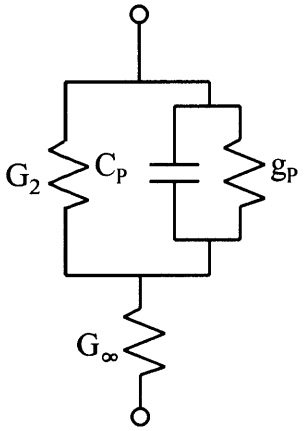

b. Yamamoto's model of the skin satisfying Cole-Cole arc's law[44]

Figure 3-1: Electrical models for skin from previous literature.

3.2 Electrical Circuit Models of Skin

To determine the circuit components that comprise that stratum corneum, the impedance values found from pigskin in 2.2.2 were used as a model. Figure 3-2 shows the impedance values that were used and how these, in turn, helped to determine the circuit and values seen in Figure 3-3. In Appendix B: Impedance, the impedance behavior of resistors and capacitors is shown. In Figure 3-2, the flat portion of the graph up to 10 kHz is mostly due to the effects of a resistor since resistors' impedance values don't change with change in frequency. But, above 10 kHz, the slope is due to a capacitor effect as seen by the downward slope which is close to a slope of one (on the log-log graph), thus is due to only one capacitor.

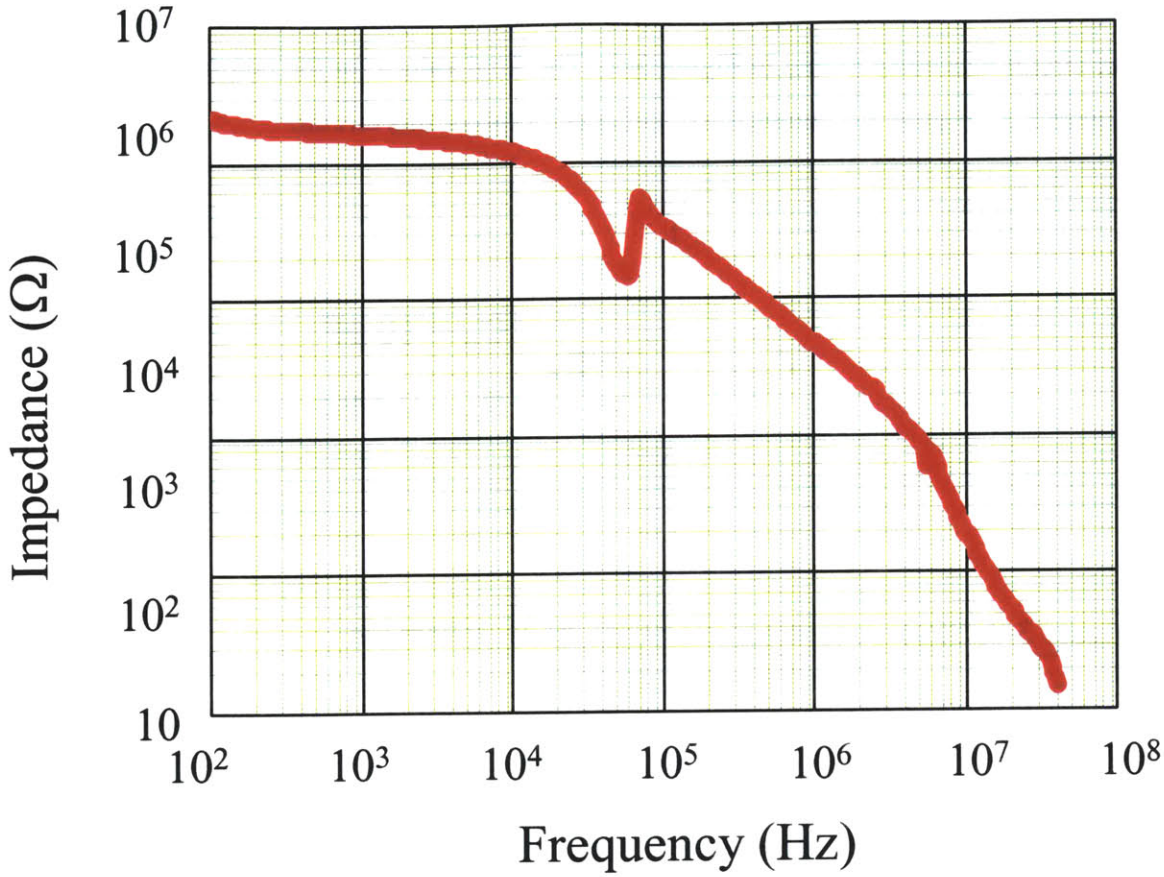

Figure 3-2: Impedance values for electrodes resting on pigskin.

From this information a basic circuit can be configured. By observation of Figure 3-2, there is going to be a resistor and capacitor in parallel. A small resistor is in series with this configuration. It is known by the impedance value of the flat portion of the graph that the resistor that is in parallel with the capacitor is approximately 2 MΩ. The capacitor doesn't take over until 10 kHz, if the impedance values of the resistor and capacitor at this value are set equal to one another, then an initial guess for the capacitor value can be found,

$$\left|Z_{10\text{kHz}}\right| = 2\ \text{M}\Omega = \frac{1}{10 \cdot 10^{3}\,\text{Hz} \cdot \text{C}} \Rightarrow \text{C} = 50\ \text{pF}. \qquad 3.1$$

Initially a capacitance of 50 pF was tried in the circuit. But, this didn't give impedance values which were a close enough match to those in Figure 3-2. Therefore, the

capacitor values were changed in the appropriate direction until the impedance graph of the circuit was close to that in Figure 3-2. The final values for the components are in Figure 3-3. Figure 3-4 shows the impedance graph of this circuit.

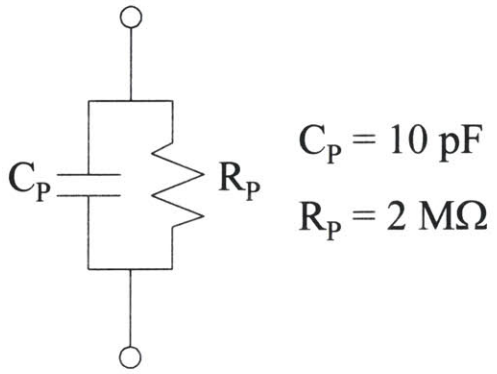

Figure 3-3: Stratum corneum electrical model schematic.

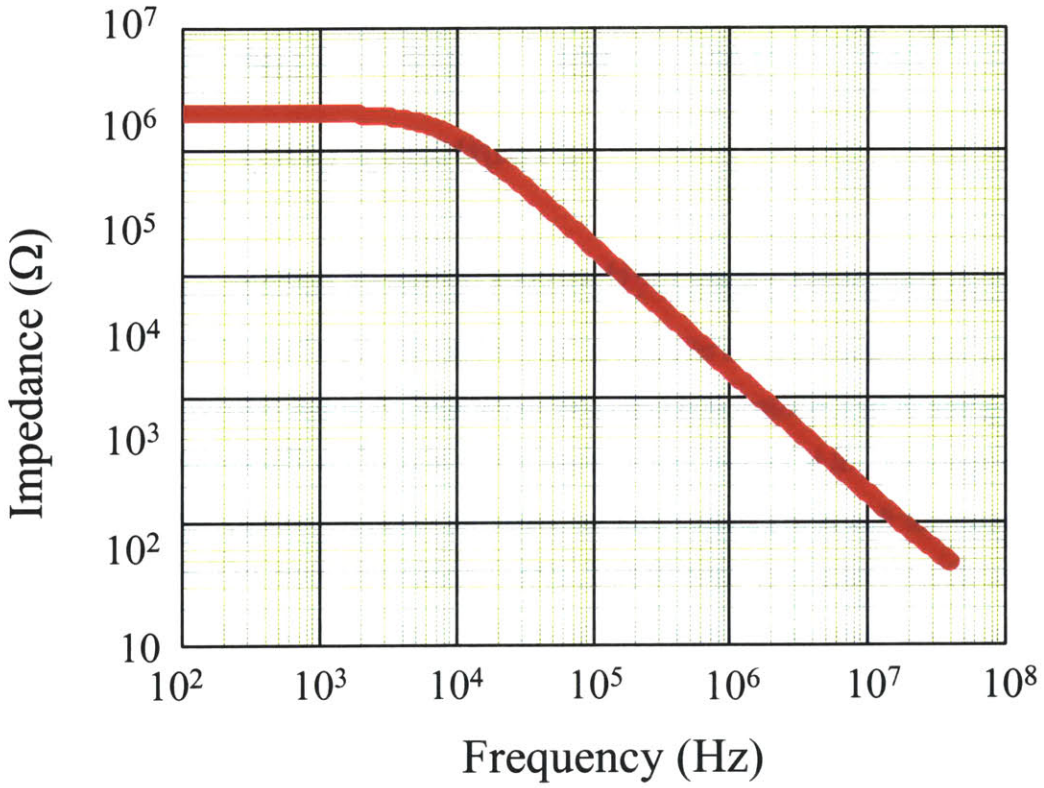

Figure 3-4: Stratum corneum electrical model transfer function.

After the stratum corneum is penetrated, a different behavior occurs in the impedance plot (see Figure 3-5). The impedance is lower than when the needles are on the skin. Also, the trend of the plot is much different. In the first part of the graph, up to 30 kHz, the plot is dominated by the effects of a capacitor. The beginning value for the graph is approximately 3,000 Ω, so this should be the initial impedance value. The circuit schematic, seen in Figure 3-6, was determined to give similar values to those seen in Figure 3-5 (see Figure 3-7).

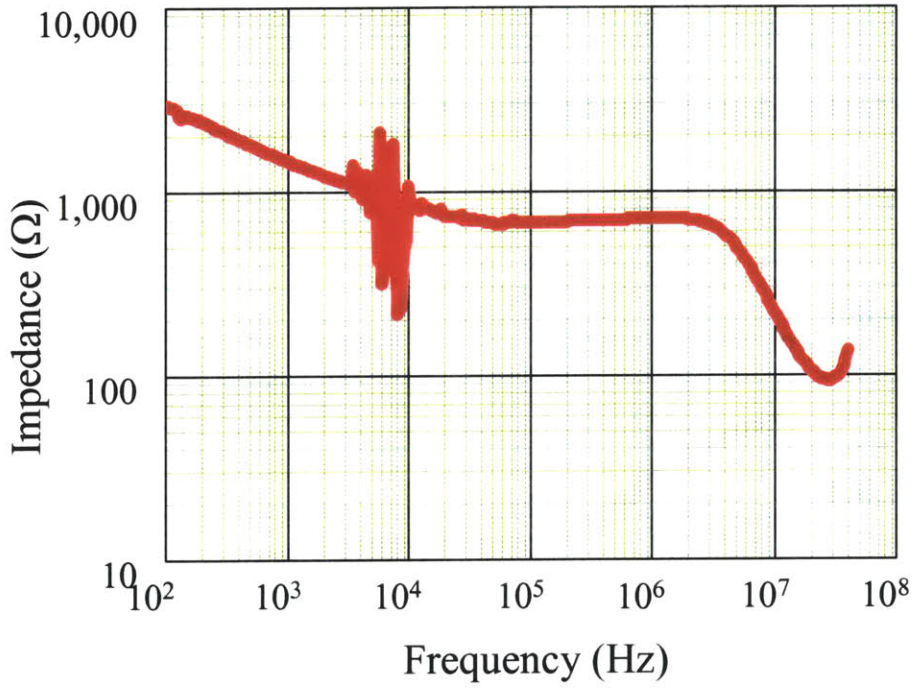

Figure 3-5: Impedance values for electrodes plunged into pigskin.

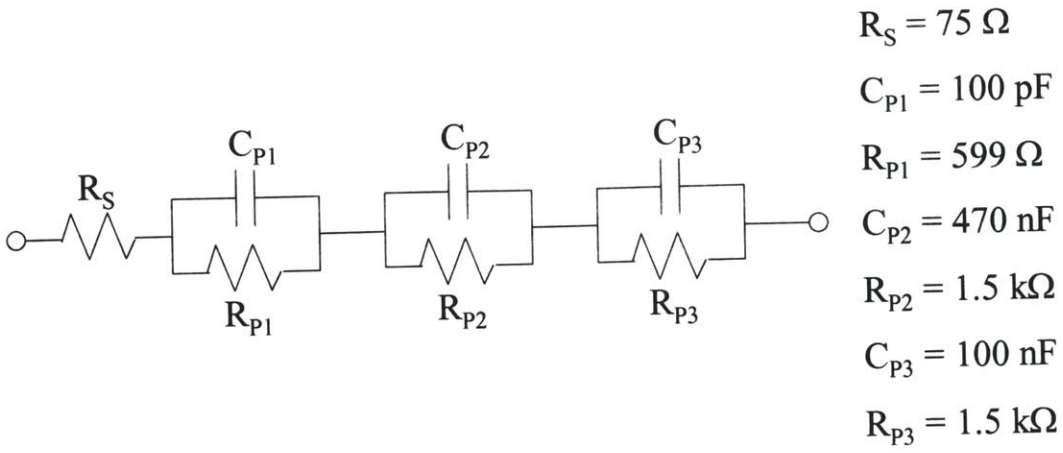

Figure 3-6: In skin electrical model schematic.

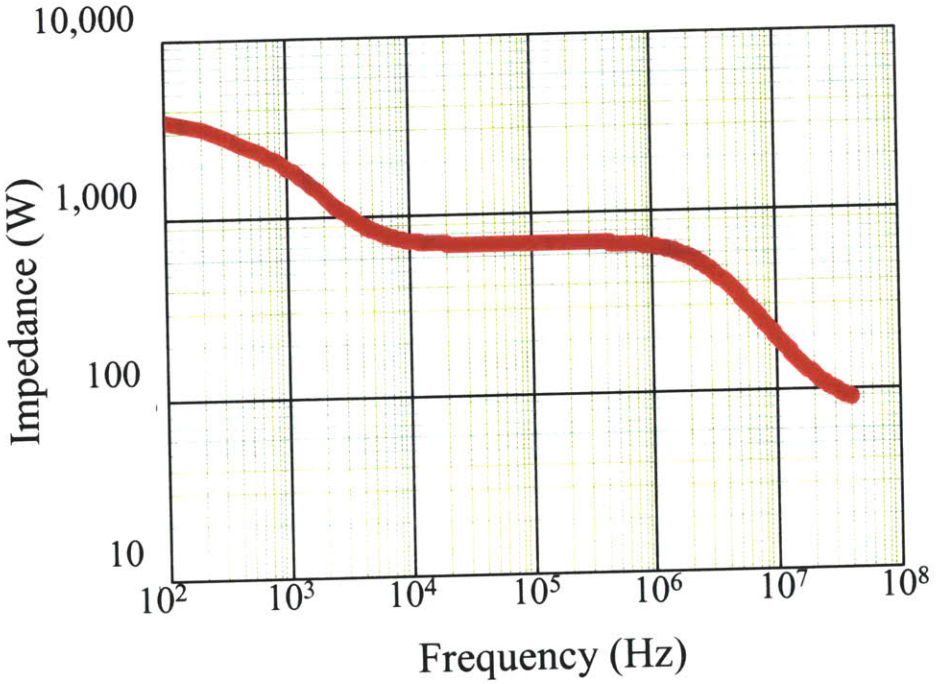

Figure 3-7: In skin electrical model.

Chapter 4: Electrical Circuit Design for Impedance Testing

The purpose in designing a circuit to test impedance is so that it can be included in the portable limpet drug delivery device. There were several stages of testing, redesign, and retesting. There are five major components of the analog portion of the circuit. Included here will be an overview of the different components and how they operate (see Figure 4-1). Many different integrated circuits (ICs) were considered for the design. It's important to know why the final design uses the ICs it does, and what the differences are between the initial components considered and the final components decided upon. In the end, it became important to miniaturize the circuit so that the drug delivery device could be portable and interfere with the patient as little as possible. A short profile is necessary. Also, a small footprint for the whole device would allow it to deliver drugs into the forearm where there is less flat skin surface than other areas (e.g. the thigh or stomach). Steps were taken to complete this task using the most appropriate, smallest number of, most economical, smallest size, modern components available. Each component was analyzed to be an optimal blend of the above characteristics.

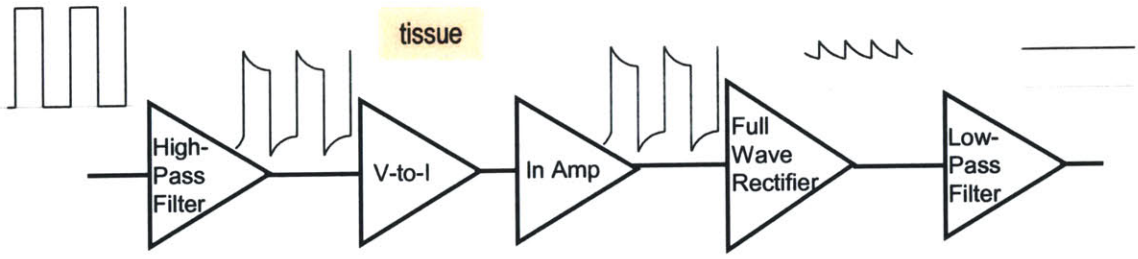

Figure 4-1: Block diagram of analog portion of impedance circuit with waveforms.

The five major portions of the analog circuit are the: high-pass filter, voltage to current converter, instrumentation amplifier, full-wave rectifier, and low-pass filter. The flow of the circuit and the resulting waveforms may be seen in Figure 4-1. First, a 1 kHz

square wave comes from the microcontroller that oscillates between 0 and 3 V. This is put through the high-pass filter which removes the DC component of the waveform. From this, the voltage is put through a voltage to current converter which puts the small current through the tissue. The instrumentation amplifier measures the voltage over the load. Then, the full-wave rectifier rectifies the wave in the positive direction so that it can go into the analog to digital converter in the microcontroller (which can only measure positive voltages). Finally, the signal, which is oscillating at 1 kHz, is sent through a low-pass filter for smoothing.

There is also a digital portion of the circuit portion which provides the input signal, a square wave with a frequency of 1 kHz, and also takes the output data through an ADC. The major component on the digital side of the circuit is the microcontroller. This microcontroller is used for other aspects of the drug delivery system; it will control the movement of the limpet needles and will also provide the operator insight as to whether or not the limpet has injected drug into the patient. For the impedance aspect of the limpet, the microcontroller has two major operations. First, it puts out a square wave to the analog portion of the circuit. It also has a 12-bit ADC which takes in the output of the analog portion of the impedance circuit. This ADC can determine values only between 0 V and 3 V. So, no negative values should go into the microcontroller's ADC nor should any values much larger than 3 V (thus the rectification). See Figure 4-2 which shows how the different components link up to one another.

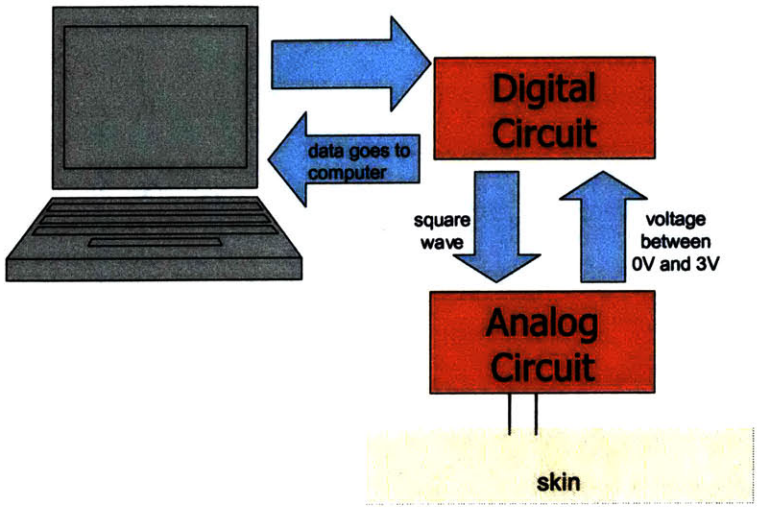

Figure 4-2: The flow of data through the circuit and how it interfaces with the computer. The digital circuit starts sending a square wave to the analog circuit as soon as it's powered up. The skin serves as the load on the analog circuit and determines the voltage output that goes into the digital circuit. This data, in turn, is sent through the ADC, which is part of the microcontroller on the Digital Circuit, then sends the data to the computer through the RS-232 Driver/Receiver.

4.1 Analog Impedance Circuit

As shown in Equation **B.1**, impedance is determined from current and voltage. The idea behind this circuit design is to have a known current drive through the skin and measure the voltage output. This is generally done with an AC sine wave. The circuit in question uses the TI MSP430F149 (see Appendix C.6) mixed signal microcontroller to deliver a 1 kHz square wave to the circuit (see Figure 4-1). The microcontroller is not able to deliver a sine wave easily, thus a square wave is used. The amplitude of the square wave is equal to that of the power supply to the microcontroller. The microcontroller is powered by a three volt lithium button battery.

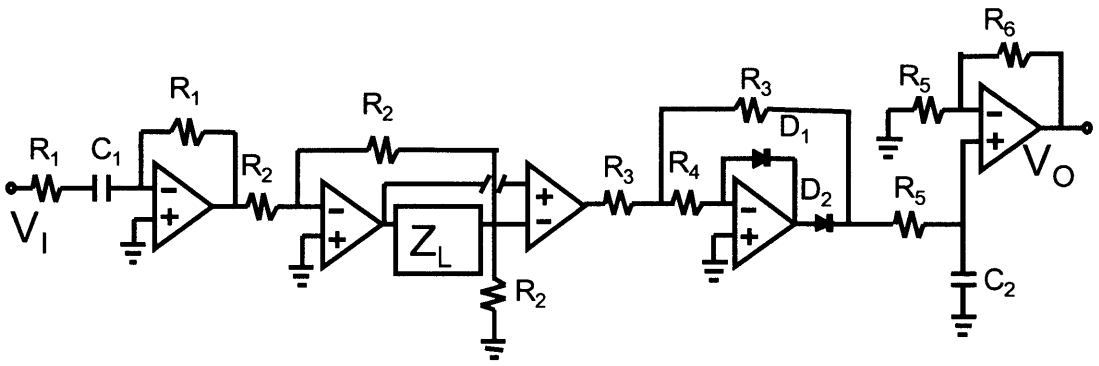

Figure 4-3: Analog impedance circuit schematic.

The circuit schematic of the analog portion of the impedance circuit is shown in Figure 4-3. Each different segment of the circuit is discussed in the following subsections.

4.1.1 High Pass Filter

In order to determine impedance, the delivered periodic signal must oscillate about zero. If the waveform does not oscillate about zero, the waveform will have a direct current (DC) component to it. This is a problem because of the nature of biological tissue, in this case skin. Skin is an ionic conductor, meaning that free ions are in suspension within the skin. Polarization will occur if a direct current tries to pass through the skin, therefore a direct current cannot be used.

Thus, the input waveform needs to go through the first component of the impedance circuit, a high pass filter, in order to achieve this. A high pass filter will only allow high frequencies through (see Figure 4-5). The waveform in Figure 4-4 represents the output of the microcontroller; a square wave that oscillates between 0 and +3 V. The 1.5 V DC component of the input wave may be thought of as an alternating current (AC) with frequency zero; it will not be permitted through the high pass filter (Figure 4-5). Therefore, the output of the high pass filter will be approximately a square wave with a mean of zero (Figure 4-6, gain=1).

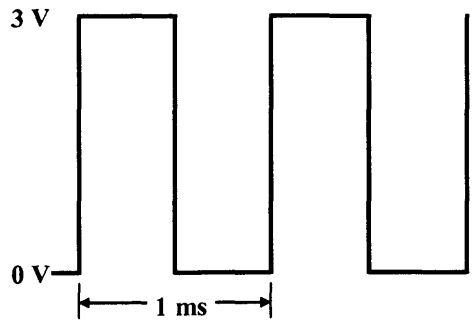

Figure 4-4: Square wave input to analog portion of the impedance circuit.

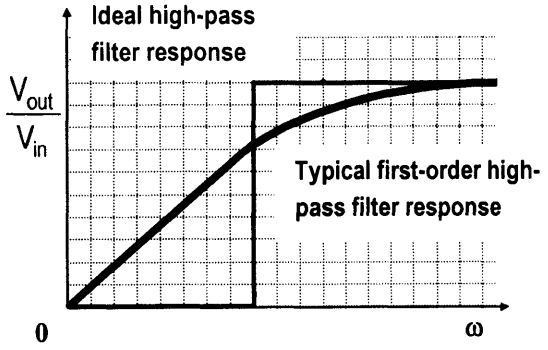

Figure 4-5: General frequency response of a high-pass filter.

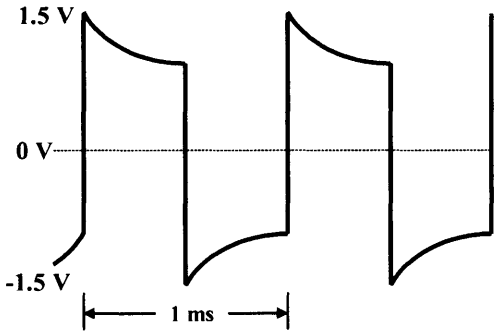

Figure 4-6: Output of the high-pass filter given a square wave input.

There are several designs for a high pass filter that may be used. The most basic high pass filter is a combination of a resistor and a capacitor (Figure 4-7). The governing equation for a capacitor is given in Equation 4.1

$$Q = CV. \qquad 4.1$$

where a capacitor with C farads and V volts across it has a charge of Q coulombs. Given the fact that the current is the derivative of charge, taking the derivative of Equation 4.1 gives the current through the capacitor,

$$I_C = C\frac{dV}{dt}. \qquad 4.2$$

By applying Kirchhoff's current law, the current into the node (through the capacitor) is equal to the current out of the node (through the resistor):

$$C\frac{d(V_{in}-V_{out})}{dt}=\frac{V_{out}}{R}. \qquad 4.3$$

Assume that $\frac{dV_{out}}{dt} << \frac{dV_{in}}{dt}$, to reduce Equation 4.3

$$C\frac{dV_{in}}{dt}\approx\frac{V_{out}}{R}. \qquad 4.4$$

This gives the output voltage as:

$$V_{out}(t)=RC\frac{d}{dt}V_{in}(t). \qquad 4.5$$

These are the equations that govern the behavior of a first-order high-pass filter. The output voltage, V_{out}, is a linear function of the change in the input voltage, V_{in}.

Another way to look at the passive high pass filter is to analyze the voltages directly in the frequency domain. This analysis gives a better understanding of how the filter works to block out low frequency signals. In the simplest terms, one can determine the current traveling through the filter assuming that the input has no impedance and the output has infinite impedance. This is done by taking the input voltage and dividing it by the total impedance. Since the values of impedance are in series, they are

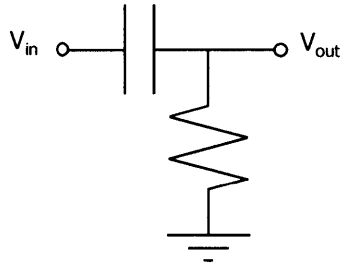

Figure 4-7: Schmatic of a passive high-pass filter.

added. The total impedance is:

$$Z_{HP}=-\frac{j}{\omega C}+R. \qquad 4.6$$

The output voltage can then be determined by multiplying the current by the impedance of the resistor,

$$V_{out}=I_{HP}R=\frac{V_{in}C\omega}{-j+RC\omega}R=\frac{RCj\omega}{1+RCj\omega}V_{in}. \qquad 4.7$$

From Equation 4.7 , it can be seen how low frequencies are attenuated but high frequencies are not.

A passive filter is not used because it is ideal only when the driving source has low impedance and the load has infinite input impedance, which is rarely the case. So, an active high-pass filter should be used because it has a high input impedance and low output impedance providing minimal loading of the source or load. In this application, an active high-pass filter (Figure 4-8) with a gain of one is used to convert the output from the microcontroller to a waveform about zero. The output from this active high pass filter can be seen in Figure 4-6.

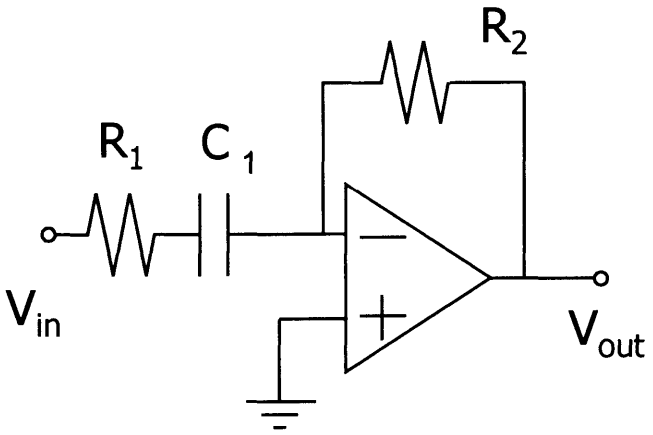

Figure 4-8: Schematic of an active first-order high-pass filter.

The high pass filter in Figure 4-8 has the following governing equations:

$$\text{Gain} = \frac{V_{out}}{V_{in}} = -\frac{R_2}{R_1}, \qquad 4.8$$

$$f_{cutoff} = \frac{1}{2\pi R_1 C_1} \text{ Hz.} \qquad 4.9$$

The signal coming in is a 1 kHz square wave of amplitude 3 V. In order to remove the DC component, the cutoff frequency should be between 0 Hz and 1 kHz. There is also concern over 60 Hz noise. Although this will be minimized by using a battery supply, there is still potential for noise from the overhead lights and surrounding devices. A high-pass filter with a cutoff frequency approximately 100 Hz is suitable for the purposes of this circuit,

$$f_{cutoff\text{-}HP} = 100 \text{ Hz.} \qquad 4.10$$

There is some freedom in choosing the values of the capacitor and resistors. A general guideline to building circuits with the most accuracy available is to use resistors between 10 Ω and 100 kΩ. There is flexibility in this, but following this guideline will reduce the overall noise of the circuit. Resistors larger than 10 Ω have the smallest temperature coefficient.[33] Also, though all resistors have thermal noise, resistors greater than 100 kΩ have a large amount thermal noise and a larger noise rating than lower valued resistors (see Appendix C.1). [33] With respect to the op amp, it is important to keep in mind that a gain of less than one is less stable than a larger gain. For this situation, that means that R2 ≥ R1. Another point to consider is the size of the components. In order to make the circuit small enough to fit into the specified dimensions, it is wise to keep each component as small as possible. This means that any component as large as the 0603's, will be adequate. The two basic sizes of resistors and capacitors used are – 0402's (1.00±0.05 x 0.50±0.05 x 0.20±0.10 mm) and 0603's (1.60±0.10 x 0.80±0.10 x 0.30±0.20 mm). In keeping the size of the capacitor within the limits, a capacitance value of 0.33 μF is used,

$$C_1 = 0.33\ \mu F. \qquad 4.11$$

In order to find the value of R_1, plug C_1 and f_{cutoff} into Equation 4.9 and solve for R_1:

$$R_1 \cong 4.82\ k\Omega,$$

$$R_1 = 5.1\ k\Omega. \qquad 4.12$$

For a 0402 surface mount, 1%, thick film chip resistor, the closest available value to 4.82 kΩ is 5.10 kΩ. Since the gain should be one, the other resistor equals the first value,

$$R_2 = 5.1\ k\Omega. \qquad 4.13$$

The cutoff frequency then becomes:

$$f_{cutoff} = \frac{1}{2\pi \cdot 5.1k\Omega \cdot 0.33\mu F} = 94.6\ Hz. \qquad 4.14$$

First, the input voltage, V_{in}, is applied across the resistor R_1 and the capacitor C_1. The inverting input (-) to the op amp is held at virtual ground. The total impedance of R_1 and C_1 in series will be the same as Equation 4.6]. What's essentially happening is that the current that's going through R_1 and C_1 is either going to go through R_2,

through the op amp, or split through both. But, we know that op amps do not allow significant amounts of current into either of their inputs (generally a couple of picoamps). Thus, the current will go through R_2 only. The output should then be:

$$V_{out} = I_{HP} R_2 = \frac{V_{in} C_1 j\omega}{1 + R_1 C_1 j\omega} R_2 = \frac{R_2 C_1 j\omega}{1 + R_1 C_1 j\omega} V_{in} . \qquad 4.15$$

In order to come up with the output seen in Figure 4-6, look at the different components that make up the input 1 kHz square wave. The square wave is centered about 1.5 V. Thus, it is a square wave with an added DC component of 1.5 V. The flat parts of the square wave that occur at 0 V and 3 V are of frequency = 0. The high-pass filter will attenuate signals smaller than 100 Hz – the smaller the signal, the more the filter will attenuate the signal. Once the signal goes through the filter, the flat parts of the input wave taper towards zero. The decay is known to be exponential. In order to determine the value to which the waveform tapers down, we calculate an exponential decay with the time constant defined with R_1 and C_1:

$$V_{decay-min} = 1.5 \cdot e^{-\frac{t}{R_1 C_1}} = 1.5 \cdot e^{-\frac{0.0005s}{5.1k\Omega \cdot 0.33\mu C}} = 1.114 . \qquad 4.16$$

Also note that the vertical components of the wave easily go through the filter since they are essentially components of the wave with an infinite frequency component.

Another way to analyze this circuit is to look at the time response (as opposed to the frequency dependence behavior discussed above). Suppose the capacitor in the circuit is initially uncharged. Before discussing what the current is through the resistor R_1 and C_1, first a review of the behavior of resistors and capacitors is necessary. The voltage drop over C_1 is V_c and the voltage drop over R_1 and C_1 is V_{in}. If V_{in} is made positive at time t = 0, the current through the resistor R_1 and C_1 will be equal to:

$$I_1 = \frac{V_{in} - V_c}{R_1} = C_1 \frac{dV_c}{dt} = C_1 \frac{dV_{in}}{dt} . \qquad 4.17$$

Notice that the change in V_c with respect to time will be the same as the change in V_{in} with respect to time. This is because both the impedance of the resistor and capacitor are stable in time. The capacitor's impedance value will only change if the frequency of the wave changes. Thus, the resistor and capacitor form a resistor bridge of sorts (as

discussed above), and the value of the voltage drop over the capacitor is proportional to the value of V_{in}. The same current that goes through R_1 and C_1 will also go through R_2:

$$V_{out} = I_1 R_2 . \tag{4.18}$$

Now, a relationship can be found between V_c and V_{out} and V_{in};

$$V_{out} = \frac{V_{in} - V_c}{R_1} R_2 \Rightarrow V_c = V_{in} - \frac{R_1}{R_2} V_{out} . \tag{4.19}$$

From this, a time dependent solution for the high pass filter is determined,

$$\frac{V_{in} - \left(V_{in} - \frac{R_1}{R_2} V_{out} \right)}{R_1} = C \frac{dV_{in}}{dt} \Rightarrow V_{out} = R_2 C \frac{dV_{in}}{dt} . \tag{4.20}$$

4.1.2 Voltage Driven Current Source

The essential part of the impedance circuit is the point where the known voltage is converted into an oscillating current of known amplitude. This known current is driven through the skin. The current is going through a load of unknown impedance (the skin). The voltage drop over the load is measured using an instrumentation amplifier, and the resulting impedance is determined by Equation B.1.

To determine impedance, drive a known current through the load and measure the voltage drop. A known voltage form is coming from the high-pass filter, the next step is to convert the voltage to a current and drive it through the load, which is, in this case, skin. The simplest voltage to current converter is a resistor (Figure 4-9). In a simple resistor circuit, a known voltage Vin is applied across a known resistance, R. This will produce a current, I, where $I = \frac{V_{in}}{R}$. This is not an appropriate method to make a voltage-driven current source where the current will go through the load (Figure 4-9) because the voltage is not only applied over the resistor, but would also be applied across the unknown load unless the load has infinite input impedance. Thus, the current will not be known, and the circuit is useless unless a follower is placed before the load. This basic circuit does lay the groundwork for the voltage to current converters that are discussed in this section.

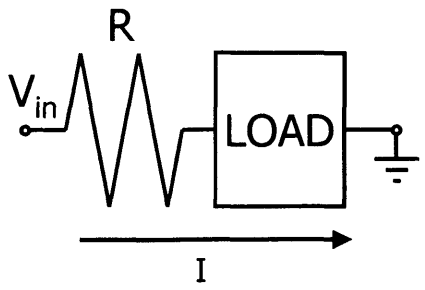

Figure 4-9: Resistor representing a simple voltage to current converter with a load added.

There are several methods of remedying this problem using operational amplifiers. Operational amplifiers (or op amps, as they are often called) have a very large input impedance, and very small output impedance. This is a very useful characteristic, as seen in the high-pass filter. The original op amp circuit used in voltage to current conversion for the impedance circuit can be seen in Figure 4-10.

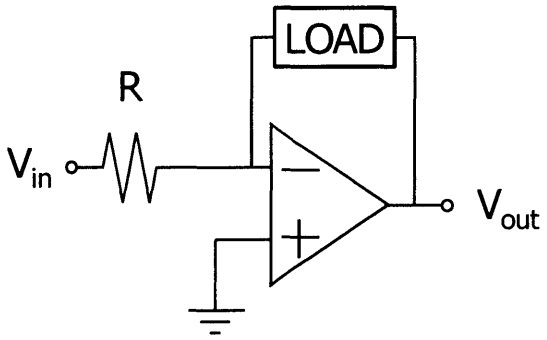

Figure 4-10: Non-inverting voltage-to-current converter.

This circuit works on the concept of a "virtual ground." The non-inverting side of the op amp (+) is held at ground. Thus, the inverting side of the op amp (-) is also at ground. When an input voltage, Vin, is applied across the resistor, R, a specific current is produced, $I = \frac{V_{in}}{R}$. This current is then applied through the load since the input impedance to the op amp is very large. When the current goes through the load, an output voltage, V_{out}, can give the particular impedance value for the load at the

frequency used. The equation for impedance is: $Z_{LOAD} = \frac{V_{out}}{I} = \frac{V_{out}}{V_{in}} R$. Vout is measured and V_{in} and R are known values.

When the current source was used on the pigskin, there was a drift in the output. Thus, a different voltage-to-current converter must be used, such as an inverting voltage-to-current converter.

The inverting voltage-to-current converter can be seen in Figure 4-11. The input voltage, V_{in}, is applied over R_1. This will produce a current,

$$I_1 = \frac{V_{in}}{R_1}, \tag{4.21}$$

because of virtual ground. This same current will go through R_2 because, as mentioned previously, negligible amounts of current flow into either input of the op amp,

$$I_1 = I_2. \tag{4.22}$$

In order to find I_{LOAD}, the current through the load, the current through resistor R_3 must be found. The voltage drop between V_{3H} and ground (over R_3) is the same as the voltage drop between V_{3H} and the inverting input to the op amp (over R_2). This voltage is:

$$V_{3H} = I_2 R_2 = \frac{R_2}{R_1} V_{in}. \tag{4.23}$$

This is needed to find I_3, as follows:

$$I_3 = \frac{V_{3H}}{R_3} = \frac{R_2 V_{in}}{R_1 R_3}. \tag{4.24}$$

To find the current through the load, apply Kirchhoff's current law, which is simply the addition of I_2 and I_3,

$$I_{LOAD} = I_2 + I_3 = \frac{V_{in}}{R_1} + \frac{R_2 V_{in}}{R_1 R_3} = \frac{V_{in}}{R_1 R_3}(R_2 + R_3). \tag{4.25}$$

The current through the load is set by varying the resistors and the input voltage, V_{in}. The measured output is the voltage drop over the load. If V_{3L} and V_{3H} are both voltages measured with respect to ground, then the output voltage will be:

$$V_{LOAD} = V_{3H} - V_{3L} = I_{LOAD} Z_{LOAD}. \tag{4.26}$$

The impedance value can be found by measuring V_{LOAD}, and plugging it into the above equation to find the impedance,

$$Z_{LOAD} = \frac{V_{LOAD}}{I_{LOAD}} = \frac{V_{LOAD}}{V_{in}} \frac{R_1 R_3}{R_2 + R_3}. \quad 4.27$$

Note: the input voltage in this case is not the input voltage to the high-pass filter, but rather the output of the high-pass filter.

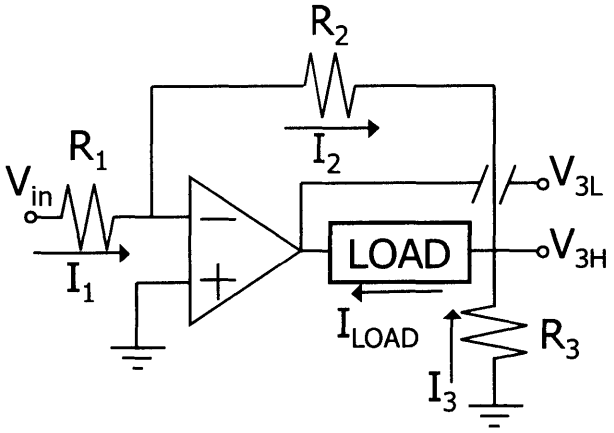

Figure 4-11: Inverting voltage-to-current converter.

Referring back to Figure 2-4, the impedance values for the pigskin at 1 kHz were:

$$Z_{on} = 1.5\ M\Omega, \quad 4.28$$

$$Z_{in} = 1.5\ k\Omega. \quad 4.29$$

These values are important in taking advantage of the range of the op amps. There are other assumptions that need to be made in order to determine some suitable values for the resistors in the inverting voltage-to-current converter.

The op amps will be powered by ±5 V sources. The op amps that are used are rail-to-rail. The specifications state that the "output voltage swings to within 40 mV of the negative supply and 220 mV of the positive supply."[24] Thus, taking the larger value of the two will give the output swing,

$$V_{out} \leq 4.78\ V. \quad 4.30$$

It is important to utilize this range to determine the optimal distance for drug injection, where the needle is deep enough without causing pain. Given that the digital circuit is

running off of one three volt battery and that 3 V is the largest voltage detectable by the microcontroller, the smallest voltage to the op amps should be ±3.22 V.

The maximum current that should be used is very important to know. The current needs to be large enough to produce minimal noise results, but small enough to be undetectable by the subject.

It also needs to be below the maximum value allowed for by the American National Standard Safe Current Limits for Electromedical Apparatus which is 10 μARMS.[4]

The frequency of oscillation is also important. The microcontroller that is used is the Texas Instruments MSP430F149 16-Bit Ultra-Low-Power Microcontroller. The inputs to the microcontroller are a 4 MHz timing circuit and a 3 V battery. The output of the microcontroller is a 1 kHz square wave from 0 V to 3 V. The 1 kHz signal was decided upon because of the distinction in impedance values from previous tests (see Section 2.2 Impedance Measurements) This is useful in determining the output from the high-pass filter. Since there is no gain in the high-pass filter and the DC component of the input signal is removed, the output of the high-pass filter will vary between ± 1.5 V.

Using the same reasoning for choosing the resistor values as in the high-pass filter, and taking the other considerations above into mind, we can determine the best values for R_1, R_2, and R_3. Using the flexibility in choosing the values, a resistance of 220 kΩ is used for all three values. Given these values, one can determine the maximum value of the current through the load from Equation 4.25

$$R_1 = R_2 = R_3 = 220\ \text{k}\Omega, \tag{4.31}$$

$$|I_{LOAD}| = \frac{R_2 + R_3}{R_1 R_3}|V_{in}| \le \frac{220\text{k}\Omega + 220\text{k}\Omega}{220\text{k}\Omega \cdot 220\text{k}\Omega}(1.5\text{V}) = \frac{2 \cdot 1.5\text{V}}{220 \cdot 10^3\,\Omega} \Rightarrow$$

$$|I_{LOAD}| \le 13.64\mu\text{A}. \tag{4.32}$$

One should note the RMS value of the above current just for comparison to the limits:

$$|\text{IRMS}| \le \frac{13.64\mu\text{A}}{\sqrt{2}} = 9.64\ \mu\text{A}. \tag{4.33}$$

Therefore, there are no problems in putting a current that is too large through the skin. Since the load is well isolated, it is not possible for the current to be higher than 9.64 μA.

It is important to note that the circuit that will measure the voltage drop over the load must have extremely large input impedance so that it doesn't load the results. Therefore, voltage followers must be used. These followers will be discussed in the following section.

Given a load impedance value of Z_{LOAD}, the values of V_{3L} and V_{3H} can be seen in Figure 4-12.

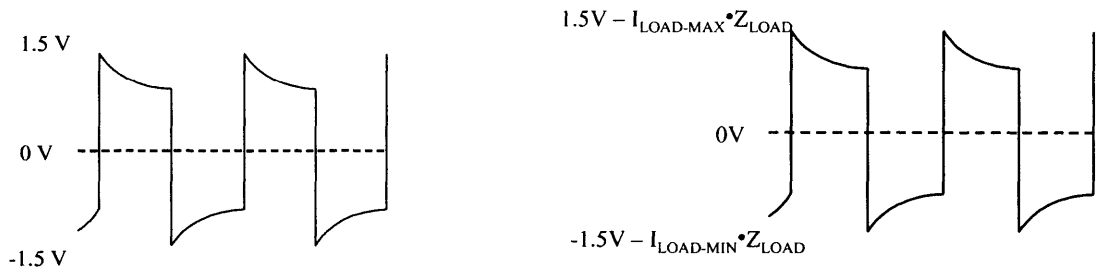

(a) V_{3H} (b) V_{3L}

Figure 4-12: Output of the voltage-to-current amplifier.

4.1.3 Instrumentation Amplifier

The next step is to find the voltage drop over the load. This may be done by using two followers that go into a difference amplifier, see Figure 4-13. The followers are there to provide infinite input

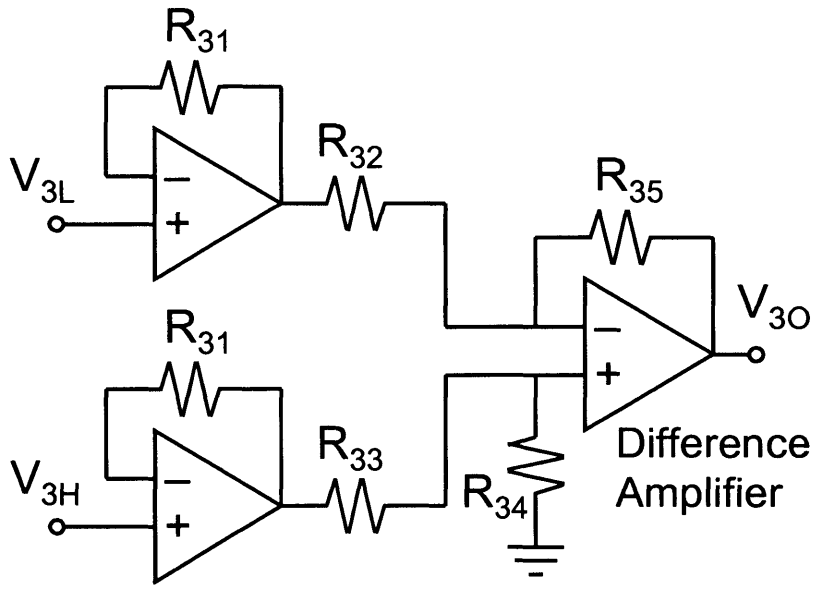

Figure 4-13: Followers with a difference amplifier to take the voltage difference $V_{3O} = V_{3H} - V_{3L}$.

impedance from the previous step. This is important so that the circuit that takes the difference between the nodes does not load the previous circuit, rendering it unreliable.

The resistors used in the feedback loop are generally very small, on the order of a couple hundred ohms. An analysis of the low input will show how the followers work:

$$V_{3L} = V_{3L-}. \qquad 4.34$$

Looking at the output of the op-amp and relating that to the inverting input:

$$V_{3LOUT} = V_{3L-}. \qquad 4.35$$

The resistor, R_{31} is quite small, and only there to take the small bit of input bias current that is expected with real op-amps.

The follower works by taking the input into the non-inverting input, then taking the difference between the inputs and multiplying it by a very large gain until the non-inverting and inverting inputs are the same values. This is done in less than 10 μs; in very little time, the input to the non-inverting end of the amplifier and the output of the amplifier are equal.

In order to find the voltage at the inverting input of the difference amplifier, treat the resistors R_{33} and R_{34} as a resistor bridge. The input voltage is essentially V_{3L}. The voltage at the inverting input is then:

$$V_{3DA} = \frac{R_{34}}{R_{33}+R_{34}} V_{3H}. \tag{4.36}$$

The voltage above is also the voltage at the non-inverting input of the difference amplifier. Given this, the voltage drop over R_{32} is known. This will help determine the current through R_{32} and thus through R_{35}. Below the current is determined,

$$I_{3+} = \frac{V_{3L}-V_{3DA}}{R_{32}} = \frac{V_{3L}-\frac{R_{34}}{R_{33}+R_{34}}V_{3H}}{R_{32}} = \frac{(R_{33}+R_{34})V_{3L}-R_{34}V_{3H}}{R_{32}(R_{33}+R_{34})}. \tag{4.37}$$

From this, the voltage output may be found. First, find the voltage drop over the resistor R_{35} by using the above current,

$$V_{35} = I_{3+}R_{35} = \frac{(R_{33}+R_{34})R_{35}V_{3L}-R_{34}R_{35}V_{3H}}{R_{32}(R_{33}+R_{34})}. \tag{4.38}$$

Now the voltage output, V_{3O} is the difference between the voltage at the input of the difference amplifier and the voltage over the resistor, R_{35},

$$\begin{aligned} V_{3O} = V_{3DA} - V_{35} &= \frac{R_{34}}{R_{33}+R_{34}}V_{3H} - \frac{(R_{33}+R_{34})R_{35}V_{3L}-R_{34}R_{35}V_{3H}}{R_{32}(R_{33}+R_{34})} \\ &= \frac{R_{34}(R_{32}+R_{35})}{R_{32}(R_{33}+R_{34})}V_{3H} - \frac{R_{35}}{R_{32}}V_{3L}. \end{aligned} \tag{4.39}$$

Thus, the voltage difference between V_{3L} and V_{3H} can be seen in the above equation. At first glance, the idea of making all the resistors equal seems to give the difference that is important,

$$\begin{aligned} R_{32} = R_{33} = R_{34} = R_{35}, \\ V_{3O} = V_{3H} - V_{3L}. \end{aligned} \tag{4.40}$$

This seems to perform well, thus choosing a value like 10 kΩ would be adequate for this situation. This is how the difference amplifier operates.

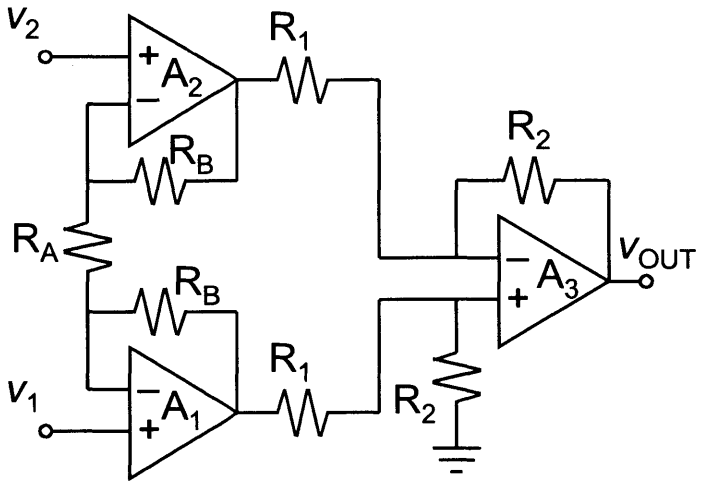

Figure 4-14: Instrumentation amplifier.

Fortunately, there is no need to use three op amps to find the voltage difference between two inputs. An instrumentation amplifier includes all of the circuitry seen in Figure 4-13 and more, but is all on one integrated circuit (see Figure 4-14). The only difference between the circuit seen in Figure 4-13 and that seen in Figure 4-14 is the addition of the resistor R_A in Figure 4-14. The addition of this resistor R_A allows one to change the gain of both input channels simultaneously. Then, the output voltage will be determined by the current going through R_1, which is the same current through R_2, consequently the voltage drop over R_2 plus the voltage at the input of the amplifier will be the output,

$$v_{out} = \left(1 + \frac{2R_B}{R_A}\right)\frac{R_2}{R_1}(v_2 - v_1). \qquad 4.41$$

More details about the specific instrumentation amplifier used for this purpose will be addressed in the second part of this chapter. Given the input to each of the needles in the previous section from Figure 4-12, the output is simply the non-inverting input minus the value of the inverting input. The results of this can be seen in Figure 4-15.

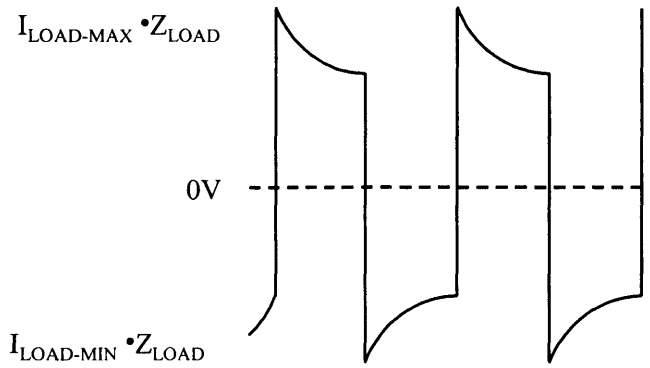

Figure 4-15: Output from the instrumentation amplifier.

4.1.4 Full-Wave Rectifier

After the instrumentation amplifier takes the difference between the voltages, the next step is to full-wave rectify the signal. The reason for full-wave rectification is because the ADC of the microcontroller does not take in negative values. As a result, it's important to have a positive rectification of the wave. In Figure 4-16 the basic full-wave bridge rectifier is displayed.

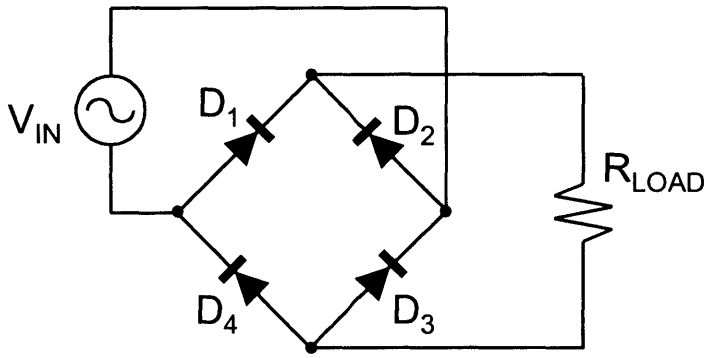

Figure 4-16: Positive full-wave bridge rectifier.

A diode is a "two-terminal passive non-linear device."[19] The symbol for a diode can be seen in Figure 4-17. Forward current flows in the direction in which the arrow points. When a current of approximately 10 mA or larger flows through the diode, it causes a typical voltage drop of about 0.6 V (the anode being more positive than the cathode);

this is called the "forward voltage drop" and can be seen in Figure 4-18. The reverse current is generally only a few nanoamps, consequently it is negligible unless it's subjected to the reverse breakdown voltage (a value generally large enough that it won't be reached in the present application).

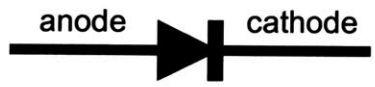

Figure 4-17: Diode.

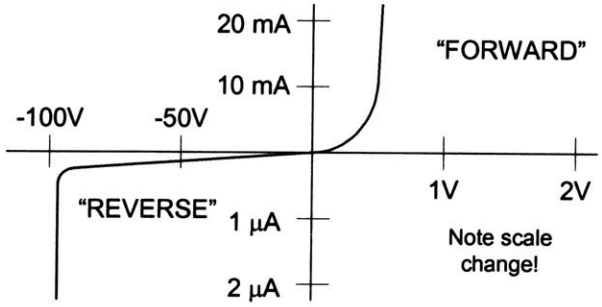

Figure 4-18: Diode voltage versus current curve.[19]

The output of the full wave rectifier may easily be determined for both positive and negative values of V_{IN}, which is always in the positive I_{LOAD} direction. For an ac input waveform, the positive portions of the input are replicated at the load, but the negative portions of the input are reversed in polarity before being applied to the load. This is achieved by using the four diode configuration as seen in Figure 4-16 where only two diodes are forward biased at any given time.

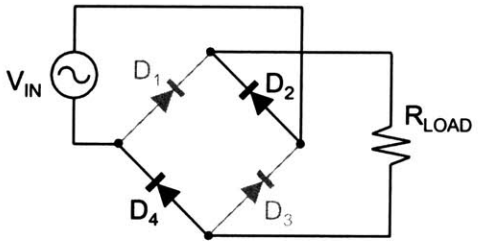

a. Positive input cycle

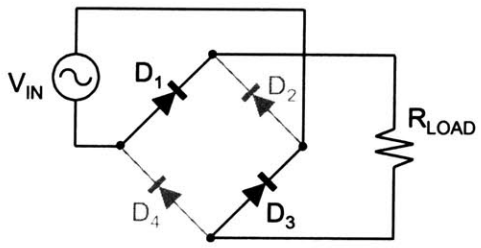

b. Negative input cycle

Figure 4-19: Full-wave rectifier.

For positive input cycles, the current flows in the positive direction through D_2 and into the top terminal of the load. The current will then flow out of the bottom of the load and through D_4 before going into the V_{IN} source. This is shown in Figure 4-19a.

During the negative input cycle, the current flows downward from V_{IN} and through D_1 which again flows into the top terminal of the load. Current then flows out from the load, through D_3, and back into the V_{IN} source as shown in Figure 4-19b. Accordingly, it can be seen that the current flows in the same direction through R_{LOAD} no matter what cycle V_{IN} is in and that will cause the voltage across the load to be in the positive direction for both negative and positive input cycles.

In the particular case of a sine wave input, the output may be seen in Figure 4-20. Notice that in the output, V_{LOAD}, there are portions of the graph that are straight across and that the output is of slightly smaller amplitude than the input. This is because of the forward voltage drop that was discussed previously. Because the current must flow through two forward-biased diodes, V_{IN} must significantly exceed two diode drops. This is not acceptable for the application at hand. If the voltage is not greater than two diode drops, then the diodes will not become forward biased and the current will be zero. Although for most applications a small diode drop would be inconsequential, for this particular case, a voltage drop of 0.6 V would cause the smallest detectable value to decrease by over 800 times (because the smallest detectable voltage from the circuit is 0.732 μV, see Figure 4-41). Therefore, it is important to use a full wave rectifier that not only rectifies the wave in the positive direction, but also causes no forward voltage drop. This can be done using op amps in addition to diodes.

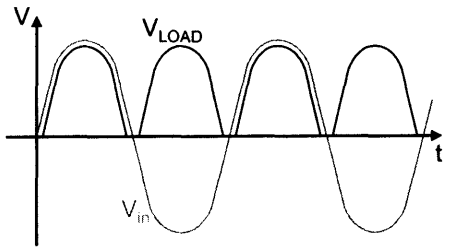

Figure 4-20: Input waveform to the positive full-wave rectifier of Figure 4-16 and the resulting load voltage.

An op-amp and a diode used in combination will remove the forward voltage drop. A general circuit that may be used to achieve this can be seen in Figure 4-21. In order to determine how this circuit works, an analysis of the negative and positive input cycles is necessary.

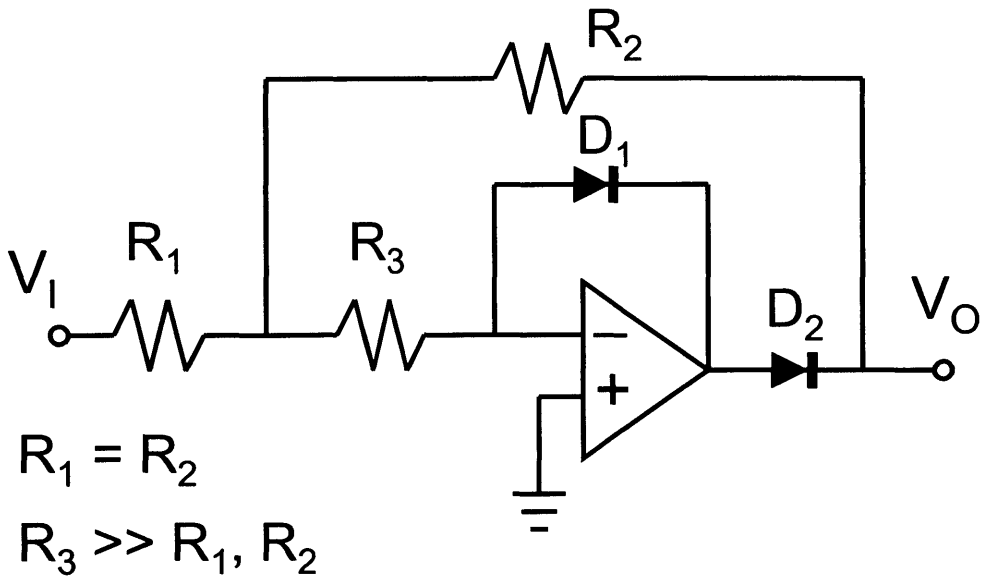

Figure 4-21: Positive full-wave rectifier with no diode forward voltage drop.

First, look at the positive input cycle, as seen in Figure 4-22. Under these conditions, diode D_1 is forward biased and the output of the op-amp will be equal to the diode drop in magnitude. The particular diodes used in the impedance circuit have a value smaller than 0.6V, they are:

$$V_{out} = - V_{\text{forward diode drop}} = - 0.41 \text{ V}. \qquad 4.42$$

Thus, diode D_2 is reverse-biased and the connection between the op amp output and V_O is open. Using Kirchoff's Current Law to analyze the node between R_1 and R_3, one gets:

$$i1 + i2 = i3 \Rightarrow \frac{V_I - v^*}{R_1} + \frac{V_O - v^*}{R_2} = \frac{v^*}{R_3}. \qquad 4.43$$

It is understood that the resistors R_1 and R_2 are equal, and also that R_3 is much larger than R_1 and R_2. In light of this, the right side of Equation 4.43 would seem to go to a very small number. If this is the case, then the difference between V_I and v^* is quite

small as is the difference between V_O and v^*. Thus, the voltage v^* can be thought of as being approximately V_I and approximately V_O. This shows that:

$$V_O = V_I. \qquad 4.44$$

It is also important to note that the forward-biased diode, D_1, does not have enough current going through it to necessarily cause the voltage to be as large as shown in Equation 4.42 .

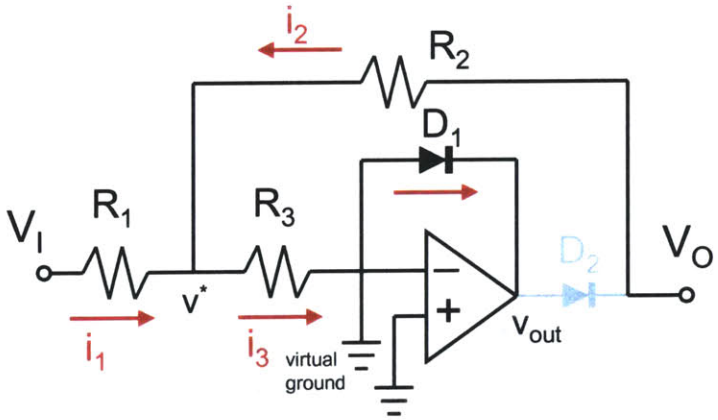

Figure 4-22: Positive input cycle of full wave rectifier.

The negative input cycle, seen in Figure 4-23, reveals that the explanation is actually simpler than that for the positive input cycle. With a negative V_I, the op amp output, v_{out}, becomes positive, and the diode D_1 is reverse biased and the diode D_2 is forward biased. The circuit will be shorted over R_3 and v^* will be held at ground since very little current goes through R_3. Use Kirchoff's Current Law to determine i_1 and i_2:

$$i_1 = \frac{-V_I}{R_1} \; ; \; i_2 = \frac{V_O}{R_2}. \qquad 4.45$$

The currents are equal to one another, therefore solving the equation for V_O gives:

$$V_O = -\frac{R_2}{R_1} V_I. \qquad 4.46$$

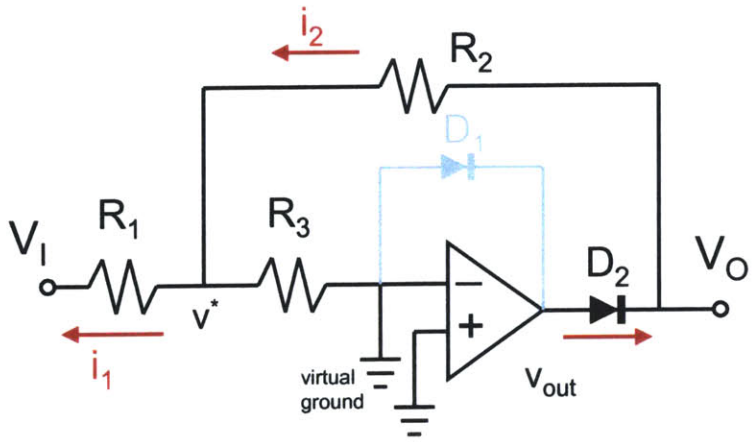

Figure 4-23: Negative input cycle of full wave rectifier.

The major advantage of this circuit is that the feedback loop is always closed via D_1 for positive input cycles and R_2 and D_2 for negative input cycles. Therefore the output will never be driven to saturation. Also, there are no diode drops in the result. Typical values for the resistors will keep R_1, R_2, and R_3 in the low noise range. Thus, choosing the following values will work.

$$R_1 = R_2 = 1k\Omega,$$
$$R_3 = 100k\Omega. \qquad 4.47$$

The output of this section of the circuit is simply the full wave rectification of the instrumentation amplifier output, see Figure 4-24.

Figure 4-24: Output from the full wave rectifier.

4.1.5 Low Pass Filter

The last part of the circuit is the low-pass filter. Now that the waveform is rectified, putting it through a low pass filter will help to keep the DC component intact

while wiping out any higher frequency noise issues or artifact spikes that tend to occur. Since a passive filter is impractical, as discussed previously, an active filter will be used.

The previous step full-wave rectified the waveform in the positive direction. Thus, the filter needed is a non-inverting low pass filter. The output from the analog portion of the circuit will be sampled at 4 Hz. The waveform in Figure 4-24 is oscillating at 1 kHz. This oscillation needs to be eliminated. A constant voltage coming out of the analog portion of the circuit with a constant depth of penetration in the skin is necessary. The needles will be moved into the skin at a rate of 10 μm/s. Accordingly, a cutoff frequency less than 2 Hz would be perfect for removing the 1 kHz components but keeping the movement of the needles. Before getting to the logistics of what values are necessary for the low pass filter, a discussion of the filter architecture is necessary (see Figure 4-25).

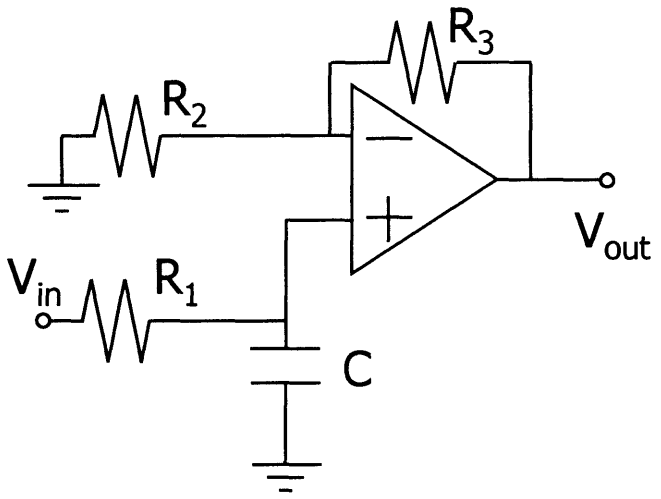

Figure 4-25: Active Low-Pass Filter.

The input signal will go through R_1 first, and any high frequency noise will be removed by the capacitor, C. The voltage drop over C will be equal to the voltage in the inverting side. Use the frequency spectrum and the values of impedance for the capacitor and the resistor to determine this voltage drop,

$$v_+ = \frac{\frac{1}{j\omega C}}{R_1 + \frac{1}{j\omega C}} V_{in} = \frac{1}{1 + j\omega C R_1} V_{in}. \qquad 4.48$$

Given that this voltage is the same as the voltage for the inverting input, the current through R_2 may be determined,

$$i = \frac{v_-}{R_2} = \frac{1}{(1 + j\omega C R_1) R_2} V_{in}. \qquad 4.49$$

This current goes through the resistor, R_3, to produce the output, V_{out}. Add the voltage at the inverting input to the op amp to the voltage drop over R_3 to determine the output voltage:

$$V_{out} = v_- + i * R_3 = \frac{1}{1 + j\omega C R_1} V_{in} + \frac{R_3}{(1 + j\omega C R_1) R_2} V_{in}.$$

$$= \frac{1}{1 + j\omega C R_1} V_{in} \left(1 + \frac{R_3}{R_2}\right) \qquad 4.50$$

As seen in Equation

4.50 , the gain is determined by:

$$Gain_{LPF} = 1 + \frac{R_3}{R_2}. \qquad 4.51$$

The other important value to know from this circuit, is the cutoff frequency:

$$f_{cutoffF} = \frac{1}{2\pi R_1 C_1}. \qquad 4.52$$

In the beginning of this subsection, an approximate value for the cutoff frequency was decided to be less than two hertz. This is a fairly small value, accordingly the first thing to decide would be the capacitor value. The largest value 0603 capacitor is 1 μF. By choosing the largest capacitor value, a resistor value can then be determined,

$$f_{cutoffF} = 2\text{Hz} \geq \frac{1}{2\pi R_1 \cdot 1\mu\text{F}} \Rightarrow R_1 \geq \frac{1}{4\pi \cdot 10^{-6}}\Omega \Rightarrow R_1 \geq 79.6\,\text{k}\Omega. \quad 4.53$$

Since the resistor needs to be 80 kΩ or larger, a value of 100 kΩ would work. This resistance will give a cutoff frequency of:

$$f_{cutoffF} = \frac{1}{2\pi \cdot 100\text{k}\Omega \cdot 1\mu\text{F}} = 1.59\,\text{Hz}. \quad 4.54$$

Now that a value for the cutoff frequency has been determined, determining a value for the gain of the filter will give the remaining resistance values. A nominal value of 100 Ω for 1 unit of output from the ADC of the microcontroller would give a reasonable amount of accuracy needed to determine whether or not the needles are penetrating the skin. 100 Ω was decided to be a good value since it will give a maximum value that is near that of when the needles are touching the skin, but small enough to detect small changes in impedance as the needles travel through the skin. The current going through the tissue, given in Equation 4.33 , is 9.64 μA. Thus, the minimum voltage that needs to be detected by the microcontroller is:

$$v_{min} = i_{LOAD} \cdot 100\Omega = 9.64\mu\text{A} \cdot 100\Omega = 0.964\text{mV}. \quad 4.55$$

Since the microcontroller can detect between 0 to 3 V with a 12 bit ADC, it gives a minimum voltage detection of:

$$v_{min} = \frac{3\text{V}}{2^{12}} = \frac{3\text{V}}{4096} = 0.732\,\text{mV}. \quad 4.56$$

Equations 4.55 and 4.56 give very close results, so no gain is needed in the low pass filter. For the configuration given in Figure 4-25, the typical value for R_2 is the same as R_1. With the knowledge that the gain needs only to be one, the value of R_3 is zero (by Equation 4.51). This simply implies that the feedback loop should be shorted.

The input into the ADC portion of the microcontroller is going to be a constant signal with amplitude slightly smaller than the value of the impedance of the skin multiplied by the load current.

4.1.6 Modifications

The analog portion of the impedance circuit is put together to give the complete architecture as seen in Figure 4-26. The circuit in Figure 4-26 was one of the first circuits used to test the impedance values of skin after first testing the circuit using resistors to see how the predicted response varied with the measured response. The values that were discussed in the preceding section are show in Figure 4-26. This shows how all of the different components are put together into one circuit.

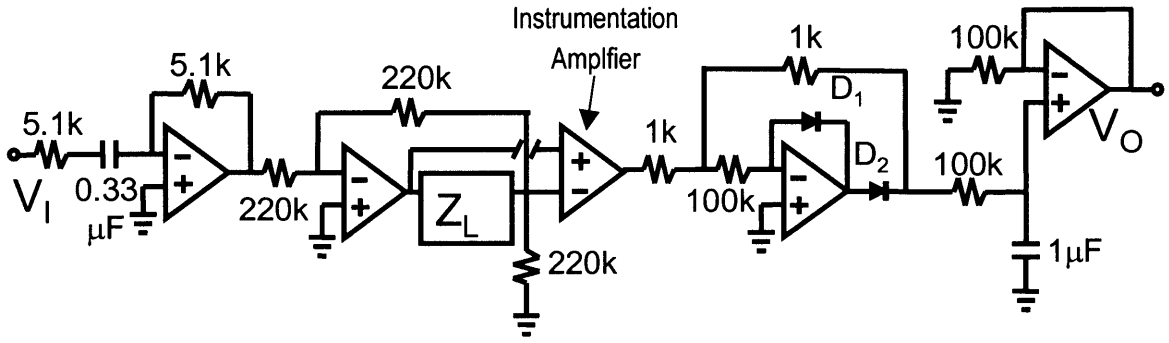

Figure 4-26: Analog impedance circuit with values.

After this circuit was complete, one small change was made which affects the last two components, the full-wave rectifier and the low-pass filter. In most applications, a low-pass filter will be inverting. In this case, that wouldn't be practical given that the full wave rectifier makes the wave positive and a positive voltage input is needed for the microcontroller. But, if the wave is rectified fully in the negative direction and then an inverting low-pass filter is used, that would remedy the problem.

Consequently, the last two components were modified. The modified portion of the circuit may be seen in Figure 4-27. A short discussion of how this portion of the circuit works follows.

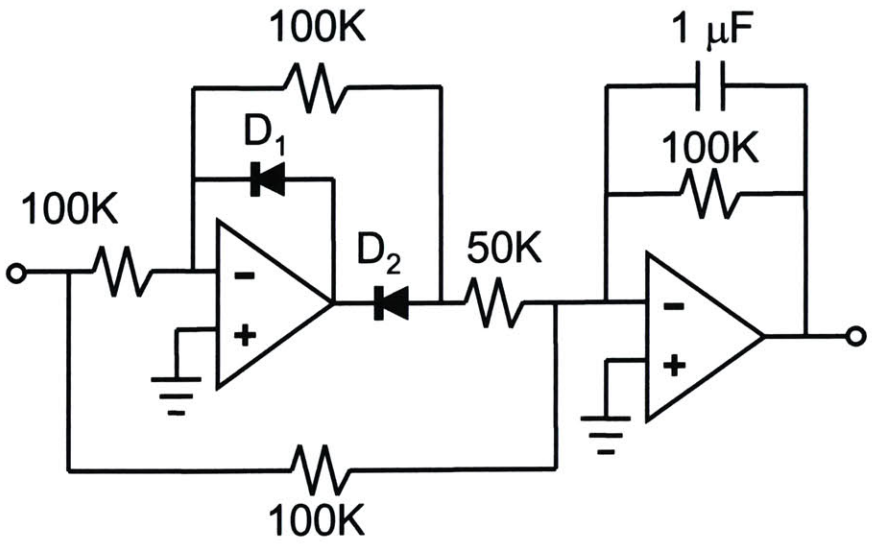

Figure 4-27: Absolute value circuit.

First, look at the positive input cycles. If a positive voltage is applied to V_{in}, as seen in Figure 4-27, what is going to happen to the output? The voltage V_{in} is applied

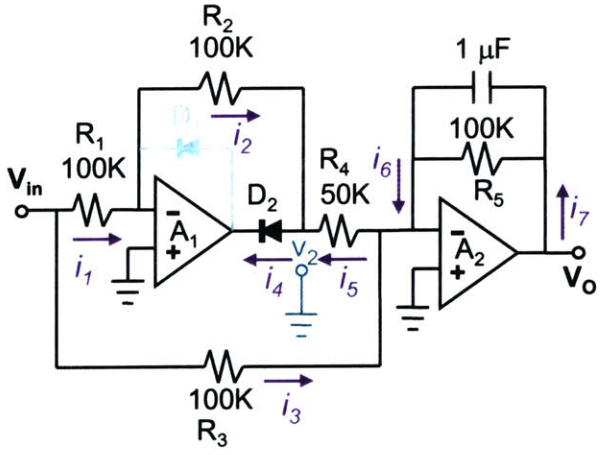

Figure 4-28: Positive input to the absolute value circuit.

over the 100k resistor, R_1, since the non-inverting input to A_1 is held at ground. Thus, the current going through the resistor is:

$$i_1 = \frac{V_{in}}{100k}. \qquad 4.57$$

This current will not go through D_1, but it will go through the 100k resistor, R_2, causing a voltage drop of V_{in} over that resistor. The voltage, v_2, is then:

$$v_2 = -V_{in}. \tag{4.58}$$

Knowing the value of v_2 shows that the current, i_5, is:

$$i_5 = \frac{V_{in}}{50k}. \tag{4.59}$$

Also, since the voltage drop over R_3 is known to be V_{in}, the current, i_6 can be determined by the knowledge of i_3 and i_5 using Kirchoff's Current Law,

$$i_6 = i_5 - i_3 = \frac{V_{in}}{50k} - \frac{V_{in}}{100k} = \frac{V_{in}}{100k}. \tag{4.60}$$

This current goes through the resistor and capacitor which are in parallel giving a positive output voltage,

$$V_O = \frac{i_6}{\frac{1}{100k} + j\omega \cdot 1\mu F} = \frac{V_{in}}{1 + 0.1 \cdot j\omega}. \tag{4.61}$$

For a negative input cycle, the circuit is somewhat simpler than the positive input cycle (see Figure 4-29). A positive input voltage will draw a current over resistor, R_1, and through the diode, D_1. No current is drawn through R_2 or R_4 since there is no voltage drop over the resistors (both inverting inputs are at ground). The voltage drop over R_3 is V_{in}. The current is then:

$$i_3 = \frac{V_{in}}{100k}. \tag{4.62}$$

This current goes through the resistor and capacitor in parallel. Since the current in Equation 4.60 is the same as the current in Equation 4.57 , and it's also going in the same direction, it will give the same voltage output as in Equation 4.58.

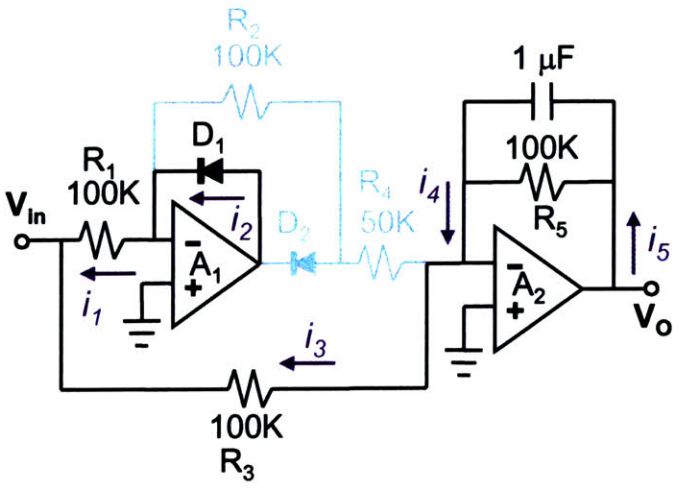

Figure 4-29: Negative input to the absolute value circuit.

4.2 Putting It All Together

Now that the above absolute value circuit has been shown to be equivalent to the full-wave rectifier in series with the low-pass filter, it will be substituted into the circuit. This allows the circuit to be simplified and uses a design which is easier to follow (the inverting form of the low-pass filter is more commonly used than the non-inverting form). The following circuit is the final product architecture for the analog side of the impedance tester (Figure 4-30).

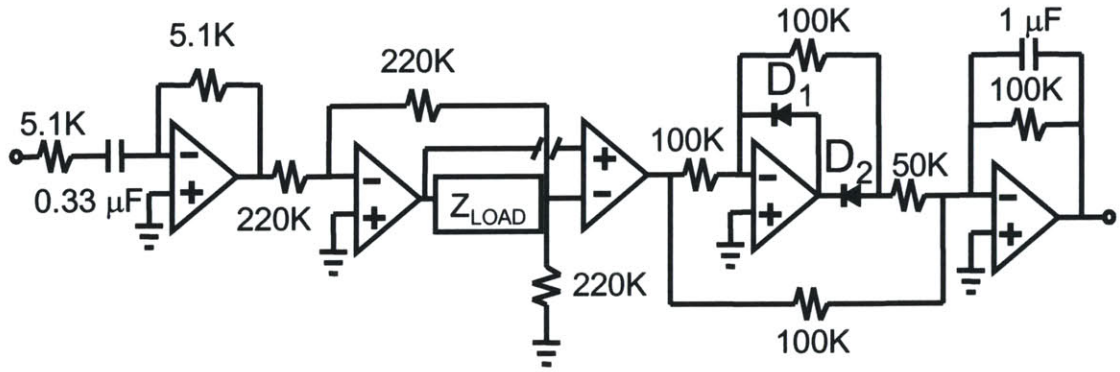

Figure 4-30: Improved analog impedance circuit.

4.3 Miniaturization and Component Selection

Now that the reasoning behind the architecture of the circuit is settled, there is the matter of the component selection. The components of this circuit have been

specifically selected for their particular purposes. There are five different types of components used in the analog portion of the circuit excluding the two different capacitors used to stabilize the power supplies (which basically adds only one more component to the list). The components will be discussed in order of physical size.

The resistors are all 0402 surface mount 1% thick film chip resistors manufactured by Yageo America (see Appendix C.1). The power level of the resistors is not significant for this application. The size and accuracy of the resistor is the primary reason that these resistors were chosen. They are 1.00 x 0.50 x 0.35 mm which makes them small enough to not take up too much room on the circuit board (Figure 4-31).

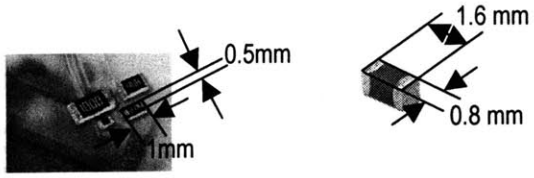

Figure 4-31: 0402 and 0603 parts.

The capacitors that are used are 0603 surface mount multilayer ceramic chip capacitors (see Appendix C.2). These capacitors are used because they are the smallest available for the capacitance value needed in the applications. They are 1.60 x 0.80 x 0.30 mm (Figure 4-31).

In the design of the circuit, there are two diodes used for wave rectification. The diodes used should be surface mount Schottky barrier diodes. Since the reverse breakdown voltage will never exceed 5 volts, it typically won't affect the diode selection. The forward voltage drop of the diode does not matter since it is used in conjunction with the op amp. Any typical value will be acceptable. Therefore, size and price are the major factors used for choosing the correct diode. Initially two SD101AWS diodes manufactured by Diodes Incorporated were used in the design. Although these diodes gave terrific results, the amount of space used up by two diodes was a bit excessive. Looking at the circuit one can see that these diodes have a common node at the output of one of the op amps. For one diode it is the anode and for the other it is the cathode. This configuration lends itself to be manifested by using one component, rather than two, in a dual diode with a series connection. In this situation,

there is very little difference in size when compared with price, so the less expensive series diode was selected. This is a Dual Schottky Barrier Diode in the SOT-323 package manufactured by Zetex Diodes (see Appendix C.3) with a footprint measuring no more than 2.2 mm squared.

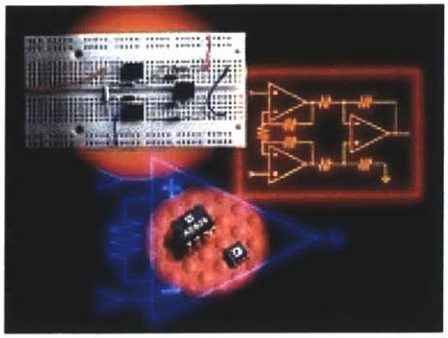

Figure 4-32: AD620 instrumentation amplifier.

The next component to consider is the instrumentation amplifier. Initially, an AMP02 by Analog Devices[1] was the selected component. This worked fine in the initial design. But, it doesn't come in a package any smaller than an eight pin DIP package. An improved instrumentation amplifier that comes in a surface mount package, the AD620, also by Analog Devices, was the selection used for this circuit (see Appendix C.4). The AD620 comes in three different packages. In the final design, the SOIC 8-pin package was used which covers an area of about 5 mm by 6 mm (Figure 4-32).

The last component in the design is the op amp. The initial design of this circuit involved using all LT1007 op amps[23]. There are four op amps used in this circuit, and in the spirit of saving space, using a quad op-amp where there are four useful op amps on one chip, would be a wise decision. For that reason, the LT1885 is a quad op amp which fits all of the qualities that are needed for the application (see Appendix C.5). It covers an area of about 6 mm by 8.6 mm.

These above components are all fairly inexpensive and will easily fit into a space of 30mm x 15 mm at this point. On the next design iteration that area can easily be made smaller. To see some of the more frequently used specification sheets, refer to Appendix C: Data Sheets

4.4 Digital Circuit

The digital end of the circuit was primarily programmed and debugged by Johann Burgert. There are three main components to the digital end of the circuit. The microcontroller is also used for other applications of the drug delivery system. This microcontroller (see Figure 4-33) needs to be driven by an oscillator and it also needs an RS-232 receiver/driver for computer communication. These are the three major hardware components in the digital circuitry (aside from the computer). The software written for this application by Martin Labrecque takes the data from the RS232 port and puts it into a text file. The data is collected at a rate of 4 Hz and is translated into a file where each line is a number between 0 and 4095 representing each unit of the ADC output from the microcontroller. The data is further manipulated to represent the impedance of the load that the current is moving through.

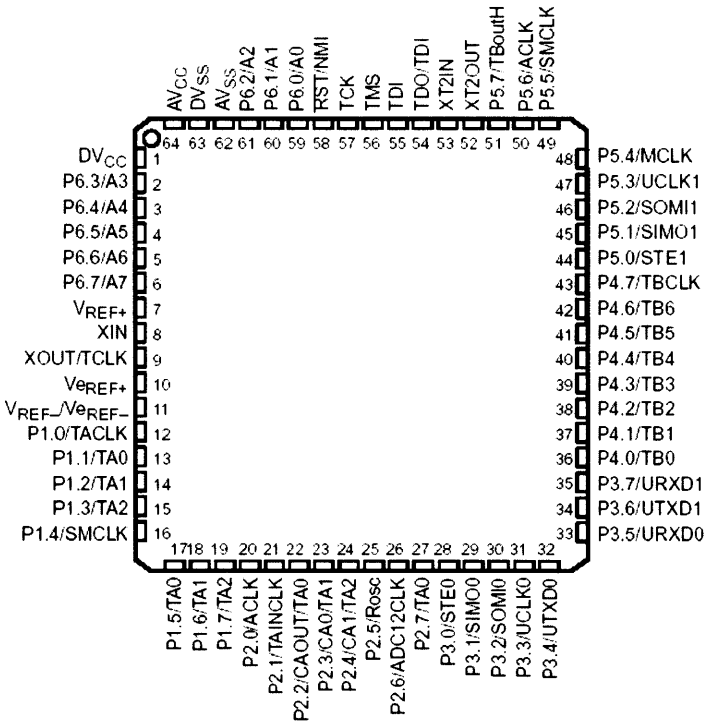

Figure 4-33: Texas Instruments MSP430F149 Mixed Signal Microcontroller.

The Texas Instruments MSP430F149 Mixed Signal Microcontroller is 12 mm by 12 mm, quite small considering what it can do. There is a low supply-voltage range, from 1.8 to 3.6 V. For the application at hand, it runs off a three volt button battery.

The driver/receiver, which is a separate component, allows the microcontroller to interact with a computer. At this point it allows the operator to collect data from the impedance circuit to analyze what happens when the needles go into skin. The 12 bit ADC takes in the data from the analog circuit and converts it to digital form to send to the computer. The data that comes through to the computer is a number between zero and 4095, which represents a unit measure from the 12-bit microcontroller ($2^{12} = 4096$). The battery supply is three volts, consequently the maximum detection of the ADC is three volts. This means that the minimum value that can be detected is:

$$V_{min} = \frac{3V}{2^{12}} = \frac{3V}{4096} = 732\,\mu V. \qquad 4.63$$

Even though this is mathematically the minimum detectable voltage level, it's important to note that because of nonlinearities and noise, the actual minimum detectable voltage is not this small, it will more likely be 1.4 mV since there is 1 LSB of noise in the microcontroller. Relating this to the minimum detectable impedance level, just take the above voltage and divide by the current that runs through the load:

$$Z_{min} = \frac{732\mu V}{9.64\mu A} = 75.9\,\Omega. \qquad 4.64$$

After that, the ADC in the microcontroller takes this information and transmits it to the line driver/receiver which in turn sends the information to the RS-232 port of the computer.

There were several choices for the RS-232 line driver/receiver which allows the output to go to a computer. This component is needed in this iteration of design, but for the final product, the microcontroller will be programmed and it will not need to communicate with a computer. Initially, the MAX233A[28] was used in a breadboard configuration (Figure 4-34), but since noise was a problem, this needed to be switched out for a smaller version that could be mounted to a PCB. Since the MAX233A is not readily available in a smaller size, it became necessary to find a good surface mount component that had the necessary features (Figure 4-35).

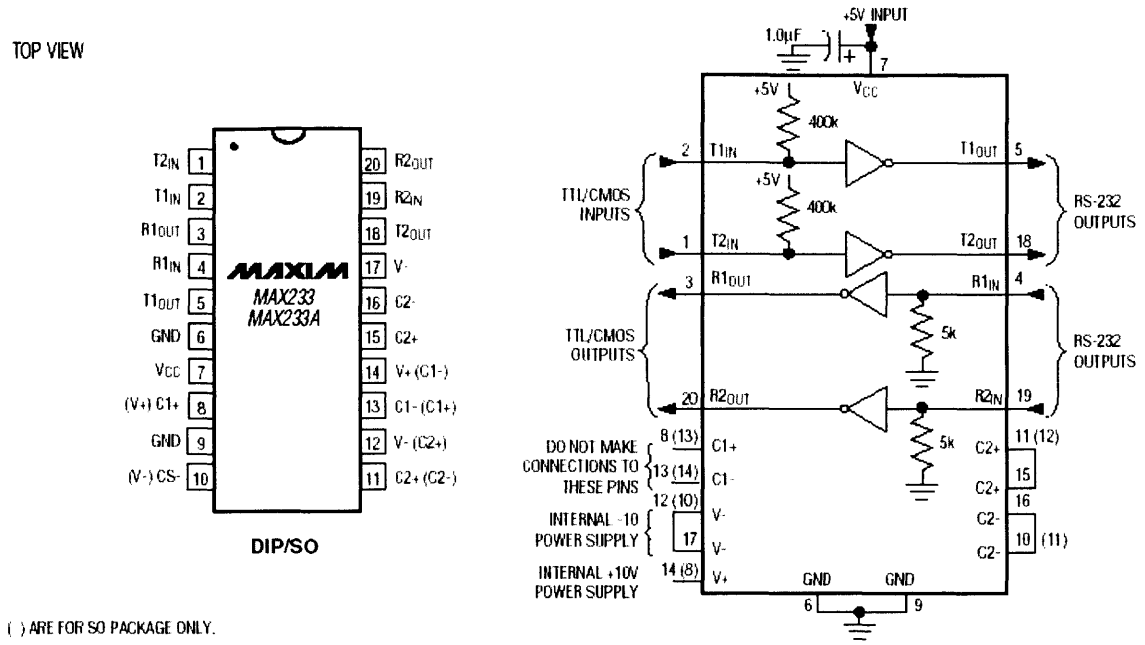

Figure 4-34: MAX233A package outline.[28]

Part Number	Power Supply (V)	No. of RS-232 Drivers/Rx	No. of Ext. Caps	SHDN & Three-State	Data Rate (kbps)	Features
MAX233A	+5	2/2	0	No	200	No external caps, high slew rate

Figure 4-35: MAX233A data.[28]

The MAX3235E was selected. The main factors used in choosing a dual transceiver were: (1) it should run from a three volt button battery source, (2) it should have no external capacitors (this just adds more components generally implying that more room will be needed), (3) it should have at least one driver and one receiver, (4) it needs to be small, (5) it should be inexpensive. These characteristics were all fulfilled with this model. It should be noted that there are very few of these types of devices that only have one driver and one receiver, and they are not as space conservative as this one selected here.

The last component used on the digital side is the oscillator. The microcontroller is programmed to run off a 4 MHz clock, thus the smallest economical

oscillator that has a high frequency output and can run off of three volts will work. The final chosen design incorporated the Epson Electronics America Surface-Mount Quartz Crystal SG-636PCE Oscillator.[11]

4.5 Final Layout

Now that all of the architecture and components of the circuit are decided, it is time to think about manufacturing the printed circuit board (PCB). There are four software programs used to bring this circuit to fruition. Each of these programs and its function in the completion of the circuit will be discussed below.

ViewDraw is used to draw up the circuit layout.[20] Using the circuit in Figure 4-30 as a guideline and the information from the data sheets the circuit is designed in ViewDraw. A similar circuit to the one designed in ViewDraw can be seen in Figure 4-36 (the ViewDraw circuit is in Figure 4-38). The pin layout from the datasheets are entered for each component symbol and added to the complete board. The major components that are added in this Figure that aren't in Figure 4-36 are the two bypass capacitors which connect each power supplies to ground. The 0.1 μF capacitor is a ceramic 0402 capacitor. The 10 μF capacitor used is a tantalum capacitor which is approximately the size of an 0603.

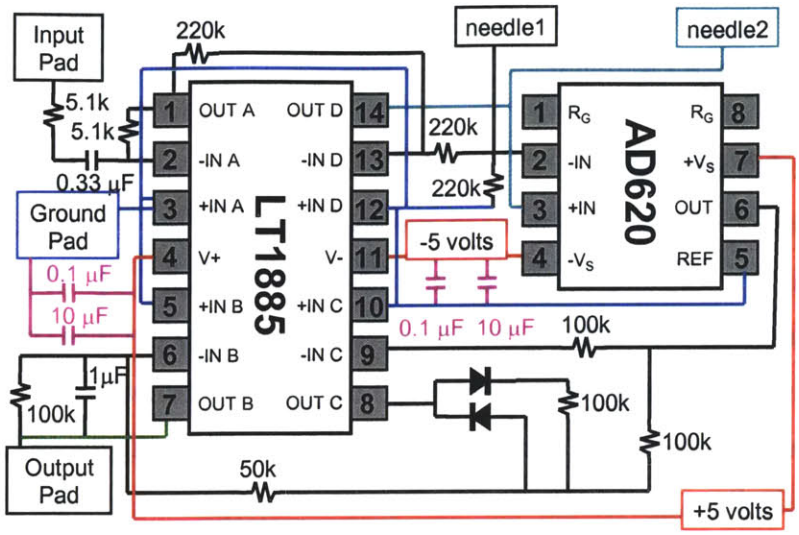

Figure 4-36: Analog layout for the impedance circuit (some of the lines are color-coded for easier viewing). The impedance value is measured between needle 1 and needle 2.

The digital components should also be placed on the same PCB for noise reduction. In the ideal case, there would be ground and power planes for the circuit, which would also reduce noise, but instead, large ground and power traces will be used. In this case, the circuit should only use one side of the PCB to avoid adding too many layers to the final design.

The final layout for the digital end of the impedance circuit is shown in Figure 4-37. The layout was determined by studying the pin outs in the data sheets that are in Appendix C: Data Sheets

. The output from the digital side is attached to the input on the analog side. Likewise, the output from the analog side is the input to the digital side.

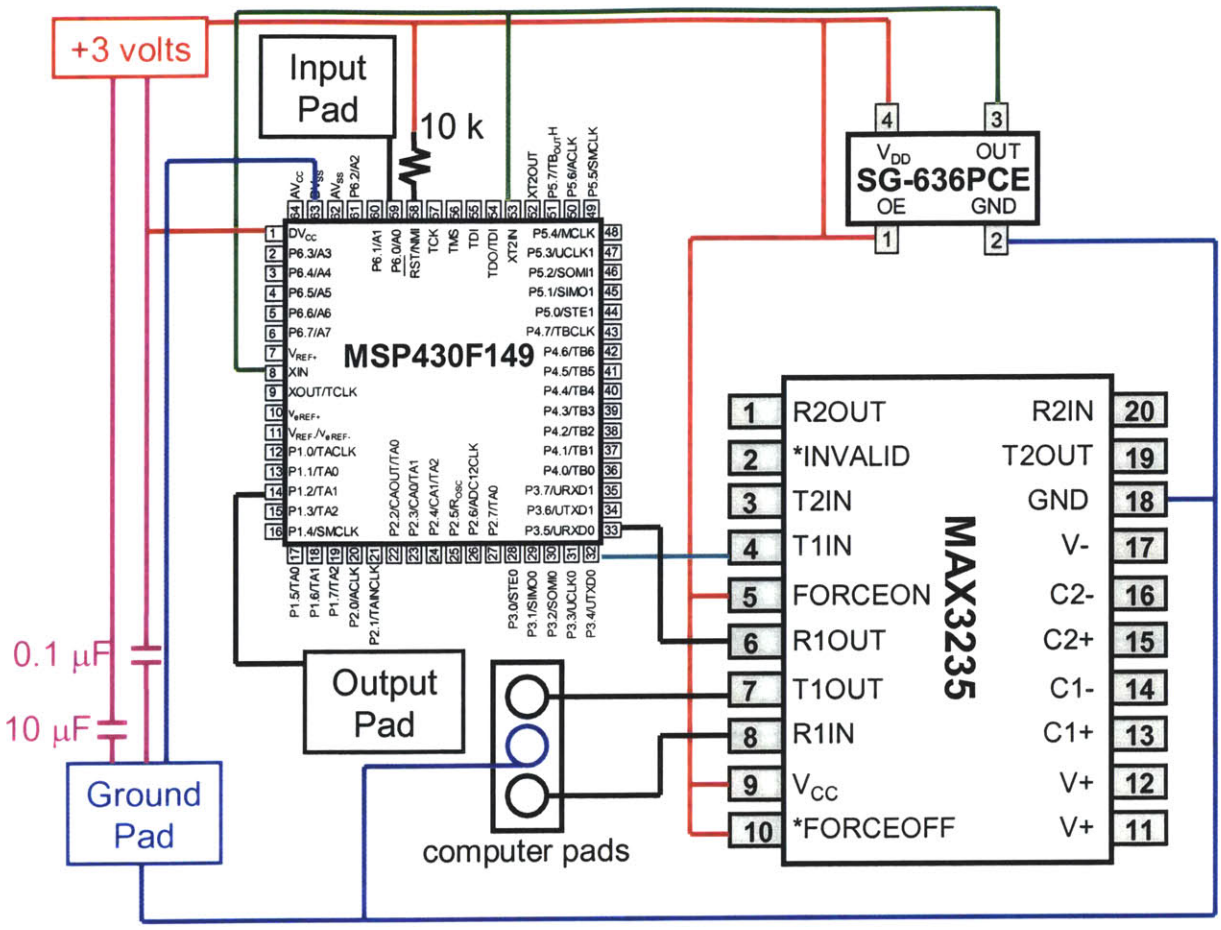

Figure 4-37: Digital layout for the impedance circuit (some of the lines are color-coded for easier viewing).

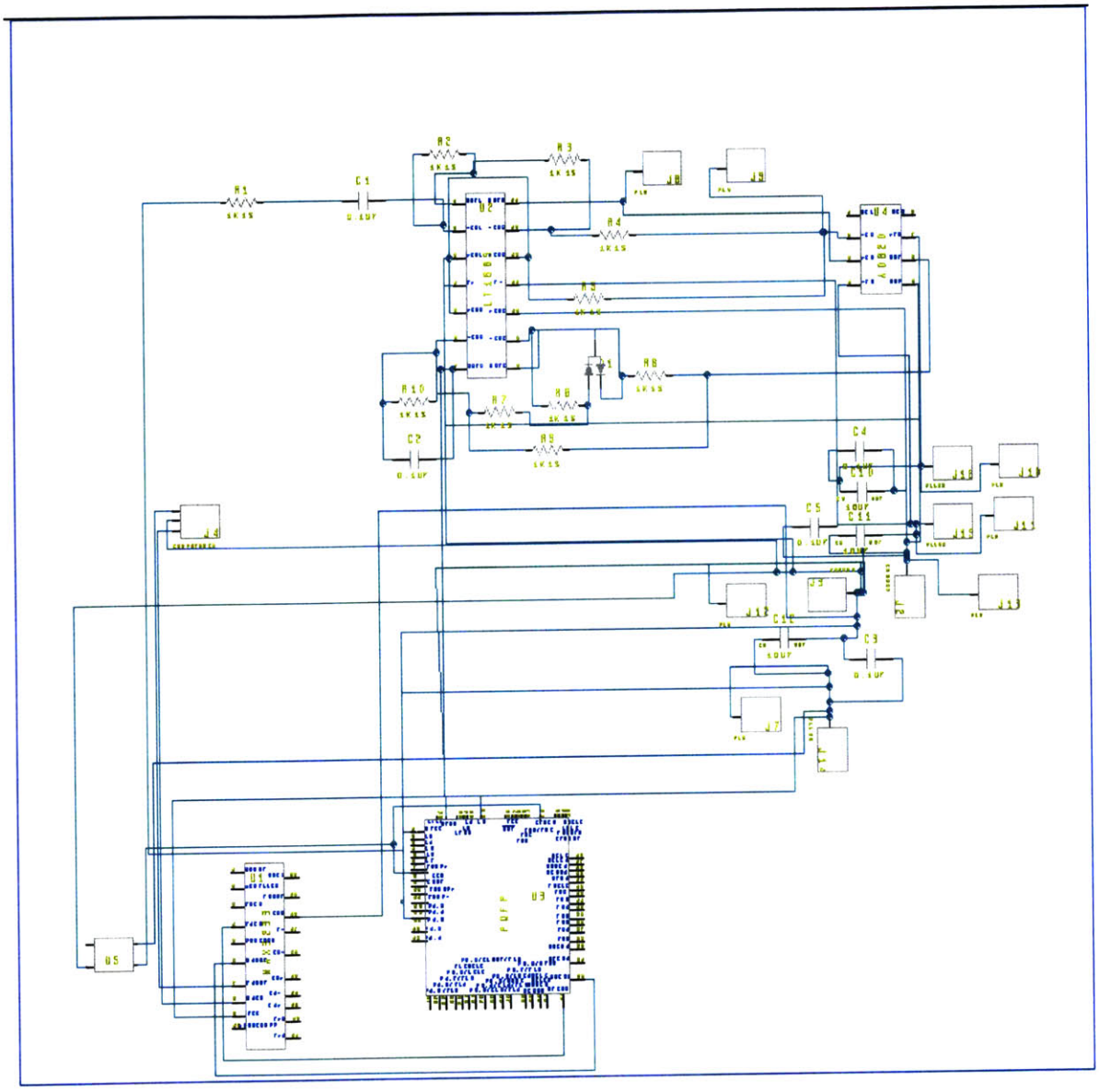

Figure 4-38: Full circuit layout in ViewDraw.

The physical layout of the circuit is done in Allegro. The challenge here was maneuvering the components and traces so that everything would fit onto one side of the board. Since this couldn't be done all on one side of the board including all the traces, some jumpers were used to facilitate this.

CircuitCAM3.2 is the program that is used to select the tooling to be used on the circuit. There were four basic tools used to cut out the circuit board. A drill is used to make the through holes. The pads and traces were cut using

one of two Universal Cutters, either the 0.4 mm or the 0.8 mm size. The 1.5 mm diameter Contour Router cuts out the circuit board.

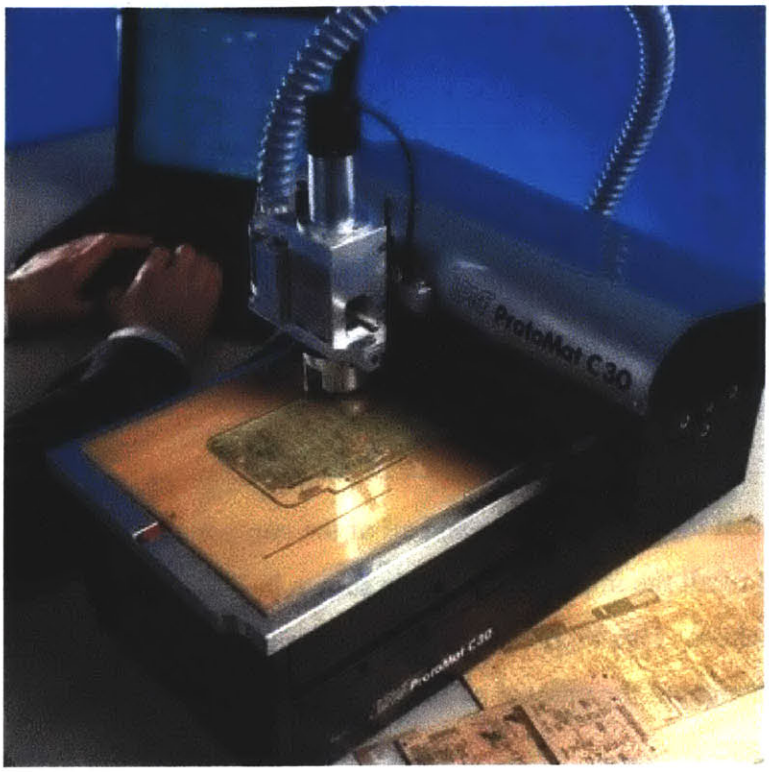

Figure 4-39: LPKF rapid PCB prototyping machine.

BoardMaster4.0 is the program that is used to control the LPKF. The LPKF is the machine that cuts out the PCBs (see Figure 4-39).

Once the PCB is complete on the LPKF, the components are soldered onto the board using the Air Pencil. The soldering paste is in a syringe and is put on the component on the pad to which the component will be soldered. If the pads are larger than a couple of millimeters in diameter, it is much more difficult to solder. Once the paste has been dispensed, the Air Pencil, which is basically held like a pencil, blows heated air out, and the operator can hold onto it over the soldering paste. This allows the person soldering to have more freedom in holding the component while soldering but is generally only good for small components. The larger components are soldered on using a typical soldering iron. The final circuit can be seen in Figure 4-40.

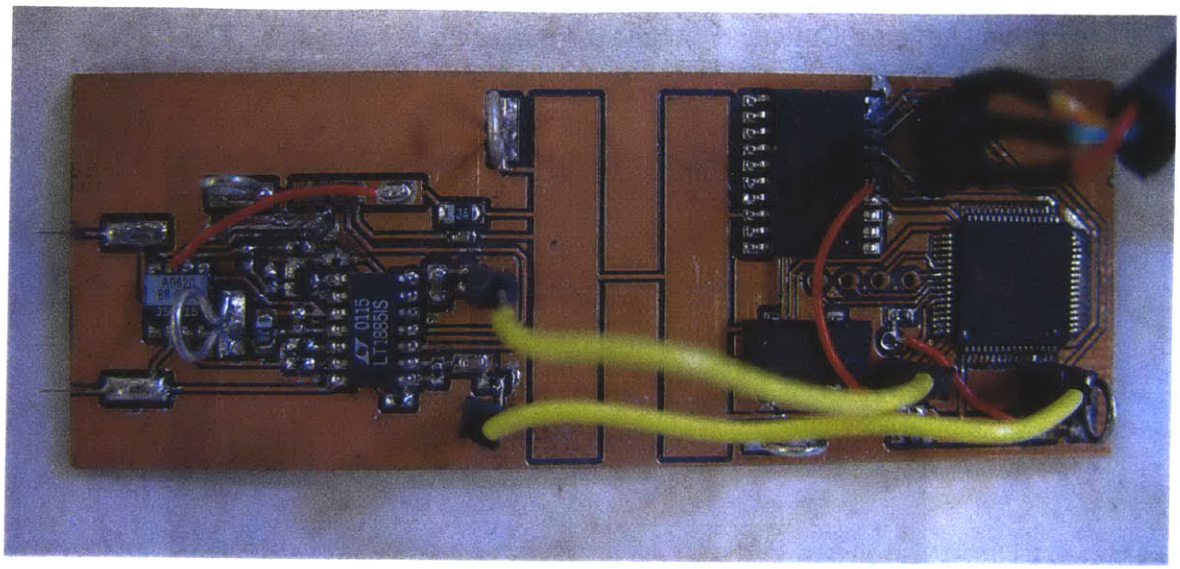

Figure 4-40: Final circuit with components.

Now that the circuit is done and all of the components have been selected, an organized list of all the important values is shown in Figure 4-41; the impedance circuit specification sheet. This Figure sheds light on the important values that are commonly referred to throughout the process of testing.

LP 2002 - Impedance Circuit Specifications

Input Parameters

Analog Side

Parameter		MIN	TYP	MAX	UNITS
V+	positive power input	+5	+5	+15	V
V-	negative power input	-15	-5	0	V

Digital Side

Parameter		MIN	TYP	MAX	UNITS
V+	power input	+1.8	+3	+3.6	V

General Parameters

Parameter		VALUE	UNITS
B	number of bits in the ADC	12	bits
	units of resolution	4096	units
I_{LOAD}	current through skin	9.642	μA
V_{MIN}	minimum voltage detection	0.732	mV
V_{MAX}	maximum voltage detection	+3	V
Z_{MIN}	minimum impedance resolution	75.9	Ω
Z_{MAX}	maximum impedance	311	kΩ

Figure 4-41: Specification sheet for the impedance circuit.

Chapter 5: TESTING AND RESULTS

Several different models for this circuit were tested before completing the final design and testing it on tissue. Even during the iterations, it was tested on tissue and problems with the different designs were discovered. This chapter overviews the basic routine used in testing the circuit to make sure that everything is running properly and finally goes through the protocol for testing the circuit on tissue and the results that were discovered.

5.1 Iterations for Testing the Circuit

Once the design was complete (see Figure 5-1 for initial design of the analog circuit), the analog portion of the circuit was tested on a solderless breadboard. Here, four discrete LT1007 op amps and one AMP02 instrumentation amplifier along with metal film resistors and polyester capacitors were designed to make sure that the proper response was elicited when different impedances were on the load. The input to the circuit came from a function generator and initially the testing was done with a sine wave of amplitude three volts and frequency one kilohertz. Once the circuit elicited the predicted response it was tested with a square wave of the same parameters.

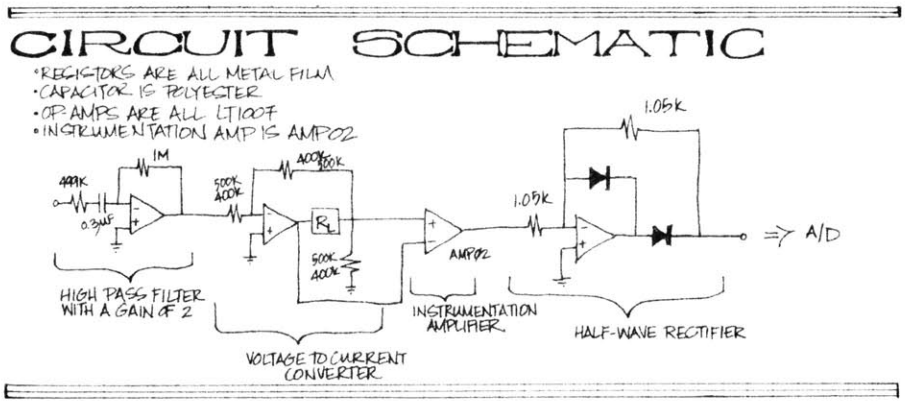

Figure 5-1: Initial design for the analog portion of the impedance circuit.

The circuit in the breadboard was also tested on in vitro pigskin to check the parameters and make sure that there was a response when plunged into skin (see Figure 5-2). This representation is rather crude and noisy, hence no quantitative data was taken

from this initial experiment. But, it did exhibit a drop in voltage output with increasing depth into the skin, which is the expected result. The predicted drop is three orders of magnitude, and the resulting drop seemed to be of that order.

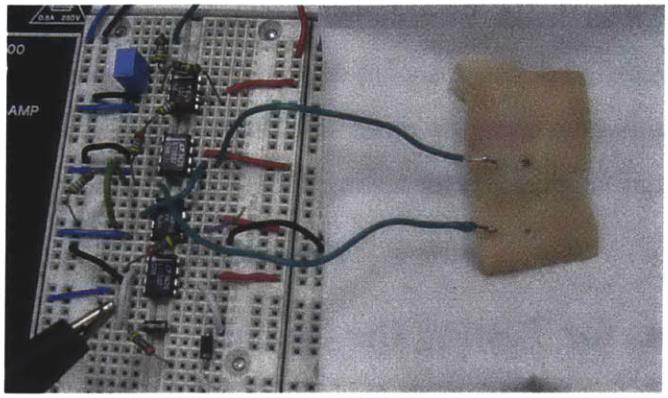

Figure 5-2: First analog iteration of the circuit being tested on porcine skin tissue.

To get an idea of how the circuit works, Figure 5-3 shows the flow of data and how the different segments relate to one another. Although this is a very simplified view of the whole schematic, it gives the general idea of how the components interact.

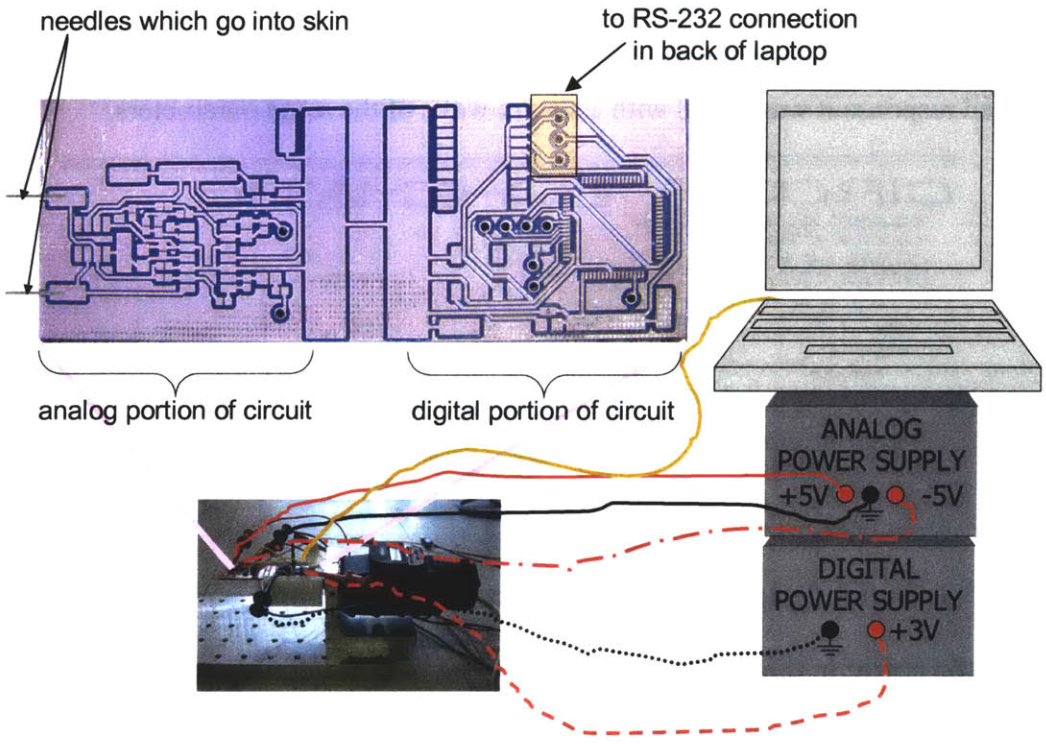

Figure 5-3: Circuit layout with components used.

After the design was tested and working, the traces and pads were laid out on a PCB (see Figure 5-4) to which the components were soldered. The details of this have been previously described. At this

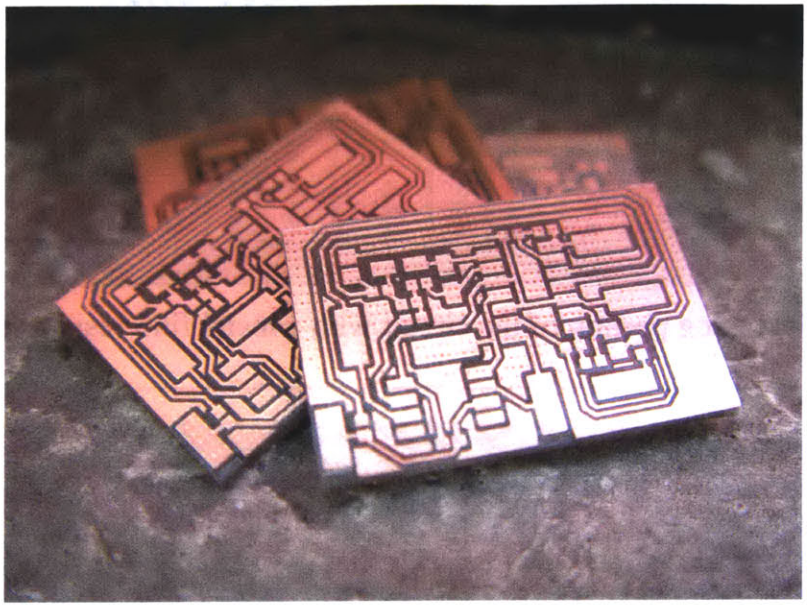

Figure 5-4: First design for analog portion of the circuit on a PCB (components not soldered to the board).

point, the analog portion of the circuit is on the PCB, but the digital portion of the circuit is on a breadboard. This allowed the circuit to be tested with the new surface mount components (see Figure 5-5). But, the noise due to the breadboard and lack of bypass capacitors was approximately three bits, much too large to get concrete results. Thus, it was important to integrate all of the components for both the digital and analog portion of the circuit onto one PCB (see Figure 5-6). Once all the components were put onto one PCB, the noise levels attenuated greatly.

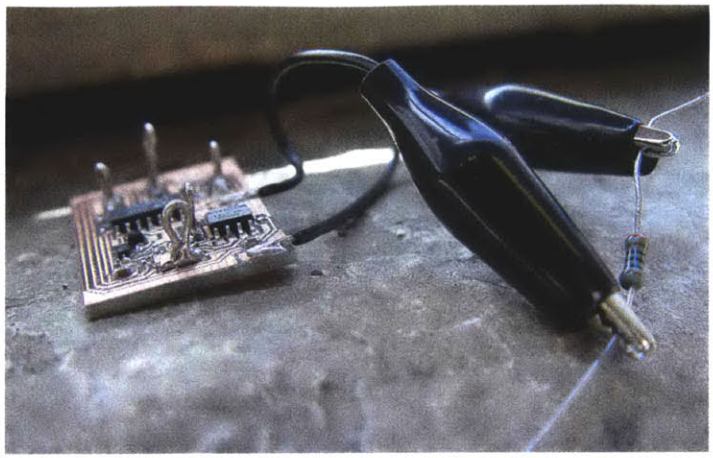

Figure 5-5: Analog portion of the circuit with a metal film resistor across it's leads.

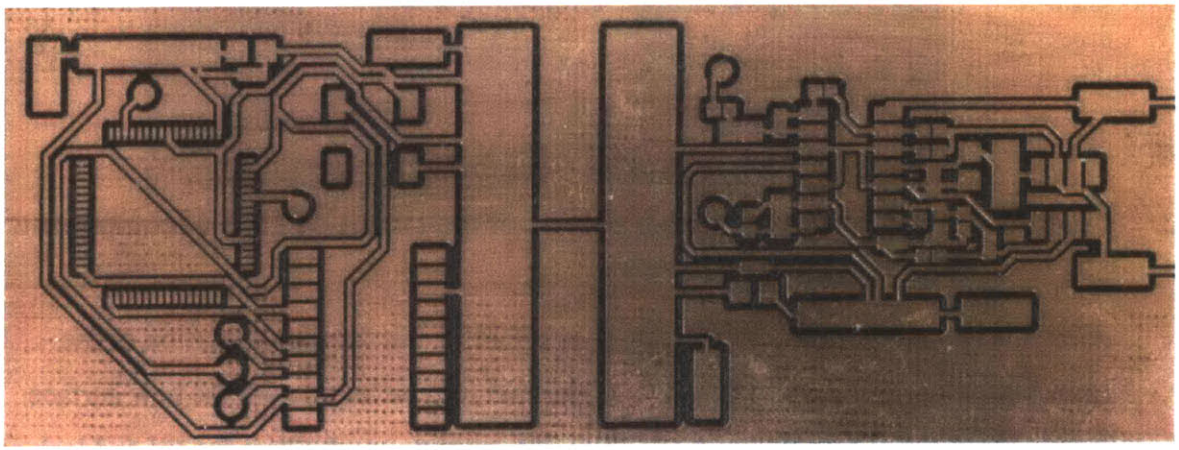

Figure 5-6: Printed circuit board for the digital components (left side) and analog components (right side) separated by a large ground pad; the components have not yet been soldered on.

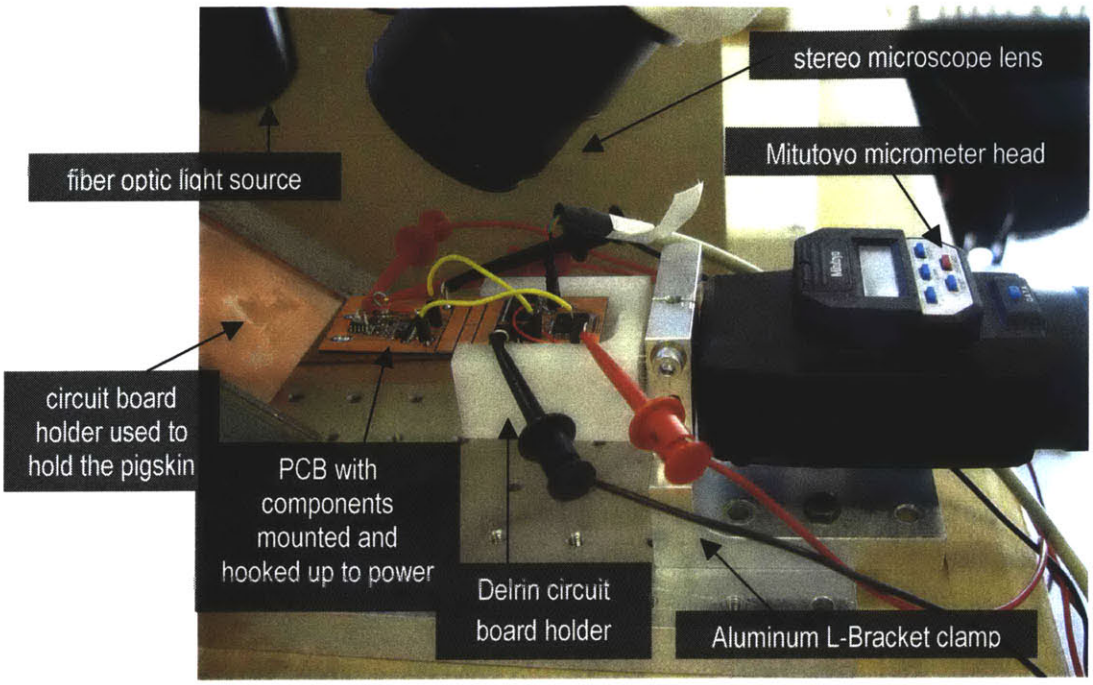

Figure 5-7: Set-up for pigskin testing.

Before testing the circuit in tissue (the set-up can be seen in Figure 5-7), testing the circuit using resistors was done so that the performance of the circuit could be measured. The method of testing was to attach several different resistor values across the leads and measure the output voltage. The output voltage cannot exceed three volts (the impedance equivalent to 311 kΩ). Any impedance values above 311 kΩ cannot be detected. The last two points on Figure 5-8 fall into this category of being too large to be detected. This is apparent by the drop off from the predicted values towards the larger numbers in Figure 5-8. The trend for the predicted impedance values versus the real values is accurate enough to start testing on pigskin.

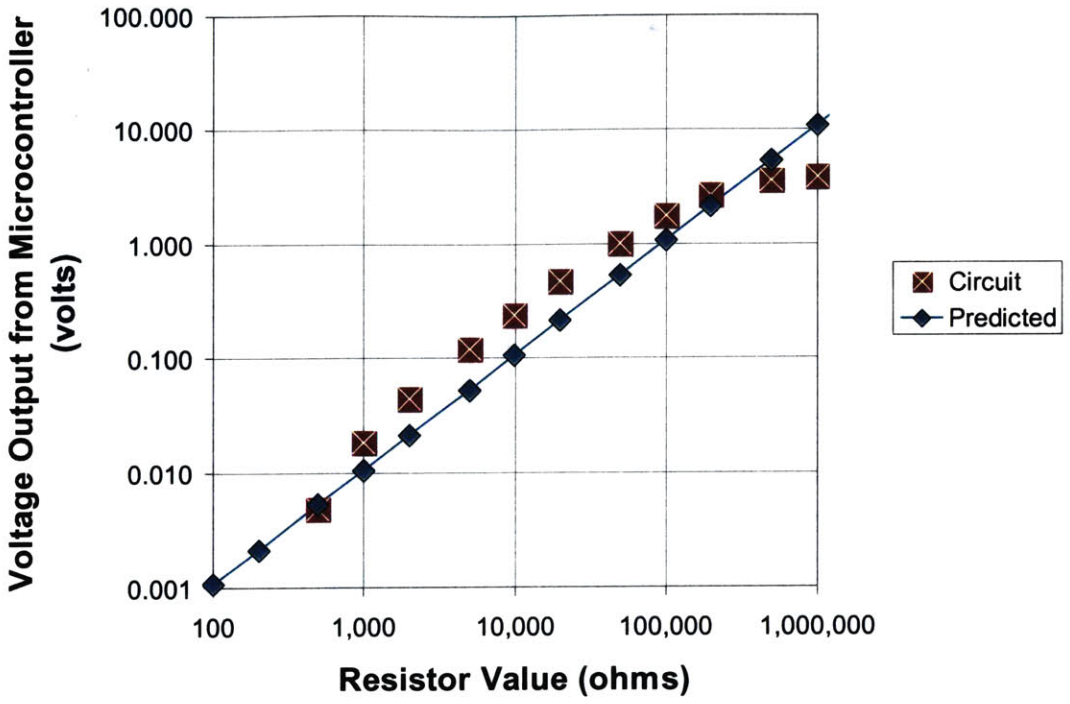

Figure 5-8: Circuit testing using resistors.

5.2 Final Results

After the circuit was tested using different valued resistors and the results were acceptable, pigskin was tried with the needle configuration seen below in Figure 5-9. The pigskin is on a stand which allows it to be positioned in two axes so that the needles will touch the skin at the same time. A stereo microscope is also included in the set-up which allows the operator to line up the needles more precisely (see Figure 5-7 for an overall view of the set-up). The needles were then plunged into the skin and the resulting impedance values measured. The micrometer to which the circuit is attached allows the operator to move the needles in the horizontal plane by as little as 1 μm. The results from initial testing are shown in Figure 5-10.

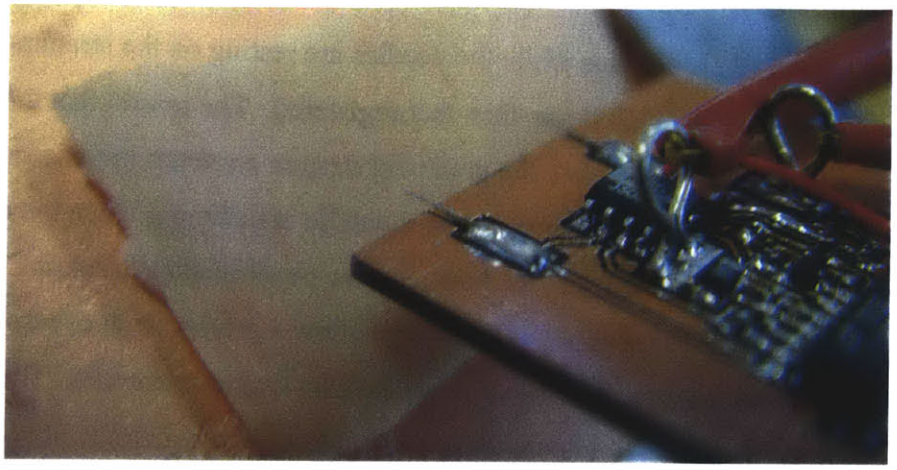

Figure 5-9: Needles going into pigskin.

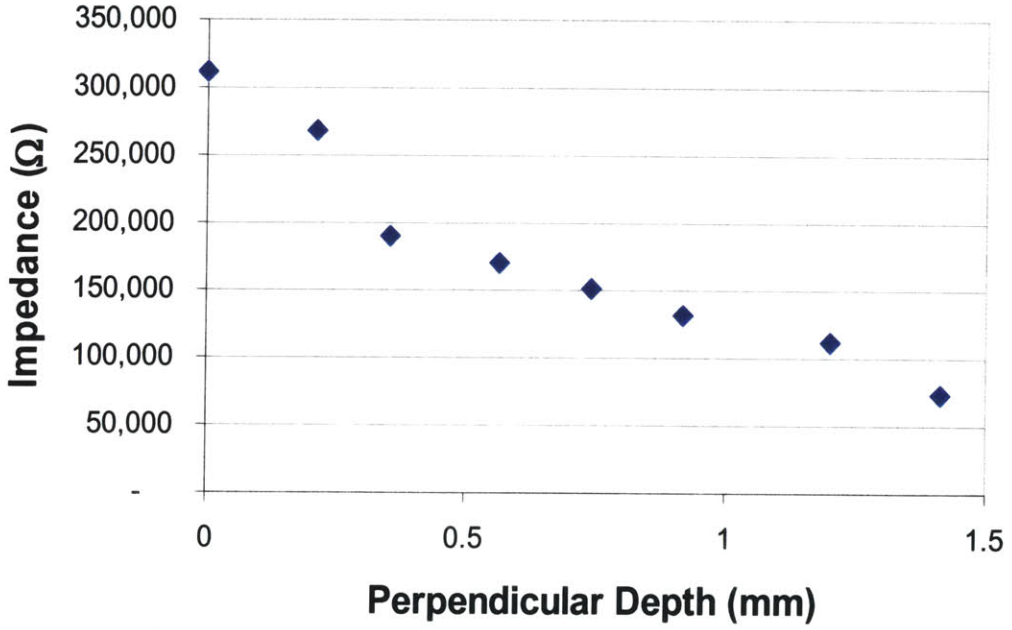

Figure 5-10: Results from impedance testing into pig shoulder skin – averaged values for approximate depth of penetration.

The values in Figure 5-10 are supportive of the earlier conclusions that the further the needles penetrate into the skin the smaller the impedance will be. The numbers at this point aren't precise enough to conclude what the changes are with respect to the different skin layers, but it does seem that there is quite a large drop between what could be the epidermis and the dermis or else the dermis and subcutaneous layer. Again, it is important to keep in mind that the upper bound of the

impedance detection is 311 kΩ, thus while the needles are resting on the stratum corneum, the actual value is much larger than that registered. The reason that the maximum value is set to a value below the predicted stratum corneum impedance value is because the interest of this project does not so much lie in detecting when the needles have touched the skin, but rather when the needles have penetrated the stratum corneum. Using a smaller value as a maximum will allow a greater level of resolution in detecting changes once the needles have penetrated the stratum corneum. There are several solutions to this issue. If it becomes important to resolve when the needles do touch the stratum corneum, then minimal adjustments need to be made. Simply changing out the resistors in the voltage-to-current converter in order to decrease the current going through the skin will allow detection of a larger impedance value. This does come at the expense of resolution for the circuit. Another solution to this issue would be to include a logarithmic circuit. But, since this would cost too much money (approximately $70), and the goal of this circuit is to make it inexpensive, this would not be a practical solution.

Further testing can be seen in Figure 5-11. More values were taken and at smaller distances apart. All points are plotted on this graph. The larger points represent the mode of the numbers for each different depth of penetration. There are several things that should be noted about this graph. First, there are points of zero impedance at many different depths of penetration that register. Typically what happens is the impedance jumps down to zero for one to three samples, and then it will jump back up to the value indicated by the mode. So, if the microcontroller can register four or more samples at two consecutive data points, then that will be enough information to determine the depth of penetration into the skin.

Something else to note about this graph is that the data points going into the skin and those coming out of the skin do not match up, especially at more shallow depths. There could be many reasons for this. One reason might be that the skin is not in vivo and therefore not as elastic as it might be if it were alive. So, perhaps the needles are going into the skin and stretching it out, but it doesn't have the elasticity to recover and the needles aren't in contact with the skin when they're pulling out. This could also

happen with skin in vivo and would take some experimentation to determine if this is or is not the case.

There are also areas on this graph that have a steep slope and other areas where the slope is rather flat. These areas might indicate changes in the structure of the skin, and if they are somewhat repeatable from test to test, they may hold clues to the configuration in the skin at different depths.

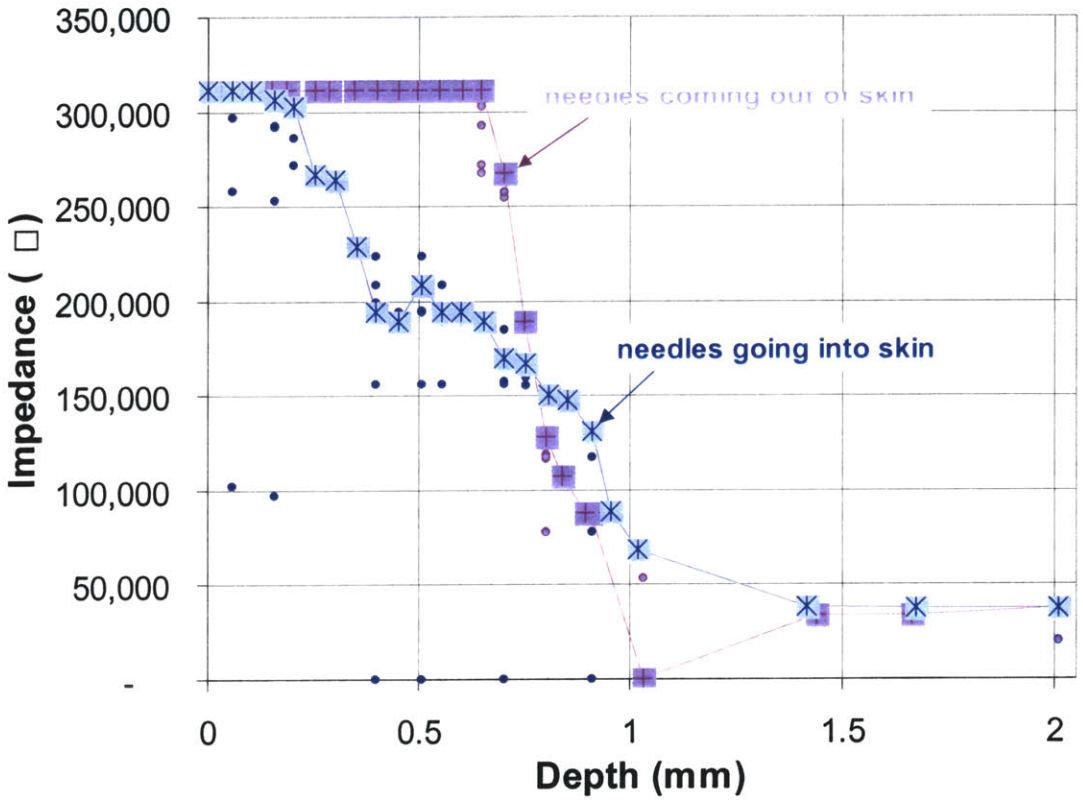

Figure 5-11: More results from impedance testing into pig shoulder skin – needles going into skin and needles being removed from skin to an ultimate perpendicular penetration depth of approximately 2 mm. The large squares represent the mode of the numbers from a sample size of approximately 90 samples per distance.

Since there seems to be a correlation between the depth of needle penetration and impedance value, this should be a useful method for determining how far the needles penetrate into the skin.

5.3 Future Tests

Now that the testing has been done on excised pig skin, testing on in vivo human skin is the next step. It would be important to determine if the tests are repeatable and if the impedance values change from person to person or even if they change with the same person in different environmental conditions. One would expect the impedance values to be lower if the skin was moist, for example. It would also be beneficial to determine how much these changes vary to see if impedance is an accurate method to determine depth of penetration of microneedles into skin.

More important than depth versus impedance, for this application, is the question of tissue structure and its relationship to impedance. If the dermis has a vastly different impedance level than the stratum corneum that will produce repeatable results from subject to subject, than that would be vastly important in the realm of drug delivery.

There may also be applications where drug dissipation versus impedance might be useful. This would be another possible subject for future testing.

Since the impedance measurements tend to follow the same form when using different tissue samples, it will be interesting to see how the porcine tissue relates to human tissue. It will also be quite fascinating to determine the variation from subject to subject at different sites in the tissue. If the impedance values at the dermis, for example, are within an order of magnitude from subject to subject, this impedance circuit could prove to be a very useful device in the medical field.

REFERENCES

1 Analog Devices. High Accuracy 8-Pin Instrumentation Amplifer AMP02. Rev. D. Norwood, MA: Analog Devices, 1999.

2 Analog Devices. Low Cost, Low Power Instrumentation Amplifier AD620. Rev. E. Norwood, MA: Analog Devices.

3 Angel A. B. A controllable, nano-volumetric, transdermal drug delivery device. Cambridge, MA: Massachusetts Institute of Technology, 2002.

4 Association for the Advancement of Medical Instrumentation. AAMI Standards and Recommended Practices (pages 87-97). Arlington, VA: Association for the Advancement of Medical Instrumentation, 1992.

5 Boyce W. E. and DiPrima R. C. Elementary Differential Equations and Boundary Value Problems, Fifth Edition. New York: John Wiley & Sons, 1992.

6 Cadence: Allegro. www.cadence.com

7 Carr, J. J. Safety for Electronic Hobbyists. Popular Electronics, October 1, 1997. http://www.britannica.com/magazine/article?content_id=54316&query=safety%20for%20electronic%20hobbyists

8 Dictionary. www.dictionary.com

9 Diodes Incorporated. SD101AWS - SD101CWS Surface Mount Schottky Barrier Switching Diode. DS30078 Rev. A-2.

10 EIT imaging. http://www.eit.org.uk/about.html

11 Epson Electronics America, Inc. Small SO J High-Frequency Crystal Oscillator SG-636 Series.

12 Fay, J. A. Introduction to Fluid Mechanics. Cambridge, MA: MIT Press, 1998.

13 Fishbane P. M., Gasiorowicz S. and Thornton S. T. Physics for Scientists and Engineers, Extended Version: Volume II. Englewood Cliffs, NJ: Prentice Hall, 1993.

14 Fox, H. W. Master Op-Amp Applications Handbook. Blue Ridge Summit, PA: Tab Books Inc, 1978.

15 Franklin G. F., Powell J.D. and Ememi-Naeini A. Feedback Control of Dynamic Systems, Third Edition. Reading, MA: Addison-Wesley Publishing Company, 1994.

16 Gandhi, O. M., DeFord, J. F. and Kanai H. Impedance method for calculation of power deposition patterns in magnetically induced hyperthermia. IEEE Transactions on Biomedical Engineering. Vol. BME-31, No. 10, October 1984.

17 Hambley, A. R. Electrical Engineering Principles & Applications. Upper Saddle River, New Jersey: Prentice-Hall, Inc., 1997.

18 Horenstein, M. N. Microelectronic Circuits and Devices, Second Edition. Englewood Cliffs, New Jersey: Prentice-Hall, Inc., 1996.

19 Horowitz P. and Hill W. The Art of Electronics, Second Edition. New York, NY: Cambridge University Press, 1989.

20 Innoveda: ViewDraw. Design Capture and Analysis Tool. http://www.innoveda.com/products/datasheets_HTML/viewdraw.asp

21 Johnson D. E., Johnson J. R., Hilburn J. L. and Scott P. D. Electric Circuit Analysis, Third Edition. Upper Saddle River, New Jersey: Prentice-Hall, Inc., 1997.

22 Kreyszig, E. Advanced Engineering Mathematics, Sixth Edition. New York: John Wiley & Sons, 1988.

23 Linear Technology. LT®1007 Low Noise, High Speed Precision Operational Amplifier data sheet, LT/CPI 1101 1.5k Rev. B. Milpitas, CA: Linear Technology Corporation, 1985.

24 Linear Technology. LT®1884/LT1885 Dual/Quad Rail-to-Rail Output, Picoamp Input Precision Op Amps data sheet, 18845fs, sn18845 LT/TP 0400 4k. Milpitas, CA: Linear Technology Corporation, 2000.

25 LPKF. http://www.lpkfusa.com/

26 LPKF: Boardmaster. http://www.lpkfusa.com/Software/boardmaster.htm

27 LPKF: CircuitCAM. http://www.lpkfusa.com/Software/circuitcam.htm

28 Maxim Integrated Products. +15kV ESD-Protected, 1 μA, 250 kbps, 3.3V/5V, Dual RS-232 Transceivers with Internal Capacitors, MAX3233E/MAX3235E, 19-1473 Rev. 1.. Sunnyvale, CA: Maxim Integrated Products, May 2000.

29 Maxim Integrated Products. +5V-Powered, Multichannel RS-232 Drivers/Receivers MAX220-MAX249, 19-4323 Rev. 10.. Sunnyvale, CA: Maxim Integrated Products, August 2001.

30 Orcutt, Niel and Gandhi Om P. A 3-D impedance method to calculate power deposition in biological bodies subjected to time varying magnetic fields. IEEE Transactions on Biomedical Engineering. Vol. 35, No. 8, August 1988.

31 Panasonic. Multilayer Ceramic Chip Capacitors (for general electronic equipment), Series: ECJ. Matsushita Electric Corporation of America, 2002.

32 Panasonic. Tantalum Solid Electrolytic Capacitors/TES, Series: TES. Matsushita Electric Corporation of America, 2002.

33 Phycomp, A Yageo Company. RC02/12/22/32 1% Precision Chip Resistors sizes 1206, 0805, 0603, and 0402, Rev. 9. Phycomp, April 9, 2002.

34 Pliquett U. F., Gusbeth C. A. and Weaver J. C. Non-linearity of molecular transport through human skin due to electric stimulus. Journal of Controlled Release 68 (2000) 373-386.

35 Roberson J. A. and Crowe C. T. Engineering Fluid Mechanics, Sixth Edition. New York: John Wiley & Sons, 1997.

36 Schauf C. L., Moffett D. F. and Moffett S. B. Human Physiology Foundations and Frontiers. Boston, MA: Times Mirror/Mosby College Publishing., 1990.

37 Schey, J. A. Introduction to Manufacturing Processes, Second Edition. St. Louis, MO: McGraw-Hill, Inc., 1987.

38 Sheingold, D. H. Nonlinear Circuits Handbook, designing with analog function modules and IC's. Norwood, MA: Analog Devices, Inc., 1974.

39 Stuchly, M. A. and Stuchly, S. S. Permittivity of mammalian tissues in vivo and in vitro Advances in experimental techniques and recent results. International Journal of Electronics. Vol. 56, No. 4, pp. 443-456: 1984.

40 Texas Instruments. MSP430x13x, MSP430x14x Mixed Signal Microcontroller data sheet. Dallas, TX: Texas Instruments, 2001.

41 Thansandote, A., Stuchly, S. S., Smith, A. M. and Wight, J. S. Monitoring variations of biological impedances at microwave frequencies. IEEE Transactions on Biomedical Engineering. Vol. BME-30, No. 9, September 1983.

42 Thomasset, A. L. Impedance of Biological Tissues. http://myweb.worldnet.net/~althomas/node12.html

43 Tortora G. J. and Grabowski S. R. Principles of Anatomy and Physiology, Seventh Edition. New York, NY: Harper Collins College Publishers, 1993.

44 Xi, W., Stuchly, M. A., and Gandhi, O. P. Induced electric currents in models of man and rodents from 60 Hz magnetic fields. IEEE Transactions on Biomedical Engineering. Vol. 41, No. 11, November 1994.

45 Yamamoto, Y. Measurement and analysis of skin electrical impedance. Acta Derm Venereol (Stockh) 1994; Suppl. 185: 34-38.

Appendix A: FLUID FLOW THROUGH MICRONEEDLES

It is necessary to determine fluid flow through the microneedles so that parameters may be set for the needles that are used. Once the microneedles have been determined, the method for impedance testing to determine how far the needles have penetrated into the skin can be built.

Fluid Mechanics will determine the pressure that is needed to force flow out of a needle. Using the Navier Stokes equation and other basic assumptions an equation can be determined that will relate the pressure gradient to the fluid flow rate and geometry of the tube. With these values, an actuation system can then be determined that will drive the drug delivery device and a method of impedance testing can begin.

A.1 Flow Through a Tube with an Angled Profile

A.1.1 Derivation of the equation

The equation for conservation of momentum is given by

$$\frac{\partial \underline{u}}{\partial t} + \underline{u} \cdot \nabla \underline{u} + \frac{1}{\rho} \nabla p = \nu \nabla^2 \underline{u} \text{ .}^{12} \qquad \text{A.1}$$

Equation A.1 is going to be applied to flow through a tube of constantly decreasing radius as seen in Figure A-1. In this equation the velocity, u, is a function of x, the axial direction and r, the radial direction. The other parameters in the equation are ρ, the mass density; p, the pressure as a function of x; and ν, the kinematic viscosity. Incidentally, the equation for kinematic viscosity as a function of the mass density and the dynamic viscosity μ follows:

$$\nu = \frac{\mu}{\rho} \text{ .}^{12} \qquad \text{A.2}$$

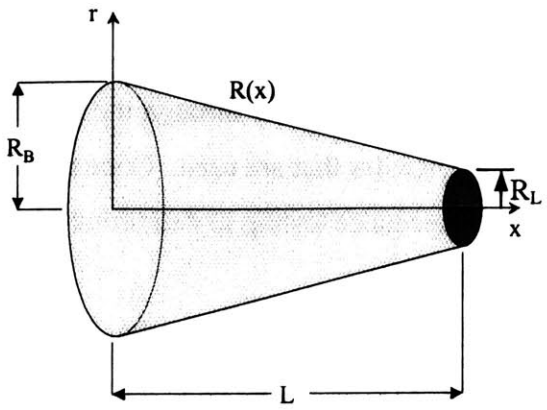

Figure A-1: Tapered tube microneedle design considered and used for fluid flow calculations

In addition to the equation for the conservation of momentum, the equation for the conservation of mass is also used in the final derivation.

$$q = \int u \cdot dA = \text{constant} \qquad \text{A.3}$$

$$\text{where} \quad A = \pi R^2(x) \qquad dA = 2\pi r \cdot dr \qquad \text{A.4}$$

and q is volume flow rate. [12]

Substituting equation

A.4 into A.3 , the result gives:

$$q = \int 2\pi \cdot u \cdot r \cdot dr = \text{constant.} \qquad \text{A.5}$$

An assumption should be made about the velocity of the flow in order to simplify equation A.5. Assuming that the tube walls taper slowly, in other words $L >> R_B$ (see Figure A-1), the velocity will only be in the axial direction, and any velocity in the radial direction will be negligible. Therefore, the velocity will assume a parabolic profile that can be generalized in the following equations:

$$u(x,r) = U(x)\left[1-\left(\frac{r}{R(x)}\right)^2\right], \qquad \text{A.6}$$

$$\frac{\partial u}{\partial r} = -2\cdot\frac{r}{R^2(x)}\cdot U(x),$$

$$\frac{\partial^2 u}{\partial r^2} = \frac{-2}{R^2(x)}\cdot U(x).$$

Substitution of equation for the velocity profile, A.6 , into the conservation of mass equation, A.5, yields the following equation:

$$q = \int_0^R 2\pi\cdot U(x)\left[1-\left(\frac{r}{R(x)}\right)^2\right]\cdot r\cdot dr = \tfrac{1}{2}\pi\cdot R^2(x)\cdot U(x) = \tfrac{1}{2}A(x)\cdot U(x). \qquad \text{A.7}$$

Taking the derivative of Equation A.7 and knowing that q=constant shows that if the area is constant, $\frac{dA}{dx}=0$, then the velocity along each axial line will also be constant, $\frac{dU}{dx}=0$; this can be seen below,

$$\frac{dq}{dx} = \frac{1}{2}\frac{dA}{dx}U(x) + \frac{1}{2}\frac{dU}{dx}A(x) = 0. \qquad \text{A.8}$$

Focusing back on the conservation of momentum equation, there are some assumptions that can be made. First, assume that the flow rate does not change as a function of time,

$$\frac{\partial \underline{u}}{\partial t} = 0. \qquad \text{A.9}$$

Second, from a previous assumption it follows that the dot product of the velocity with the gradient of the velocity will only have values in the x direction,

$$\underline{u}\cdot\nabla\underline{u} = u\hat{e}_x\cdot\left(\frac{\partial u}{\partial x}\hat{e}_x + \frac{\partial u}{\partial r}\hat{e}_r\right) = u\frac{\partial u}{\partial x}. \qquad \text{A.10}$$

Note that the pressure does not change in the radial direction; it only changes in the x-direction. Therefore, the gradient of pressure is only in the x-direction,

$$\nabla p = \frac{\partial p}{\partial x}. \qquad \text{A.11}$$

And finally, taking the Laplacian of the velocity while assuming axisymmetric flow gives the following equation:

$$\nabla^2 \underline{u} = \nabla \cdot \nabla \underline{u} = \frac{1}{r}\frac{\partial}{\partial r}\left(r\frac{\partial u}{\partial r}\right) + \frac{1}{r^2}\frac{\partial^2 u}{\partial \phi^2} + \frac{\partial^2 u}{\partial x^2}$$

$$\nabla^2 \underline{u} = \frac{\partial^2 u}{\partial r^2} + \frac{1}{r}\frac{\partial u}{\partial r} + \frac{\partial^2 u}{\partial x^2}. \qquad \text{A.12}$$

Plugging Equations A.9 through A.11 into Equation A.1 lends the following equation:

$$u\frac{\partial u}{\partial x} + \frac{1}{\rho}\frac{dp}{dx} = \nu\left[\frac{\partial^2 u}{\partial x^2} + \frac{1}{r}\frac{\partial u}{\partial r} + \frac{\partial^2 u}{\partial r^2}\right]. \qquad \text{A.13}$$

Plug Equation A.6 into Equation A.13 to get

$$\left[1-\left(\frac{r}{R}\right)^2\right]U\frac{dU}{dx} + \frac{1}{\rho}\frac{dp}{dx} = \nu\left\{\left[1-\left(\frac{r}{R}\right)^2\right]\frac{d^2U}{dx^2} - \frac{4U}{R^2}\right\}. \qquad \text{A.14}$$

Integrate Equation A.14 with respect to r:

$$\int_0^R \left\{\left[1-2\left(\frac{r}{R}\right)^2 + \left(\frac{r}{R}\right)^4\right]U\frac{dU}{dx} + \frac{1}{\rho}\frac{dp}{dx}\right\}dr = \nu\int_0^R \left[\frac{d^2U}{dx^2} - \left(\frac{r}{R}\right)^2\frac{d^2U}{dx^2} - 4\frac{U}{R^2}\right]dr$$

$$\frac{8}{15}R\cdot U\cdot\frac{dU}{dx} + \frac{1}{\rho}R\frac{dp}{dx} = \frac{2}{3}\nu\cdot R\frac{d^2U}{dx^2} - 4\nu\frac{1}{R}U. \qquad \text{A.15}$$

Given that the mass is constant, use Equation A.7 to solve for U(x) in terms of R.

$$R^2U = R_0^2U_0^2 = \frac{2q_0}{\pi} = k, \qquad \text{A.16}$$

$$U = \frac{k}{R^2},$$

$$\frac{dU}{dx} = -\frac{2k}{R^3}R'(x),$$

$$\frac{d^2U}{dx^2} = \frac{6k}{R^4}[R'(x)]^2 - \frac{2k}{R^3}R''(x). \qquad \text{A.17}$$

Plugging Equations A.17 into A.15 will put everything in terms of R:

$$-\frac{dp}{dx}=\frac{4\mu k}{R^4}\left[1-\left(\frac{dR}{dx}\right)^2+\frac{1}{3}R\frac{d^2R}{dx^2}\right]-\frac{16}{15}k^2\rho\frac{dR}{dx}\frac{1}{R^5}. \qquad \text{A.18}$$

Now, plug in from Equation A.16 into Equation A.18 , and this is the equation governing flow through a tube with a varying profile

$$-\frac{dp}{dx}=\frac{8\mu q_0}{\pi\cdot R^4}\left[1-\left(\frac{dR}{dx}\right)^2+\frac{1}{3}R\frac{d^2R}{dx^2}\right]-\frac{64}{15}\frac{q_0^2}{\pi^2}\rho\frac{dR}{dx}\frac{1}{R^5}. \qquad \text{A.19}$$

The results for a linear profile will be addressed in the next session.

A.1.2 Results

The initial design for the needle profiles assumed a linear sloping profile. Assuming that the dynamic viscosity of the drug to be delivered is approximately that of water, μ is set to $8.9\cdot10^{-4}\frac{N\cdot s}{m^2}$. Using a fixed base radius of R_B=150 μm and a length of 500 μm, the data in Figure A-2shows how much the pressure needs to change with changing flow rate for several different internal tip radii on the needle.

Look at Figure A-2 to see when the tip radius is larger, less pressure is required to push a specific flow rate through a needle. Figure A-2 also shows that for a flow rate of 1 mm^3/s = 1 μL/s, with a base radius of 150 μm and a tip radius of 32 μm, the pressure used to drive the liquid through one needle is about 100 Pa. Thus, for an array of four by four needles, given that the total flow rate must be 1 μL/s and the other dimensions are the same, the pressure reduces to 6.25 Pa.

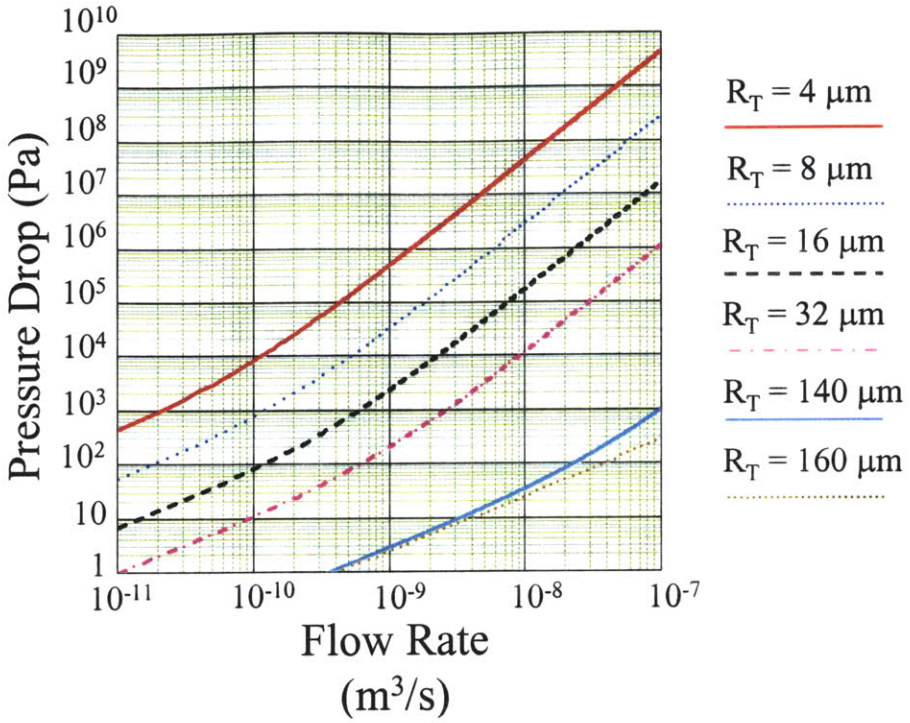

Figure A-2: Tapered tube with a base radius of 150 micrometers, a length of 500 micrometers for one needle. Change in pressure drop with a variable flow rate using several different tip radii.

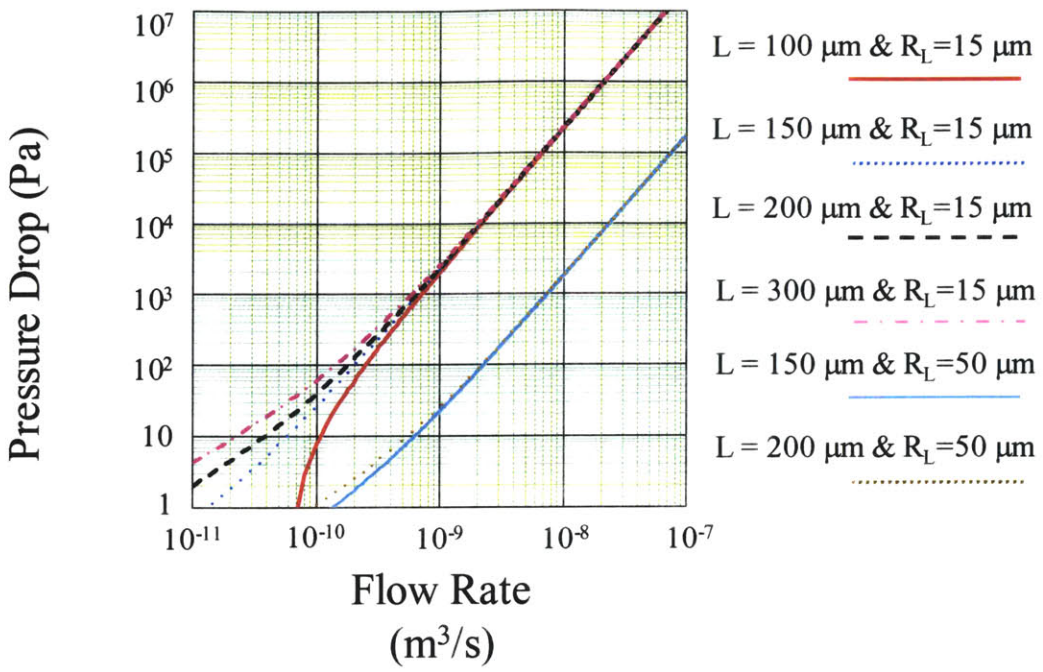

Figure A-3: Flow rate and pressure drop for tapered profile needles of a given base radius of 150 μm, a tip radii of 15 μm (upper cluster) or 50 μm (lower lines), and several different lengths.

Figure A-3 shows what happens when the length of the needles is varied between 100 μm to 300 μm for two different tip radii. For flow rates above 1 μL/s, there is almost no difference with increasing length for a given tip radius. This is because the speed required is sufficiently large and requires the same amount of pressure regardless of the length of the tube. For lower flow rates, increasing the length requires more pressure.

A.2 Flow Through a Straight Tube

A.2.1 Derivation of the equation

Flow through a straight tube is called Poiseuille Flow. If the tube is straight, as in Figure A-4, then the change in radius with respect to x is zero, $\frac{dR}{dx} = 0$. This also implies that the second derivative is zero, $\frac{d^2R}{dx^2} = 0$. Thus, if these assumptions are

applied to Equation A.19, the result will be Equation A.20 , the equation for Poiseuille Flow:

$$-\frac{dp}{dx} = \frac{8\mu q_0}{\pi R^4}. \qquad \text{A.20}$$

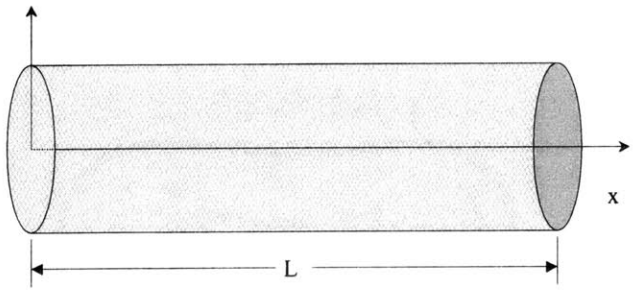

Figure A-4: Straight tube for Poiseuille Flow.

A.2.2 Results

After several different design modifications for the needles in the limpet drug delivery device, a straight needle was decided upon with an inner radius of 31.75 μm (see Figure A-5). The previous needle designs proved to be too strenuous to manufacture and given that the straight needles were already available, it allowed the group to focus more upon the actual delivery of the drug rather than how to manufacture the needles. If a given pressure of 1 MPa, an amount predicted for the pumping mechanism, is put on the end of the needle, then for longer tubes, the flow rate will decrease one decade per decade increase of tube length (see Figure A-6). For needles in the order of 10 mm in length, the flow rate should be over 10 μl/s, which is better than the minimum value of 1 μl/s.

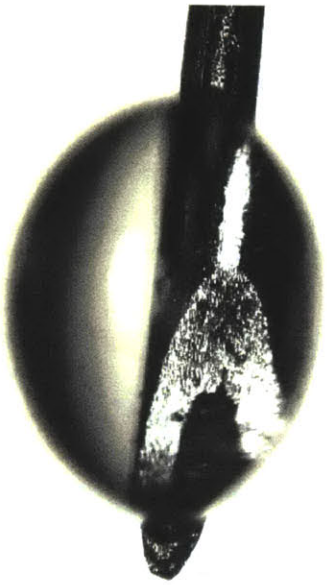

Figure A-5: Microscopic image of needle used for drug delivery device (inner diameter of 50 μm and outer diameter of 100 μm). Droplet of water is coming from the tip while picture is taken from below.

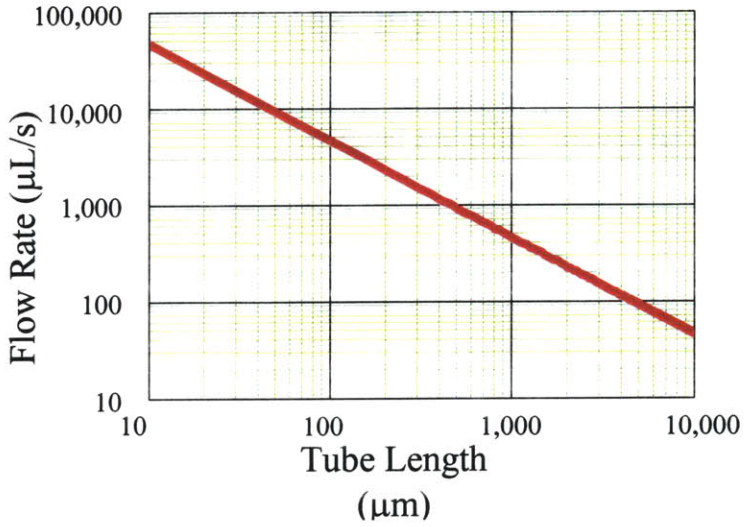

Figure A-6: Flow rate versus tube length for a constant tube radius of 31.75 μm and an applied pressure of 1 MPa.

Figure A-7 shows the flow rate for increasing pressure difference going from 1 kPa to 10 MPa. Needles of different lengths from 100 μm to 20 mm are plotted. In the final design, the needles are between 10 mm to 20 mm in length. A flow rate of 1 mm^3/s for a needle of length 20 mm, needs a pressure drop of approximately 45 kPa.

Because the predicted pumping mechanism can produce approximately 1 MPa of pressure, producing 45 kPa should not be difficult.

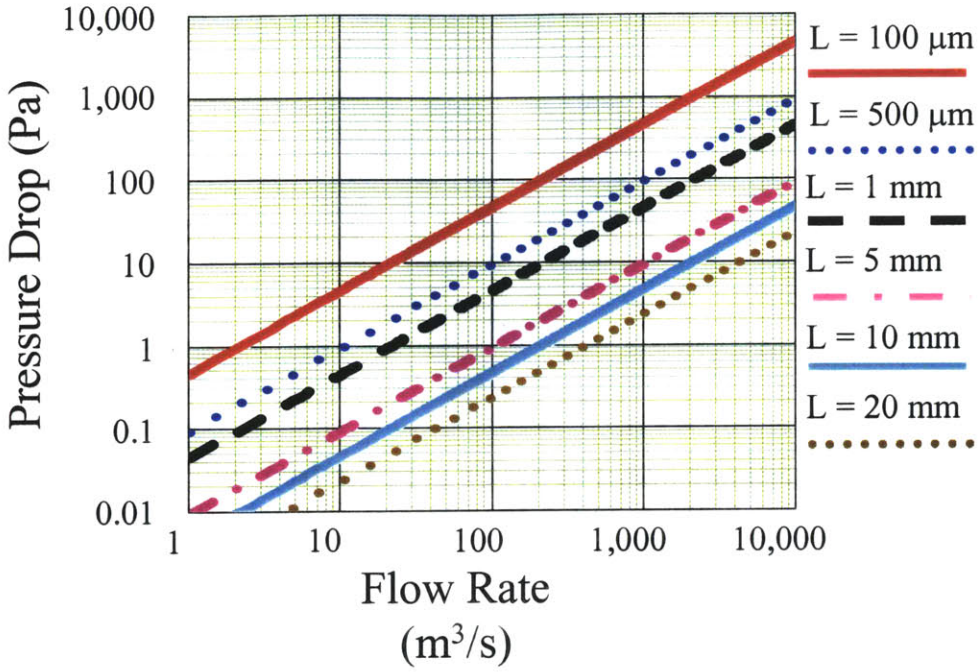

Figure A-7: Pressure Drop versus flow rate for a tube of constant radius 31.75 μm and several different lengths.

Appendix B: IMPEDANCE

Electrical impedance is resistance to current measured in ohms. In general, one can find the impedance of an object at a specific frequency by putting a known current through, then measuring the voltage drop,

$$Z = \frac{\Delta V}{I} \ [Ohms]. \qquad \text{B.1}$$

Impedance values may change for an alternating current when the frequency changes. Three objects that a current may go through are resistors, capacitors, and inductors. Each of these objects has a different impedance equation.

B.1 Resistors

The resistance of a material is defined as the potential difference across the material over the current that flows through it. Ohm's law shows this relationship:

$$R \equiv \frac{V}{I}. \qquad \text{B.2}$$

This means that the impedance of a resistor is equal to the resistance, as seen in Equation B.3 ,

$$Z_R = R. \qquad \text{B.3}$$

Thus, an ideal resistor is not frequency dependent. An ideal resistor will hold its impedance magnitude steady over all frequency ranges, and will have a phase of zero throughout all frequencies, as there is no imaginary term in the equation for impedance of a resistor. Resistors are not ideal, and will typically be frequency dependent in a high frequency range (see Figure B-1). The magnitude graph shows that above frequencies of 500 kHz, the magnitude of the resistor starts to decline and it acts like a capacitor. The phase graph shows that above frequencies of 200 kHz, the resistor no longer has a phase of zero. The phase seems to approach -90°, which is also like a capacitor. So, at higher frequencies, a real resistor tends to act like a capacitor. For the application of the impedance circuit, where the frequency is at 1-2 kHz, this behavior of the resistor will not be a problem.

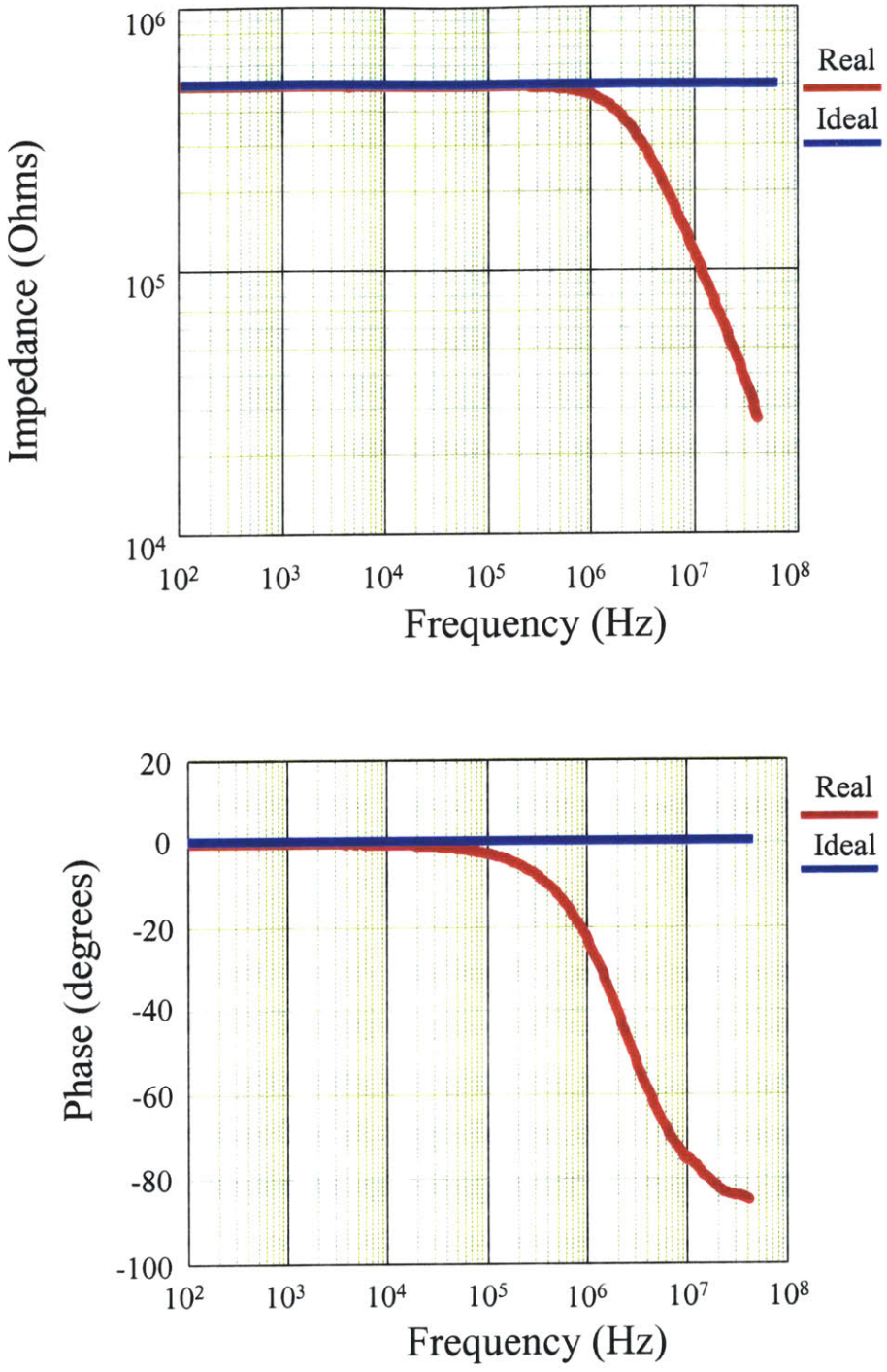

Figure B-1: Impedance values for a 499 Ω resistor.

B.2 Capacitors

Capacitors are time-dependant and thus an ideal capacitor will have a frequency dependent impedance value:

$$Z_C = \frac{-j}{\omega C}. \qquad \text{B.4}$$

From this equation, one can see that the magnitude of the impedance of a capacitor should be at a value inversely proportional to the frequency. In a logarithmic graph, one can see that there is one decade of magnitude decrease per decade frequency decrease (see Figure B-2). Equation B.4 also shows that the phase value should be at -90° because of the –j term. A capacitor may begin to show characteristics of an inductor above a specific frequency. The magnitude graph in Figure B-2 shows that a capacitor has ideal behavior until 1 MHz, at which point, it makes an abrupt transformation into inductor-like behavior. The phase of the capacitor is approximately -90°, as it should be, until approximately 100 kHz, where it seems to gradually move to +90°, the value for an ideal inductor. Again, with the circuit in question, these variables should not be a problem seeing as the frequency is in the 1-2 kHz range.

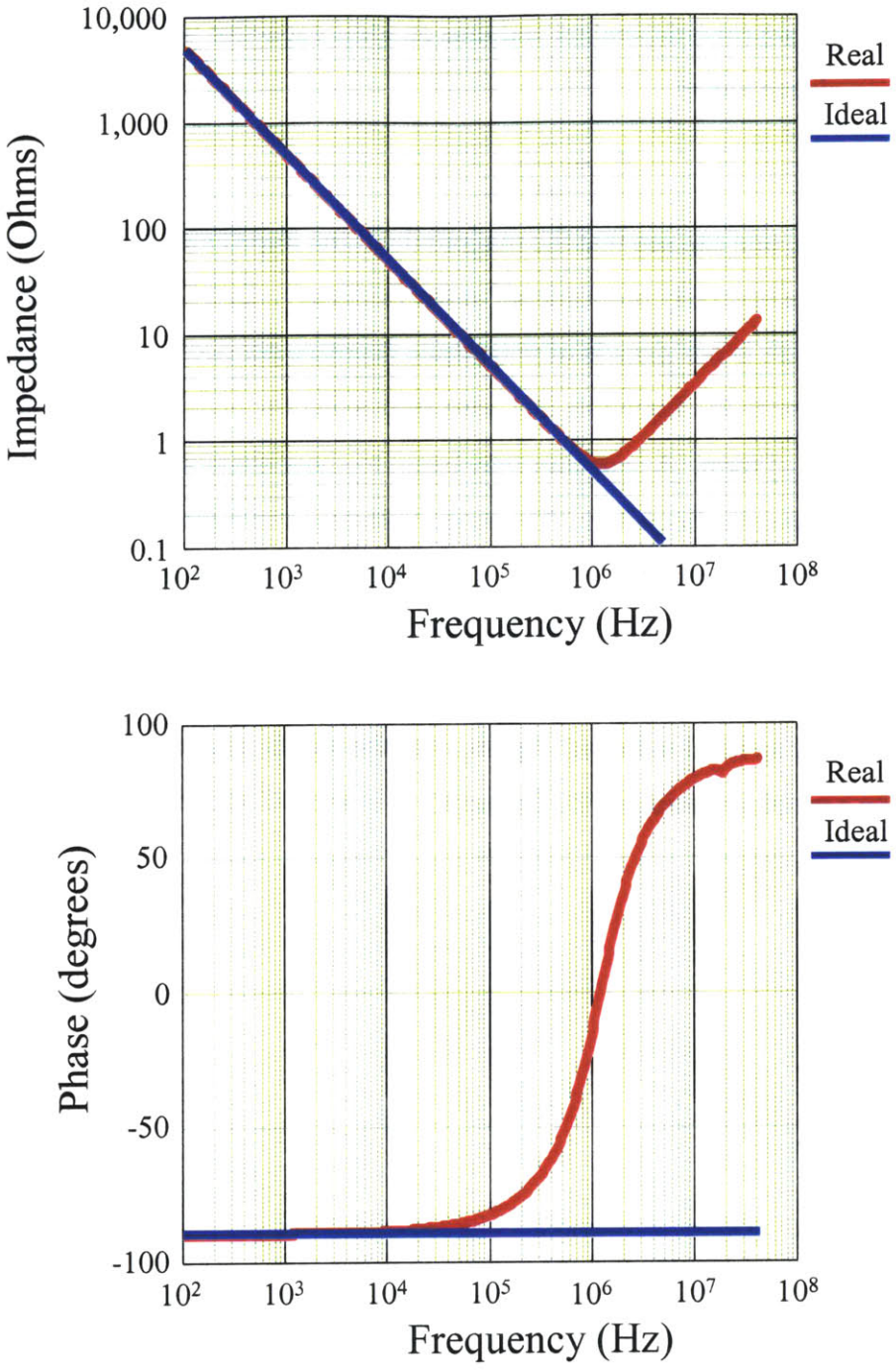

Figure B-2: Impedance values for a 3.33 μF capacitor.

B.3 Inductors

Inductors are also frequency-dependent elements. The equation for the impedance of an inductor is given by Equation B.5 :

$$Z_L = j\omega L . \qquad \text{B.5}$$

The magnitude of the impedance is proportional to the frequency, as given in Equation B.5 . From the magnitude plot of Figure B-3, one can see that this inductor varies from ideal under 300 Hz and over 1 MHz. It seems that over 1 MHz, the behavior varies between inductor and capacitor. The phase from 2 kHz to about 2 MHz corresponds to what is expected of an inductor, +90°.

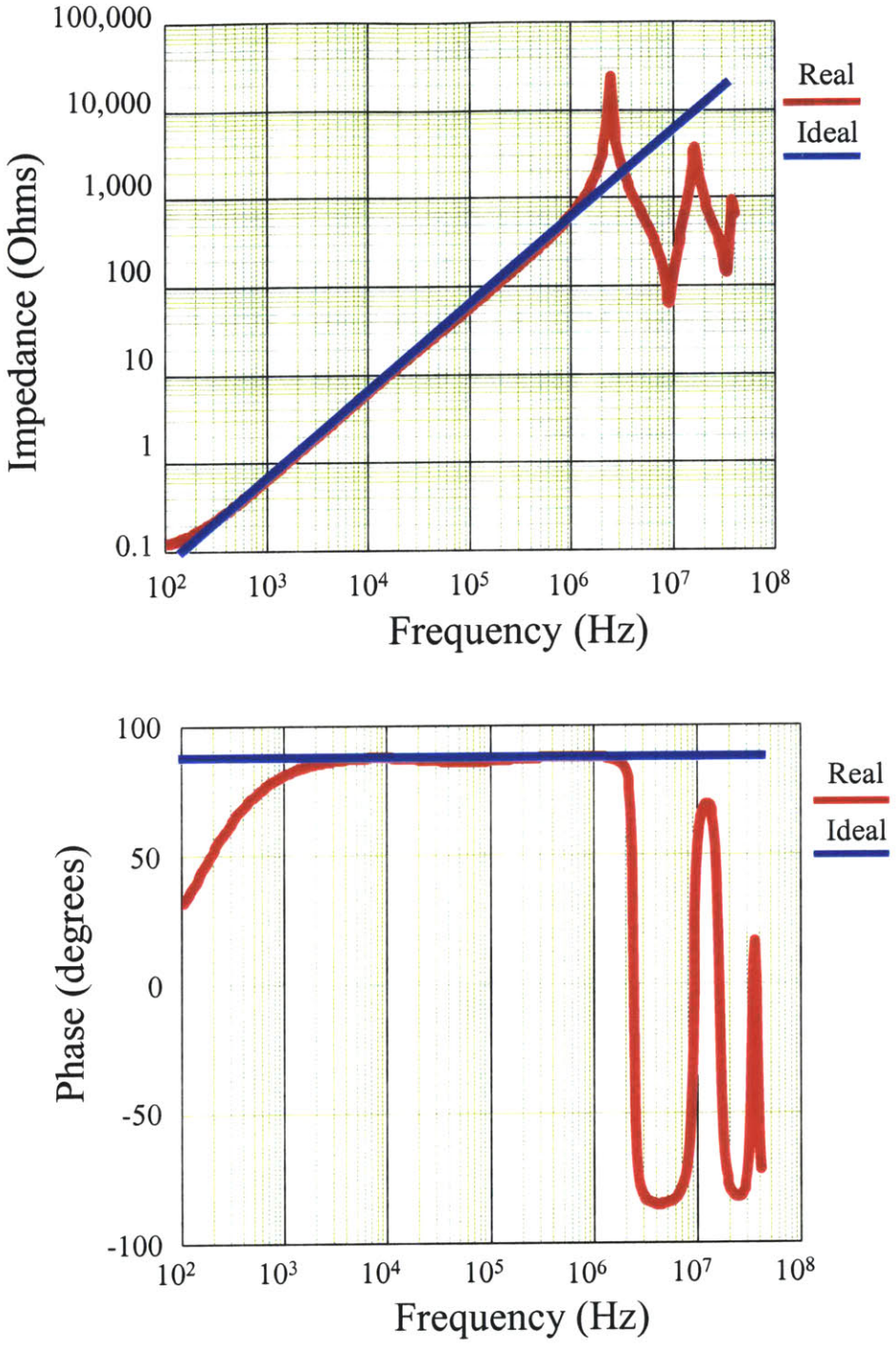

Figure B-3: Impedance values for a 0.5 μH inductor.

Appendix C: DATA SHEETS

The data sheets in this section are either components that are integrated into the final product of the impedance circuit or were considered to be a part of this circuit.

C.1 0402 Surface Mount 1% Resistors

http://www.phycomp-components.com/pdf/rc02.9.pdf

C.2 0603 Surface Mount Ceramic Chip Capacitors

http://www.panasonic.com/industrial/components/pdf/003_ec020_ecj_2_dne.pdf

C.3 Diodes

http://www.zetex.com/

C.4 Instrumentation Amplifier

http://products.analog.com/products/info.asp?product=AD620

C.5 Operational Amplifier

http://www.linear-tech.com/prod/datasheet.html?datasheet=550

C.6 TI MSP430F149 Microcontroller Data Sheet Excerpts

http://focus.ti.com/docs/prod/productfolder.jhtml?genericPartNumber=MSP430F149

C.7 RS232 Driver/Receiver

http://dbserv.maxim-ic.com/quick_view2.cfm?qv_pk=2008